UNIVERSITÀ DEGLI STUDI DI PADOVA
DIPARTIMENTO DI INGEGNERIA CIVILE, EDILE E AMBIENTALE
Department Of Civil, Environmental and Architectural Engineering

Corso di Laurea Magistrale in Environmental Engineering

TESI DI LAUREA

DESIGN OF A LANDFILL GAS COLLECTION LAYER USING RECYCLED MATERIALS

Relatore:
Chiar.mo PROF. MARCO FAVARETTI

Laureando: DAVIDE GARGHELLA
Mat. 2027164

Correlatori:
Chiar.mo ING. STEFANO BUSANA
Chiar.mo PROF. GIAMPAOLO CORTELLAZZO

ANNO ACCADEMICO 2022-2023

ABSTRACT

This thesis focuses on the design of a landfill biogas collection layer (BCL) considering the use of recycled materials, aiming to address the increasing demand for sustainable and environmentally friendly solutions in various industries. Moreover, this study, especially in its final section, seeks to outline an effective approach to choosing the right material for the BCL construction.

The research methodology aims to identify existing practices and technologies related to the design of this layer with the purpose of decreasing biogas dispersion in the environment, which may pose risks to humans and the ecosystem.

In the first place, the various components and considerations involved in designing an effective landfill cover will be explored, including engineering principles and regulatory requirements. This work will evaluate the different cover system components and finally concentrate on the BCL. This layer, located in the top cover, works as a homogenization for the biogas collection, helping the gas to flow into the collection points avoiding the formation of potential local runaways.

A significant portion of this paper will focus on the analysis of the landfill body's stability, which must be guaranteed in the presence of uplifting pressures on the top cover caused by biogas migration from the underlying waste mass. For this purpose, the infinite slope approach and the Koerner & Soong (1998) method will be applied for the analyses. After the evaluation of an allowable biogas pressure, the method proposed by Thiel (1998) will be used as the groundwork to calculate a suitable coefficient of permeability of the granular filter forming the BCL. Moreover, in the final sections, an acceptance procedure for choosing a proper material will be carried out.

Throughout this work, a case study will be examined regarding the stability of the top cover of an existing landfill located in Torretta di Legnago (VR), Italy.

The final objective of this work is to provide a framework for the development of an approach that considers factors such as gas flow dynamics and geotechnical properties, giving instructions for an effective and sustainable BCL design.

SOMMARIO

Questa tesi è incentrata sulla progettazione dello strato di drenaggio del biogas da discarica considerando l'uso di materiali riciclati, con l'obiettivo di rispondere alla crescente domanda di soluzioni sostenibili ed ecologiche nei vari settori civili e industriali. Inoltre, questo studio, in particolare nei capitoli finali, cerca di delineare un approccio efficace per quanto riguarda la scelta del materiale idoneo da utilizzare nella costruzione dello strato di drenaggio del biogas. La ricerca è mirata a identificare le pratiche e le tecnologie esistenti relative alla progettazione di questo strato, con l'obiettivo di minimizzare la dispersione di biogas nell'ambiente, evitando quindi rischi per l'uomo e l'ecosistema.

In primo luogo, verranno esplorate le varie componenti coinvolte nella progettazione di un'efficace copertura di discarica, considerando i fondamentali principi ingegneristici e i requisiti normativi, presentando i diversi componenti del sistema di copertura e concentrandosi infine sullo strato di drenaggio del biogas. Questo strato, situato nella copertura superiore, fornisce un'omogeneizzazione dell'afflusso del biogas tramite un filtro poroso, favorendo il deflusso verso i punti di raccolta evitando la formazione di potenziali instabilità locali.

Una parte significativa sarà dedicata all'analisi della stabilità della discarica, che deve essere garantita in quanto è da tenere in considerazione la presenza di pressioni sulla copertura superiore causate dalla migrazione del biogas dalla massa di rifiuti sottostante. A tal fine, per le analisi di stabilità verranno applicati l'approccio del pendio indefinito e il metodo di Koerner & Soong (1998). Dopo la valutazione della pressione ammissibile del biogas, il metodo proposto da Thiel (1998) sarà utilizzato come base per calcolare l'adeguato coefficiente di permeabilità del filtro granulare che costituisce lo strato di drenaggio del biogas. Nelle sezioni finali verrà infine presentata una possibile procedura di accettazione per garantire una corretta scelta del materiale.

Inoltre, verrà preso in considerazione come caso studio quello relativo alla stabilità della copertura superiore della discarica di Torretta di Legnago, in provincia di Verona. L'obiettivo finale di questo lavoro è di fornire un riferimento e un approccio progettuale sistematico che considera fattori quali la dinamica del flusso di gas e le proprietà

geotecniche, fornendo indicazioni per una progettazione efficace e sostenibile dello strato di drenaggio del biogas.

SUMMARY

Still today, landfilling represents an important and necessary method of waste disposal, especially in poor areas that do not possess adequate and modern recycling facilities. However, too often landfills are not adequately designed, and the potential negative effects exceed the advantages of this solution, leading to air, water, and soil pollution, as well as many other environmental problems. For this reason, especially in the last few decades, national and continental regulations have tried to define various guidelines for engineers to follow when designing a landfill. Recently, the term "sanitary landfill" has been used to refer to a well-engineered construction that is designed, operated, and monitored in accordance with the norms of a certain country or region, with technical standards that are the same as those of other infrastructures.

In the first two sections, the main aspects and design criteria for modern landfills will be presented, with special attention to the Italian guidelines contained in *D. Lgs. 121/2020*. While these indications give a general framework for the designer to start with, they must not become the only instrument to rely on. The core of this work, the profound reason behind the study carried out in this paper, derives from the observation of problems that could arise even when all the norms are fulfilled. In fact, the first objective of this research is the correct design of the biogas collection layer (BCL), whose purpose is the drainage and collection of the biogas that is formed in the underlying waste mass. This layer, located in the top cover of the landfill, has been introduced by the Italian regulation with *D. Lgs. 36/2003*. The importance of this element is given by the fact that, consisting usually in granular material that acts as a filter, it provides a homogenization of the biogas inflow arriving from the waste mass. This homogenization is intended to avoid the formation of preferential pathways for the gas, that could eventually result in local instabilities on the top cover. Thus, the primary function of the BCL is to guarantee an efficient transport of the biogas to the collection points, usually consisting in wells or horizontal drains.

For what concerns the Italian regulation, the only indication is that this layer must have a thickness $s \geq 0.5$ m and a suitable transmissivity and gas permeability. This is a general rule, which leaves the designer a certain amount of discretion in the planning of this layer. However, the biogas could cause important problems for the landfill cover, thus making

it crucial to adopt an efficient method to prevent unexpected issues. In fact, the gas that ascends from below the BCL creates a pressure and, consequently, an uplifting force on the interface between the BCL and the upper clay liner. For this reason, this interface becomes a potential failure surface that, if the pressures are too high, could lead to the sliding of the upper layers.

After a brief overview of biogas characteristics and collection methods based on literature, an assessment of the stability of the landfill top cover in the presence of biogas will be carried out. The main model that will be used for the analyses will be the one developed by Thiel (1998). This model considers a series of strip drains installed inside the BCL, which have the function of collecting the biogas that flows through the layer.

First, the estimation of the biogas flux that can be found with different gas generation models will be assessed. After this preliminary action, a slope stability analysis is carried out to determine the maximum gas pressure $u_{g,max}$ that guarantees a suitable Factor of Safety (FoS). Finally, when the evaluation of the maximum pressure is complete, a series of design equations will be used to determine the required permeability k_w of the material used for the BCL, relating to the distance between the strip drains.

In order to achieve a clearer understanding of the process to follow, a case study of an existing municipal solid waste (MSW) landfill will be used to perform the calculations. This landfill is located in Torretta di Legnago, in the province of Verona, Italy. Since 1982, this facility has undergone several changes and expansions, and nowadays the project for the adjustment of some areas is currently being carried out. In particular, calculations will concentrate on the escarpments constructed following the prescriptions of *D. Lgs. 36/2003*, which present a slope of approximately 21°. The new projects, on the other hand, are being carried out following *D. Lgs. 121/2020* and plan the use of geogrids in the top cover, which provide a major resistance to the instability of the slope and are therefore not presenting relevant stability problems.

The slope stability methods that are going to be used to assess the maximum gas pressure are the infinite slope approach and a slightly modified version of the method proposed by Koerner & Soong (1998), less conservative than the previous, since it also considers the toe buttressing of the slope. All results will be presented in the appropriate graphs and the permeability of the material chosen for the BCL will be assessed. Moreover, different

design solutions that have already been implemented in the landfill, such as coils instead of linear drains, will be considered and presented.

Finally, the last part of this work will be dedicated to the materials and aims to determine an appropriate acceptance procedure for a general material to be utilised in the BCL as a granular drainage. This procedure is crucial, since permeability is not the only parameter to be measured when designing a granular filter, and there is a need to understand if the material is suitable also in terms of mechanical and chemical resistance, internal stability, and compatibility with the other layers' materials.

In the end, this thesis intends to give the designer a possible efficient method for the choice and assessment of a suitable material to use as a granular filter in the BCL, trying not to overlook important factors that may compromise the stability of the top cover when in the presence of biogas pressure, resulting in major damage to the environment.

TABLE OF CONTENTS

LIST OF FIGURES

LIST OF TABLES

1 INTRODUCTION

1.1 THE ECOLOGICAL TRANSITION

As it is well known, improper waste management and disposal can have a major environmental impact, causing air, water, and soil pollution. For this reason, the European Union has made serious efforts in recent decades to enact laws to reduce waste's environmental and health impact and improve resource efficiency. These new guidelines, in particular the European Green Deal, have led member states to adapt and pay more attention to environmental issues. The European Green Deal (2020) is a package of strategic initiatives that aim to set the EU on the road to a green transition, with the ultimate goal of achieving climate neutrality by 2050.

Italy, for example, established the Ministry for Ecological Transition ("Ministero della Transizione Ecologica") with *Law of 22 April 2021, n. 55*. This replaces, to all intents and purposes and in all regulatory acts, the Ministry of the Environment. Now renamed as Ministry of Environment and Energetic Efficiency ("MASE, Ministero dell'Ambiente e della Sicurezza Energetica"), this ministry oversees and organizes the strategies to be implemented to guide the so-called "Ecological Transition".

The ecological transition is, together with decarbonization, one of the greatest challenges of our time. It is a way to combat climate change and support future generations with a view to sustainable development. It is also referred to as the "Green Transition", emphasizing how to reduce human activities' impact on the environment. This takes up many of the 17 Sustainable Development Goals set out in the 2030 Agenda for Sustainable Development.

The Ecological Transition focuses on a few key aspects that can be summarised as follows: circular economy, responsible agriculture, soil management, transition to renewable energy sources, energy efficiency of buildings, air pollution, waste management, water management, protection of biodiversity, sustainable mobility and much more.

The ecological transition is one of the pillars of the National Recovery and Resilience Plan ("PNRR, Piano Nazionale di Ripresa e Resilienza") and the European programme "Next Generation EU". In Italy, the objectives of the green revolution are contained in

Mission 2 of the PNRR. Many of the investments and funding are directly provided by the MASE, which also monitors the achievement of the planned targets.

1.2 WASTE GENERATION IN EUROPE

A total of 2153 million tonnes of waste were produced in the European Union in 2020, as a result of all economic activity and domestic waste. This translates into an average of 4813 kg per person (Eurostat, 2023). Northern countries account for the majority of the production, with Italy producing 2942 kg/year, below the European average (**Figure 1.1**).

Figure 1.1 *Waste generation in European member states for the year 2020 (Eurostat, 2023)*

In general, Europe produces significantly less garbage than nations like the USA or China when the kg/year per resident is taken into account. Additionally, all information pertaining to the recovery, reuse, and recycling of waste demonstrates how the European Union's efforts are producing excellent outcomes. **Figure 1.2** illustrates current waste management practices in the EU, which take into account the two primary treatment categories: recovery and disposal. From 870 million tonnes in 2004 to 1164 million tonnes in 2020, the amount of waste recovered used for backfilling or burnt with consequent energy recovery increased by 29.4%; as a result, the share of such recovery in total waste treatment increased from 45.9% in 2004 to 59.1% in 2020. The three main methods of recovery for waste are recycling, backfilling and burning with energy production. Waste that does not undergo one of these processes can be either landfilled, incinerated without any energy recovery or, in the worst case, have a different path and end up dispersed in the environment.

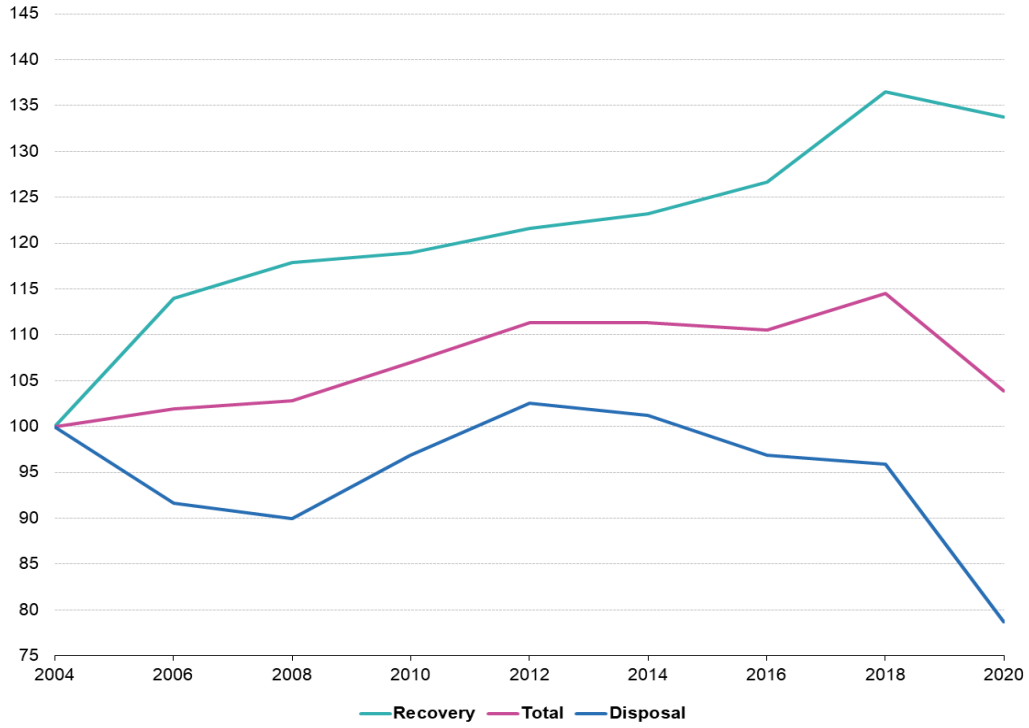

Figure 1.2 *Trend for waste management for the period 2004-2020 (Eurostat, 2023)*

One thing that needs to be made clear is that landfilling is still necessary and essential to safeguard the environmentally responsible management of garbage, despite the general improvements in waste recovery. Moreover, landfilling is still the main treatment method for some countries like Romania, Bulgaria, Finland, Sweden and Greece (**Figure 1.3**).

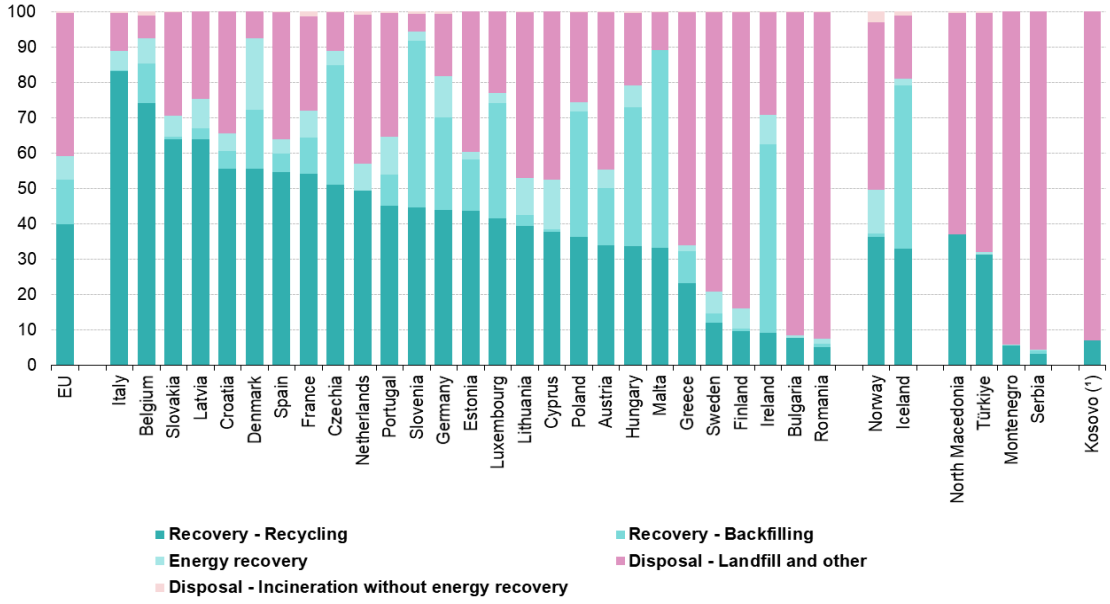

Figure 1.3 *Waste treatment by type of recovery and disposal (Eurostat, 2023)*

1.3 THE IMPORTANCE OF LANDFILLING

Although many people can think of landfill as an obsolete system of waste management, most of the time influenced by extremely negative depictions in public media, this type of disposal is still vital for the preservation of the environment. This is valid especially for less developed countries that do not possess modern technologies and facilities for the recovery and recycling of waste. Moreover, the majority of these countries also struggle with the problem of overpopulation and extremely rapid demographic growth. In these cases, recycling cannot keep up with the pace of waste generation and, consequently, phenomena like open dumping and sea littering begin to spread (**Figure 1.4**).

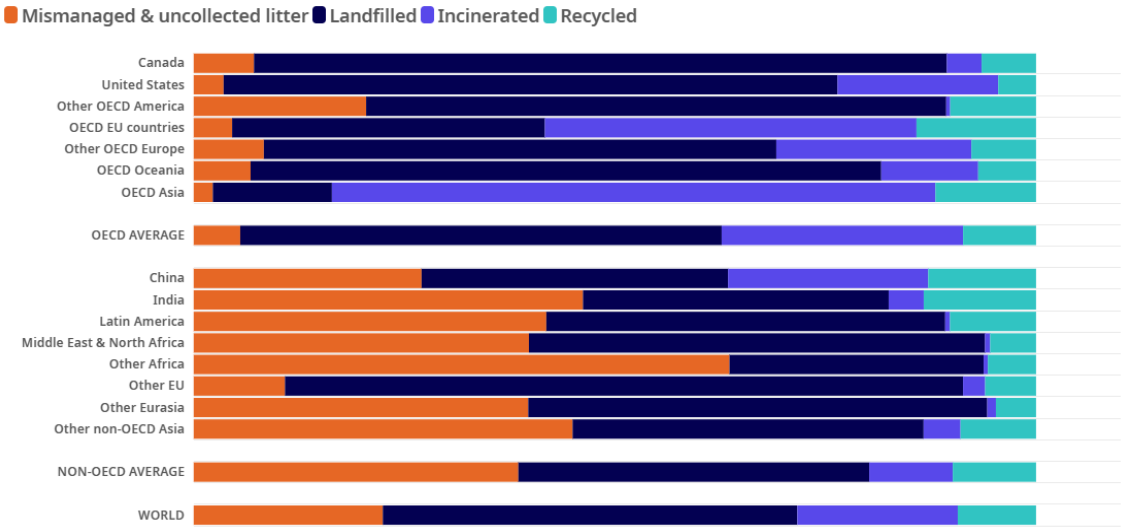

Figure 1.4 Share of plastics treated by waste management category, after disposal of recycling residues and collected litter in 2019 (OECD, 2019)

Landfills continue to be used as a waste management method in many countries for several reasons that can be resumed as the following:

- ***Cost-effectiveness***: Landfilling is often considered a cost-effective waste management option, particularly in areas with limited financial resources. Compared to other waste management methods, such as incineration or advanced technologies, landfills typically require less initial investment and operational expenses.
- ***Infrastructure availability***: Landfills require relatively basic infrastructure and equipment, making them accessible in areas with limited resources and technology. They can be constructed and operated with the existing local infrastructure and expertise, making them a practical choice for waste

management in poor countries with limited access to advanced waste treatment facilities.

- ***Flexibility and scalability***: Landfills can accommodate a wide range of waste types and quantities. They can be scaled up or down based on the waste generation rate, allowing for flexibility in waste management strategies. In areas where waste composition and quantities fluctuate, landfills provide a practical solution that can adapt to changing circumstances.
- ***Job creation***: Landfills, especially the larger ones, help create employment opportunities in waste collection, sorting, and landfill operation and maintenance. In countries with high unemployment rates, landfills can provide job opportunities for local communities, offering economic benefits.
- ***Limited alternatives***: In some cases, poor countries may lack access to alternative waste management technologies, such as waste-to-energy facilities or advanced recycling infrastructure. Landfills become the default option due to limited resources, infrastructure, and technical expertise to implement and operate alternative waste treatment methods.

It is crucial to emphasize, however, that while landfills can be a viable short-term option, they are not without limitations. If landfills are not adequately managed, they can have negative environmental and health consequences. If not planned and run in compliance with suitable environmental standards and procedures, they can contribute to air and water pollution, greenhouse gas emissions, odour and aesthetic inconveniencies, and pose health risks to local people.

Sustainable waste management practices, such as trash reduction, recycling, and the development of more advanced waste treatment technology, should be promoted. Supporting capacity-building activities, raising public awareness, and offering financial support can all help to improve waste management methods and, in the long term, reduce dependency on landfills.

2 THE SANITARY LANDFILL

Modern landfills need to be well-engineered structures that are positioned, run, and monitored to guarantee adherence to the rules of a specific country or region. Landfills for solid waste, comprehending municipal solid waste (MSW) landfills, must be constructed with the aim of safeguarding the environment from contaminations due to potentially harmful substances present in the disposed materials and should be built, controlled, operated, and maintained to the same high technical requirements as other civil work installations of public importance (buildings, roads, airports, waste treatment facilities etc.). While on-site environmental monitoring systems keep an eye out for any indication of groundwater pollution, landfill gas and other dangers, the landfill siting plan avoids the placement of landfills in environmentally sensitive regions. Furthermore, a large number of recent landfills capture potentially dangerous landfill gas emissions and turn the gas into electricity, as it will be addressed in Chapter 3.

2.1 STRUCTURE OF A SANITARY LANDFILL

2.1.1 Different geometries

The structure of a sanitary landfill varies from case to case, according to the needs and the criticalities of the ecosystem in which it is integrated. After the decision on the site location, an extremely precise technical survey should be conducted during the design phase to characterize the area in detail. This survey should use topographic data and evaluate factors such as climatic regimes, geological structures, groundwater and surface water hydrology, and geomechanical problems.

Currently there are five main methods for the construction of a landfill, as visible in **Figure 2.1**. As far as possible, landfills should be built above ground level (mound landfill, option B and D). In this case, leachate will be able to flow out from the landfill by gravity and will not need to be pumped off from deep shafts, as would be the case for below ground level landfills (pit landfill, option A, C, and E). In addition, for options B and D, cleaning and maintenance of drainage pipes is undoubtedly easier. Moreover, the landfill is more visible, which is of importance in view of the long-term life span and the risk of overlooking its presence. Additionally, landfill mining can be carried out with greater ease.

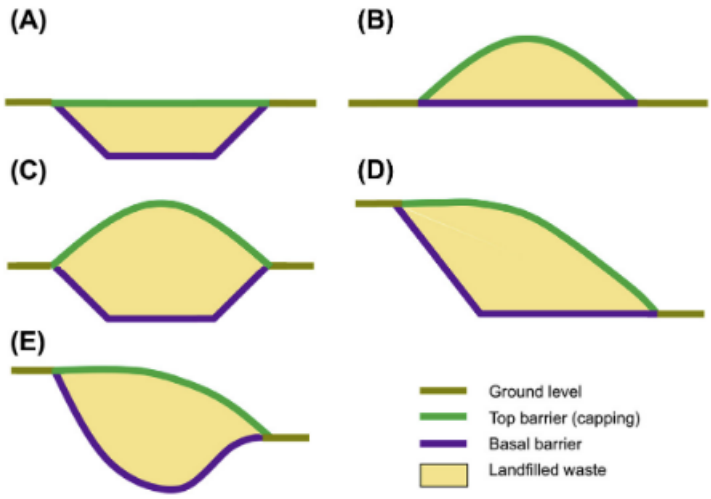

Figure 2.1 *Different landfill morphologies. (A) Below grand level, (B) Above the ground level, (C) Below and above ground level, (D) On a slope, (E) On a valley (Cossu & Stegmann, 2018)*

Option D, a landfill located on a slope, would be another suitable morphology if it proves impracticable to build the dump above ground level. Controlling the water regime is essential in this situation for preventing issues with mechanical instability. Rainfall and clean drain water should be effectively routed away from the landfill, as well as being adequately drained. In general, it is never a good idea to build up a landfill to cover a valley since this might lead to the creation of uncontrolled waterways and the contamination of waterways that are already present under the landfill. The base barrier system should meet the same exact requirements as the mound landfill for both slope and pit landfills.

When a landfill is built in a pit, the same level of construction as that intended for the bottom liner should be used to install the drainage and lining at all surfaces between soil and garbage. Leachate extraction should also be done using a specialized design.

2.1.2 The landfills' cover

Any site's design and operation must meet four essential characteristics (Thurgood, 1999) before it can be considered a sanitary landfill:

1. ***Full or partial hydrogeological isolation***: if a site cannot be located on naturally leachate-secure land, additional lining materials should be brought to the site to reduce leakage from the site's base (leachate) and help reduce contamination of groundwater and surrounding soil. If no leachate collection system is provided with a liner, whether soil or synthetic, all leachate will eventually reach the

surrounding environment. The collection and treatment of leachate must be emphasized as a basic necessity.

2. ***Accurate engineering preparations***: plans should be based on local geology and hydrogeological studies.
3. ***Permanent control***: trained personnel should be stationed at the landfill to oversee site preparation and construction, waste deposition, and regular operation and maintenance.
4. ***Planning of waste disposal***: waste should be scattered in layers and compacted. A small working area that is covered daily reduces the accessibility of garbage to pests and rodents.

All these characteristics led engineers to the construction of landfills as multi-layered systems, in order to achieve the best results in terms of isolation and pollution control. The general scheme of a modern landfill and its components can be seen in **Figure 2.2**.

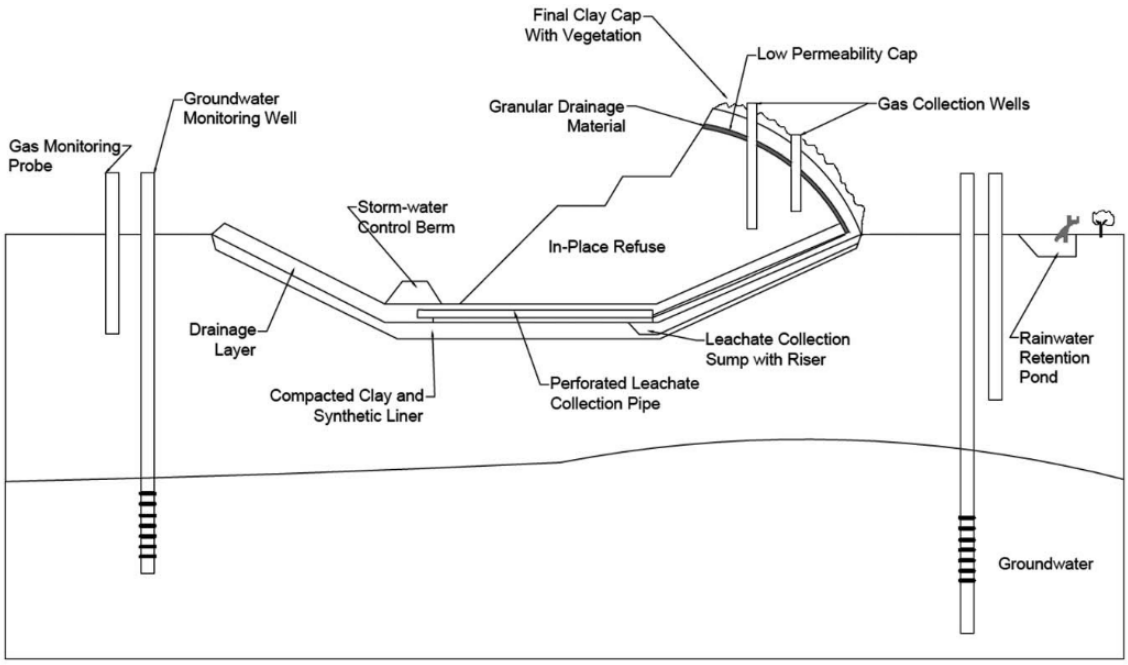

Figure 2.2 *Cross section of a typical modern sanitary landfill (Meegoda et al., 2016)*

However, this is just an overview and the choices between different materials, components, thickness of layers, etc. need to be assessed by the engineer in charge of the design. Moreover, every area or country is subjected to a regulation that must be observed. The specific Italian regulation concerning landfill construction will be briefly presented in Chapter 2.2.

It is very important to note that, if the design has been performed correctly, the landfill should be easy to control and limit the number of problems that could arise. Instead, most of the problems may come out during the construction phase. For that reason, it is important to guarantee the security of both the environment and the workers during this phase. In fact, to ensure general safety, different types of landfill covers must be used as follows (**Figure 2.3**):

1. ***Daily cover***: daily cover is an intralayer cover that is applied on a regular basis at an active landfill site to reduce windblown litter, dust, odour, disease vectors, fire hazard, scavenging, and all possible unpleasant situations. Usually, soil-based materials are used for this type of cover, but also plastic tarps, foams, and sprays that may be removed are used. In any case, regulations govern the quality and prescriptions for products used as daily coverings. For example, volume occupancy, interference with gas extraction wells, and poor draining quality are all critical factors to consider.
2. ***Intermediate cover***: when filling in a designated region is temporarily paused and exposed for a period of time, intermediate coverings are required. Controlling water infiltration, erosion, fugitive gas emissions, leachate breakouts, air intrusion, fire hazards, and littering is the goal. These covers should provide several months of service until landfilling is resumed. Furthermore, regular inspections and erosion control are required.
3. ***Temporary capping***: when waiting for waste to settle before laying permanent capping, a landfill may use intermediate covers. If there is the need to place other batches of waste, temporary cappings serve as top barriers until mechanical and biological stability is achieved. They must be functional to the landfill design idea, controlling water infiltration, reducing gas emissions, contributing to rainwater management, promoting vegetation development, and protecting against erosion. Physical barriers such as low permeability soil and materials accomplishing specific functions, such as methane oxidizing material, natural soil to sustain vegetation, and low stem vegetation with high evapotranspiration (ET)[1] effect is suitable for temporary cappings.

[1] Evapotranspiration is the sum of transpiration through plant canopy and evaporation from soil, plant, and open water surface. It can be the largest component of the hydrologic cycle.

4. ***Permanent capping***: permanent capping gets adopted in landfills after mechanical stabilization and significant pollutant mobilization. It must drain and control water infiltration, as well as attenuate gas emissions, contribute to rainwater management, support vegetation development, and control erosion. It must also meet certain landfill afteruse requirements, such as easy vehicle movement, gas emission prevention, effective water runoff management, and erosion resistance. Permanent capping must be maintained in an effective way until the final quality of landfilled waste and emissions is reached.

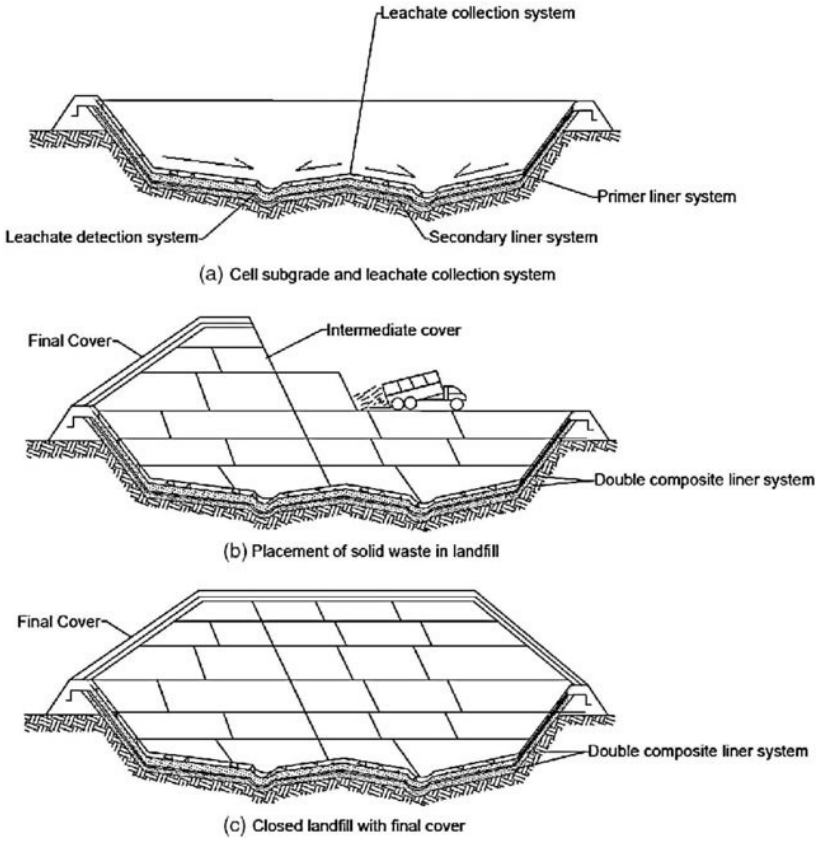

Figure 2.3 *Construction sequence of a solid waste landfill (Meegoda et al., 2016)*

2.1.3 Stratification

For the purposes of this thesis, which aims to investigate the gas collection layer's design, it is important to pinpoint where this layer is situated. In fact, it is part of the landfill top cover, also known as the final cover or cap. As just explained, this multi-layered structure acts as a barrier to minimize the potential for environmental contamination. It helps prevent the infiltration of rainfall, mitigates odours that may arise from the decomposing waste, and discourages the intrusion of pests, animals, and vectors into the landfill. It also

helps prevent erosion of the landfill surface due to wind and water, providing stability and protecting the underlying layers. In some cases, the top cover may be designed to incorporate a gas collection system, as it will be further analysed in Chapter 3.3. This allows for the efficient capture and management of landfill gas, including methane, which can be utilized as a renewable energy source or properly controlled to minimize its impact on climate change.

In **Figure 2.4**, the usual layers of a top cover are visible.

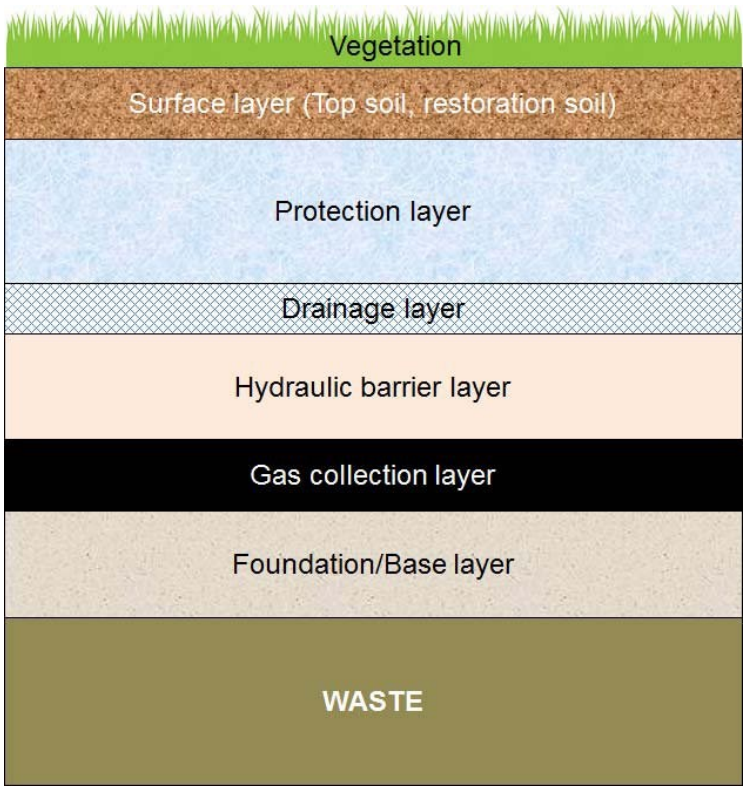

Figure 2.4 *Landfill top cover (Othman, 2016)*

The stratification of the landfill top cover includes certain elements, each one with its own purpose. The principal components are:

- ***Surface layer***: the surface layer is the most exposed part of a cover system. This layer's primary roles are to prevent erosion caused by water and wind and, if existent, to offer a substrate for the growth of vegetation. Suitable topsoil encourages the growth of vegetation, enhancing the ET component of the cover system water balance. Plants also help a lot in reducing the volume and velocity of rainwater flow on cover system slopes.

- ***Protection layer***: the main role of the protection layer is to protect the lowermost portions from wet-dry and freeze-thaw cycles, as well as the infiltration of plant roots and animals.
- ***Drainage layer***: the drainage layer, also known as the rainwater collection layer or rainwater drainage system, is crucial in landfill top cover management. It collects and channels excess rainwater, preventing pressure build-up and enhancing stability. It also ensures water movement away from sensitive areas, directing it to designated collection points for efficient collection and management. The drainage layer also prevents saturation by facilitating efficient drainage, ensuring the cover system remains efficient and free from excessive loads. This layer plays a crucial role in the long-term effectiveness of landfill covers by maintaining their integrity and functionality. Common materials used include gravel, sand, and perforated pipes or geocomposites.
- ***Hydraulic Barrier***: the hydraulic barrier serves the purpose of minimizing or controlling the movement of liquids within the landfill. By restricting the movement of liquids, the hydraulic barrier helps to safeguard water quality and prevent the spread of pollutants. The hydraulic barrier is designed to have low permeability. This is typically achieved by using impermeable materials such as clay, geomembranes, and geosynthetic clay liners (GCLs). It should be compatible with the other components of the liner system and be resistant to chemical degradation, withstanding the long-term exposure to liquids and other landfill conditions without compromising its effectiveness. It is crucial that this layer is free from defects, such as punctures or tears, that could allow the migration of these liquids. In some cases, geosynthetic materials, such as geotextiles or geocomposites, may be used in combination with the hydraulic barrier to enhance its performance. These geosynthetics can provide additional strength, filtration, or separation properties to improve the overall functionality of the barrier system.
- ***Gas collection layer***: the biogas drainage layer helps remove the biogas produced by anaerobic waste digestion and is in charge of draining and distributing the gas to the pipelines that transport it to combustion systems. Gravels, sand, or waste

treatment leftovers may be employed. This layer can be spanned by both vertical extraction wells and horizontal pipes, as better detailed further in Chapter 3.3.

- ***Base layer***: the base layer, also defined as foundation layer, is the first element to be built and is located directly above the waste mass. Since it will serve as the foundation for all the layers above it, it should provide a smooth surface that allows construction (it must have an optimal bearing capacity) while avoiding problems caused by eventual differential settlements that may occur during the consolidation of the underlying waste mass. The most common materials utilized for the base layer are on-site or locally accessible soils and waste sieve fractions.

2.2 REGULATION IN ITALY

Concerning Italy, recent environmental legislation is under the light, because of the new reforms implemented to put European directives into practice. In fact, several legislative decrees that recently took effect represent a significant shift in the legislation governing the entire industry. The most recent laws include those that took effect in September 2020 and allowed Italy to implement the four European directives, also known as the "Circular Economy Regulatory Package".

Countries will be required to improve the recovery of matter and energy from "waste" and reduce waste by utilizing alternative options, like product recovery or reuse, as a result of the new regulatory scenario.

Following *D. Lgs. 102/2020*, concerning air quality protection, *D. Lgs. 121/2020*, in particular, intervenes in the regulation of waste landfills, also to simplify and strengthen it. Implementing the *Continental Directive (EU) 2018/850*, this legislative decree reforms the regulations previously in force and provided for by the historical *D. Lgs. 36/2003*.

In reality, the latter measure, which essentially repeated the requirements of *Directive 1999/31/EC*, was becoming outmoded in light of the EU's growing demands for the effective realization of economic sustainability. Step by step, Italy too is, at last, implementing the transition from a national environmental legislation based on the concepts of the linear economy, to a circular system where the reuse of materials even in subsequent production cycles is decisive. There are many new aspects introduced and changes made to the regulations on waste landfills with the entry into force of the new

decree although, it should be noted, at the moment the focus is mainly on municipal waste, which accounts for only a portion of the waste produced nationwide.

In Article 1, in particular, attention is paid to the «Promotion of procedures and guidelines to prevent or reduce as far as possible adverse impacts on the environment, in particular pollution of surface water, groundwater, soil and air, agri-food heritage, cultural heritage and landscape, and the global environment, including the greenhouse effect, as well as risks to human health resulting from waste landfills, throughout the complete life cycle of the landfill»[2].

Based on the criteria defined in the different attachments, Article 7 defines a new classification for landfills, based on the type of waste that will be conferred on the site. These three categories are:

- Landfills for inert waste;
- Landfills for non-hazardous waste, including municipal solid waste (MSW) landfills;
- Landfills for hazardous wastes.

These categories are then further divided into sub-categories. It is important to note that the waste producer is required to perform a basic characterization of each type of waste delivered to the landfill, to establish its eligibility in each landfill category. Characterization must be done after the final treatment, which is before landfilling.

For this thesis, particularly important is Attachment 1 to the *D. Lgs. 121/2020*, because it defines the design criteria for the construction and maintenance of a landfill.

2.2.1 Stratification of a landfill in Italy

Taking into account the case of landfills for non-hazardous waste, hence the vast majority of the MSW landfills, Attachment 1 gives important indications on how to build a proper facility. All new construction designs must attain these rules.

Considering the bottom liner, the elements that must be present are the following (from bottom to top):

1. Natural or artificially completed geological barrier, with thickness $s \geq 1$ m and permeability $k < 1 \times 10^{-9}$ m/s;

[2] Decreto Legislativo 3 settembre 2020, n. 121 "Attuazione della direttiva (UE) 2018/850, che modifica la direttiva 1999/31/CE relativa alle discariche di rifiuti", translated.

2. Artificial impermeable layer, with thickness $s \geq 1$ m and permeability $k \leq 1 \times 10^{-9}$ m/s, using natural soils or compacted soil mixtures that guarantee the prescribed permeability;
3. HDPE geomembrane, with thickness $s > 2.5$ mm;
4. Protective layer, made of suitable natural or artificial material, to prevent damage to the waterproofing system caused by atmospheric agents during the construction phase and by loads during the landfill management phase;
5. Drainage layer, with thickness $s > 0.5$ m, permeability $k \geq 1 \times 10^{-5}$ m/s, classes A1 and A3 of the HRB-AASHTO classification[3].

For what concerns the top final cover, the elements are (from top to bottom):

1. Surface layer, with thickness $s \geq 1$ m, that promotes the growth of cover plant species, providing adequate protection against erosion and protecting the underlying barriers from temperature fluctuations;
2. Drainage layer of granular material, with thickness $s \geq 0.5$ m, of suitable transmissivity and permeability ($k > 1 \times 10^{-5}$ m/s). This layer may be replaced by a draining geocomposite of equivalent performance and characteristics. In any case, the drainage layer must be protected with a natural or geotextile filter to prevent possible clogging associated with the entrainment of fine material from the surface overburden;
3. Compacted mineral layer, with thickness $s \geq 0.5$ m and hydraulic conductivity $k \leq 1 \times 10^{-8}$ m/s, supplemented by a surface waterproofing layer. This layer must also be protected with a layer of suitable natural or artificial material to prevent damage from weathering and loads during construction. It may also utilize geosynthetic waterproofing materials that ensure that the overall performance in terms of water penetration is equivalent. Particular design solutions in the construction of the compacted mineral layer of the parts with a slope greater than 30°, which nevertheless guarantee equivalent protection, may exceptionally be adopted and implemented, even with thicknesses of less than 0.5 m, provided they are approved by the competent territorial authority;
4. Gas drainage layer, with thickness $s \geq 0.5$ m of suitable transmissivity and gas permeability, capable of draining the gas flow produced by the waste into its

[3] CNR-UNI 10006 "Classificazione dei terreni HRB-AASHTO", 2002.

plane. In all cases, the drainage layer must be protected with a suitable natural or synthetic material;

5. Base layer, with the function of ensuring the correct installation of the overlying layers.

2.2.2 Some notes on the current regulations

Landfills are very complex systems, and every single constituting element must be studied taking into account a huge number of factors. This makes it crucial for the engineer in charge to be critical and question the limitations imposed by these regulations. In fact, blindly relying on these guidelines may result in a superficial project that could face some serious problems. A landfill could, in fact, be perfectly adherent to all the parameters requested in the regulation, but still have many drawbacks that compromise its efficiency. While aiming to ensure safety, they may actually not address all possible risks or cover every unique situation.

Regulations often provide general guidelines applicable to a wide range of circumstances. Each engineering project is unique, with specific site conditions, environmental factors, and project requirements. By being critical, engineers can assess the specific context and tailor their designs and solutions to address site-specific challenges. This customization ensures that the engineering solutions are optimized for the specific project, leading to better outcomes and performance. In addition, regulations are typically based on knowledge, understanding, and societal priorities available at the time of their publication. However, technology and society are continually evolving, and regulations may not always keep pace with these changes. Being critical allows engineers to anticipate future needs and challenges, developing solutions that are more resilient and adaptable to changing circumstances. In brief, by going beyond regulations, engineers can always optimize designs and processes to achieve better outcomes.

2.3 THE TORRETTA DI LEGNAGO LANDFILL

For the purposes of this thesis, the case of an Italian landfill will be taken into consideration. This landfill is located in northern Italy, precisely in the municipal territory of Legnago, under the Verona province, on the border with the provincial territory of Rovigo (**Figure 2.5**). The neighbouring region is distinguished by the presence of small

rural areas; it is essentially flat, with the presence of numerous irrigation canals, and has a predominantly agricultural vocation with extensive cereal cultivation, whereas livestock farming practices and industrial activities appear to be less prevalent.

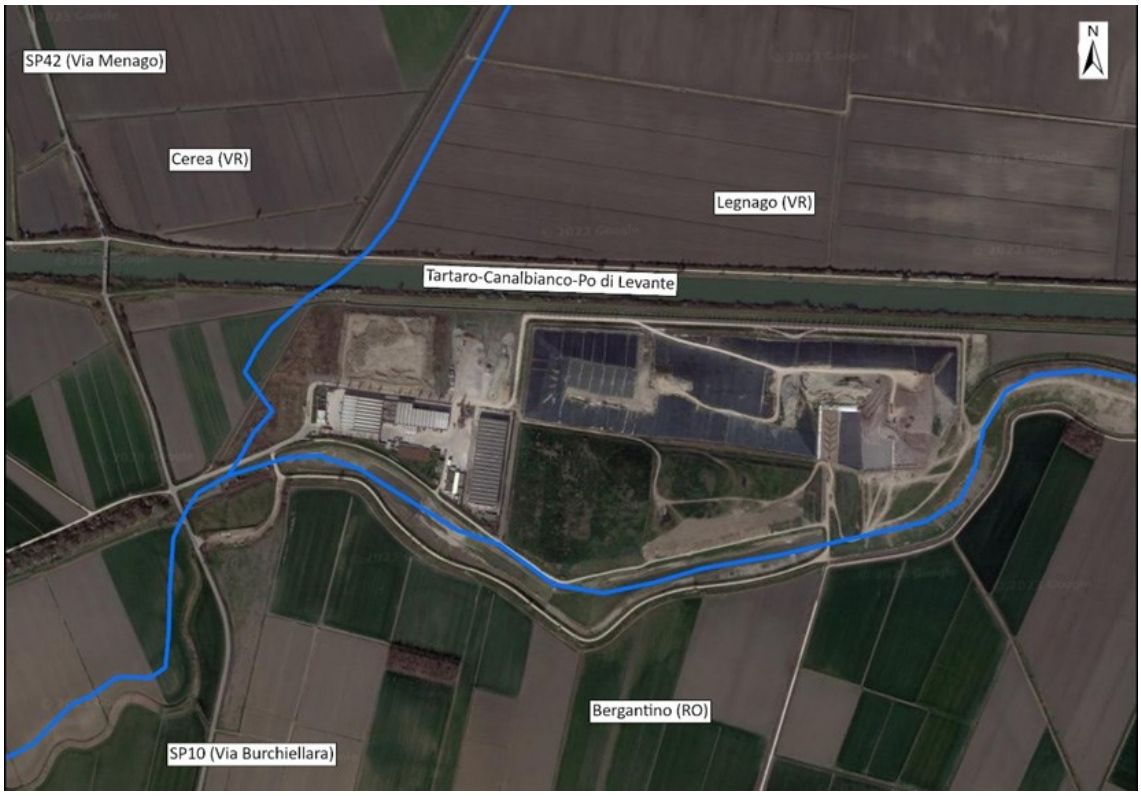

Figure 2.5 *Aerial view of the landfill site (Google Earth, 2023)*

From 1982 to 1990, the 1st riverbed section was cultivated while from 1990 to 1996 of the 2nd riverbed section has undergone the same process.

Figure 2.6 *Planimetry of the site (Google Earth, 2023)*

From 1996 to 1998, lot A was cultivated; from 1998 to 2002, lot B; from October 2002 to October 2010, lot C. Lots A, B, and C, visible in **Figure 2.6**, are above the riverbed in the form of above-ground embankments.

In August 2007, the Verona department of Veneto's Regional Agency for Environmental Prevention and Protection ("ARPAV, Agenzia Regionale per la Prevenzione e Protezione Ambientale del Veneto"), detected ongoing contamination in groundwater in the "first riverbed section" sector. Following this event, procedures were initiated to assess the actual state of contamination of the site, while the Municipality of Legnago, the landfill's owner, initiated the procedure for obtaining an opinion of environmental compatibility, project approval, and the issuance of the Integrated Environmental Authorization ("AIA, Autorizzazione Integrata Ambientale") for the intervention of environmental restoration of the first riverbed section, with simultaneous expansion of the landfill operation. Accordingly, with the project of 2009, the landfill expansion consisted of the construction of lots D, E, and F.

To date, the authorization in effect is the "Decree of the Director of the Land Protection and Development Area" dated March 31, 2020. Nowadays, the mechanical sorting plant at the landfill is intended to separate the dry fraction of MSW from upstream using the MSW as is. On the other hand, the composting facility receives the organic fraction, obtained following mechanical separation or even from external plants, for the production of "landfill biostabilized" material that can be used as daily cover.

In addition, along the western boundary of the landfill is the service area, which contains offices, warehouses, workshop, and a series of plant equipment, also visible in **Figure 2.6**. More specifically, these are:

- Biogas plant: the biogas plant configuration can currently be divided between "reclamation" equipment, consisting of the extraction fans and the biogas thermodestruction flare, and energy recovery equipment, consisting of a cogeneration plant;
- Leachate plant: leachate generated from the landfill is sent to the existing storage tanks, and consequently pretreated in a reverse osmosis and in situ distillation purification plant. The permeate is discharged into the Fosso Val di Zona, while the concentrate is sent to an evaporator/distiller that produces a

"superconcentrate", containing almost all contaminants, sent for disposal at an approved external facility;

- Sorting and composting plants;
- Rainwater treatment plant, with discharge into the Fosso Val di Zona;
- Sheds, dedicated to warehouse and mechanical workshop;
- Office building and janitor;
- Technological equipment such as weighbridges, well for drawing groundwater to be used as industrial water and to be sent to potable water plant for sanitation, etc.

Figure 2.7 and **Figure 2.8** show the landfill area in its current state.

Figure 2.7 *Aerial view of the landfill site at the actual state, view from West*

Figure 2.8 *Aerial view of the landfill site at the actual state, view from South-East*

2.3.1 Geological and geotechnical aspects

The area is flat and located in the southernmost part of the Veronese Plain, with elevations ranging from 7-8 m a.s.l. at the plant area to 13-14 m a.s.l. toward the south.

From a lithological standpoint, the subsoil is composed of alternating levels of medium and fine sands, clays, and silts, with the presence of coarser sediments identified only locally; these lithological characteristics have a direct impact on the local hydrogeological setting, which is defined by the presence of a series of overlapping aquifers separated by levels of deposits with low or no permeability.

On the surface there are almost exclusively deposits of locally peaty silty-clay lithology which, due to their characteristics of low permeability, limit the direct infiltration of precipitation water into the subsoil, thus favouring its stagnation or runoff into the drainage network; on a local scale, in fact, following the reclamation and hydraulic regulation interventions carried out, the hydrographic system consists of a set of natural and artificial watercourses.

The site has previously undergone remediation, expansion, and remodelling, all of which required detailed geognostic investigations. In particular, for the project of 2009, an extensive survey campaign was conducted, which, combined with information derived from previously consulted studies, allowed the following local lithostratigraphic setting to be reconstructed from top to bottom:

- **Agricultural topsoil**: weakly sandy clayey loam with plant fragments. Present from ground level to about 0.5 m depth;
- **Silty clayey unit I**: clayey silt transitioning to clay with silt with local presence of shell fragments and local centimetre-thick peaty levels. Levels of silt with sand are also present. Present up to about 3.2 m depth from ground level, with thickness appearing to be gradually decreasing from west to east;
- **Sandy unit I**: weakly silty to silty fine sand of grey colour. The unit is characterized by a substantial homogeneity of the grain size of the deposits and has an average thickness of about 7.5 m and reaches a depth of about 11 m from ground level;
- **Silty clayey unit II**: clayey and locally weakly sandy grey silt with local transitions to weakly sandy silty clay with grey-black peaty levels. The unit is about 1 m to 2 m thick;

- **Sandy unit II**: fine silty sand, transitioning locally to fine sand with silt, dark grey in colour. The unit varies in thickness from about 5.6 m to 12 m, reaching up to the depth of about 28 m from ground level;
- **Alternations unit**: sandy clayey silt transitioning to predominantly silty clay with interbedded levels of locally silty fine sand, with a total thickness of about 38 m; locally, levels of peaty clay have been observed.

Furthermore, in situ and laboratory geotechnical investigations were primarily aimed at verifying the stratigraphic characteristics of the landfill foundation soils and determining geotechnical parameters relevant to project work verifications. Consistent with the subsurface geological model, the results of the investigations and consultation of previous studies allowed for the identification of a stratigraphic alternation at the depth of interest. **Figure 2.9** shows a schematic representation of the stratigraphic succession for the first 20 m depth from ground level.

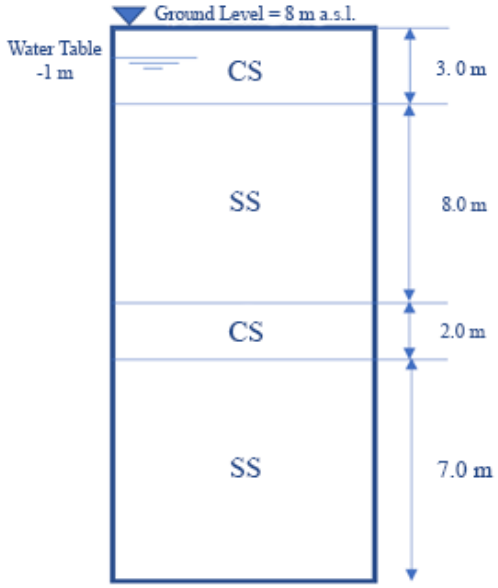

Figure 2.9 *Subsoil geotechnical model (CS = Clayey silty unit, SS = Sandy unit, with local presence of silty or clay)*

Table 2.1 shows the relevant geotechnical parameters for the identified stratigraphic units.

Table 2.1 *Geotechnical characterization of subsoil in the area*

Formation	$\gamma\ (kN/m^3)$	$c'\ (kPa)$	$\phi'\ (°)$	$c_u\ (kPa)$	$k\ (m/s)$
CS	18.0	17.0	25	90	$5*10^{-9}$
SS	19.0		38		$1*10^{-5}$

The issue of liquefaction was also addressed as part of the geotechnical verifications, as the SS formation possesses grain size characteristics that indicate a susceptibility to liquefaction. As a result, a very advanced study was conducted on the possibility that such coarser formations could liquefy in the event of a seismic event, with positive results in terms of liquefaction stability verification.

3 BIOGAS IN LANDFILLS

Biogas is of primary interest to this thesis, being the main component that is going to be taken into consideration when analysing the biogas drainage layer in the following chapters. It is important to correctly treat this gas because it is not just a problem in terms of landfill design, but it can become an efficient source of energy if properly collected and treated.

3.1 BIOGAS CHARACTERISTICS

3.1.1 Composition

By definition, landfill gas (LFG) is a gas that is generated in landfills under anaerobic conditions. It does not have a unique composition, although the two primary substances are carbon dioxide (CO_2) and methane (CH_4). Gas from landfills generally comprises between 40% and 60% carbon dioxide and between 45% and 60% methane by volume (ATSDR, 2001). Non-methane organic compounds (NMOCs), such as trichloroethylene, benzene, and vinyl chloride, are also found in limited quantities in landfill gas, along with nitrogen, oxygen, ammonia, sulphides, hydrogen, and carbon monoxide. The primary elements of landfill biogas are presented in **Table 3.1**.

Table 3.1 *Typical Landfill Gas Components (Tchobanoglous et al., 1993)*

COMPONENT	*% BY VOLUME*	*CHARACTERISTICS*
Methane	45 – 60	Naturally occurring gas. Colourless and odourless.
Carbon dioxide	40 – 60	Naturally found at small concentrations in the atmosphere (0.03%). Colourless, odourless, and slightly acidic.
Nitrogen	2 – 5	Comprises approximately 79% of the atmosphere. Odourless, tasteless, and colourless.
Oxygen	0.1 – 1	Comprises approximately 21% of the atmosphere. Odourless, tasteless, and colourless.
Ammonia	0.1 – 1	Colourless gas with a pungent odour.
NMOCs	0.01 – 0.6	May occur naturally or be formed by synthetic chemical processes.
Sulphides	0 – 1	Naturally occurring gases that give the landfill gas mixture its rotten-egg smell. Can cause unpleasant odours even at low concentrations.

Hydrogen	0 – 0.2	Odourless, colourless gas.
Carbon monoxide	0 – 0.2	Odourless, colourless gas.

It is very important to underline that LFG contains hundreds of trace constituents, some of which are organic (halogenated hydrocarbons) and some of which are inorganic (hydrogen sulphide, ammonia). Some of these gases are naturally produced in landfills, while others are anthropogenic. In particular, some components are considered greenhouse gases, therefore it is good practice to try to capture them effectively to avoid their dispersion in the atmosphere and minimize the potential risks.

3.1.2 Phases of bacterial decomposition

Chemical reactions as well as volatilization are two processes that can generate biogas in a landfill. However, the main process that produces biogas is bacterial decomposition, which occurs when bacteria naturally found in organic waste and soil used to cover the landfill break down the waste molecules. Landfill waste decomposes through four phases, with the quantity and quality of gas produced that variate within each phase.
Briefly, the four stages of decomposition are the following:

1. **Phase I**: the vast molecular chains of complex carbohydrates, proteins, and lipids that make up organic waste are broken down by aerobic bacteria, which can only exist in the presence of oxygen. Carbon dioxide is the main output of this process. This phase's nitrogen level is considerable at first, but it gradually decreases as the landfill goes through the other three stages. Phase I continues until there is no more oxygen left. Depending on the amount of oxygen present when waste is dumped, this type of decomposition may take days or months to complete.
2. **Phase II**: this phase begins once the landfill's oxygen supply has been depleted. Bacteria transform substances generated during Phase I into acetic, lactic, and formic acids as well as alcohols like methanol and ethanol through an anaerobic process, turning the landfill significantly acidic. As the acids and moisture in waste combine, they break down some nutrients and make nitrogen and phosphorus available to the landfill's numerous bacterial species. Carbon dioxide and hydrogen are the gases produced as byproducts of these processes.

3. **Phase III**: in this stage, phase II organic acids created by specific anaerobic bacteria are consumed to create acetate, an organic acid. The landfill turns into a more neutral environment, where methane-producing bacteria can flourish. Bacteria that produce both methane and acid work in cooperation with one another. Acid-producing bacteria produce chemicals that can be then consumed by methanogenic bacteria, like carbon dioxide and acetate.
4. **Phase IV**: This phase starts when the content and production rates of landfill gas stay mostly unchanged. Phase IV landfill gas is typically consisting of between 45% and 60% methane by volume, 40% to 60% carbon dioxide, and other gases. Gas is produced at a consistent rate, typically for around 20 years. In some cases, the gas generation could also last longer than 50 years.

In **Figure 3.1**, the four main phases are visible.

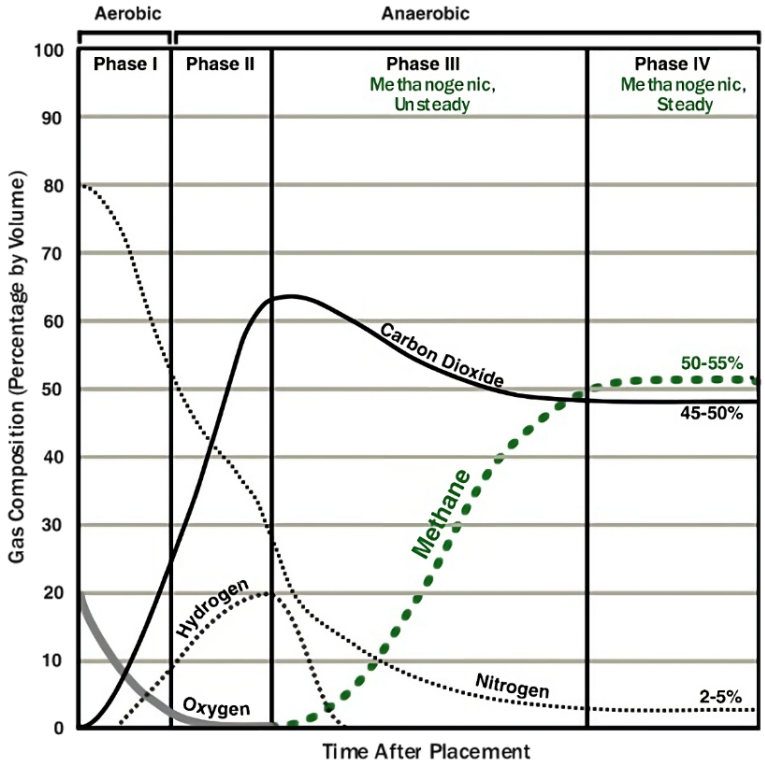

Figure 3.1 *The four phases of landfill gas generation (EPA, 2021)*

3.1.3 Main variables affecting biogas production

According to Ünvar et al. (2018), the most important factors affecting the production of biogas are essentially five:

1. **Temperature**: at extremely high and extremely low temperature values, methanogenic bacteria are not active. Thus, the rate of biogas production is influenced by the temperature of the reactor where it will occur. The ideal temperature range is typically 30-35 °C. There are three different temperature zones during anaerobic fermentation depending on the type of waste materials, the pH of the area, and the microorganisms formed. These zones are psychrophilic (3-20 °C), mesophilic (20-40 °C), and thermophilic (40-70 °C). The most suitable temperature zone for biogas production is the mesophilic fermentation zone.

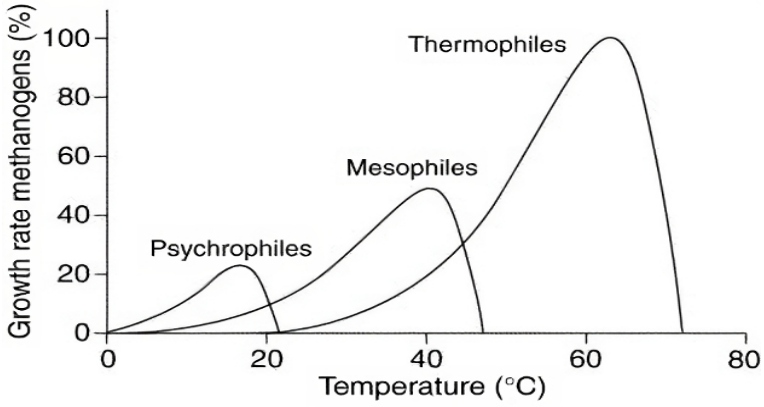

Figure 3.2 *Relation between temperature and growth rate of methanogens (Ünvar et al., 2018)*

2. **C/N Ratio**: nitrogen and carbon are both required to produce biogas, as well as for the growth and development of aerobic bacteria. The C/N ratio should be between 10/1 and 23/1. For the production of biogas, a C/N ratio of 25-30 is ideal.
3. **Distribution of the organic matter**: the mixing process must be carried out to ensure the even distribution of the solids and to make it easier for the created gas to be discharged. It enables uniform bacterial interaction with the organic materials. As a result, gas production rises by 10-15% on average. Other benefits include arranging the bacterial population density in the slurry and balancing the temperature fluctuation of the waste.
4. **Different pH**: the ideal pH range for biogas production in anaerobic environments is 6.6 - 7.6. It has toxic effects on methane bacteria when it goes below 6.2 and has a significant negative impact on gas production efficiency when it drops below 5.0.
5. **Waiting time**: The amount of time the wastes are left in the generator (the landfill in this case) is referred to as the waiting time. The duration of storage affects the

rates of reproduction of the bacteria that decompose organic materials and cause gas levels to increase.

3.2 LANDFILL GAS MIGRATION

In practically all landfills, the created LFG should be extracted and used. However, the extraction is hardly ever completely successful. In many landfills worldwide, the LFG is still not removed and reused. As a result, there is a possibility of off-site gas migration through nearby soil strata. **Figure 3.3** depicts the possible outcomes of emitting and migrating LFG related to several scales. The effects, as depicted in the picture, might be local (less than 1 km radius), regional (1–10 km), and global. The consequences could also be very different from one another.

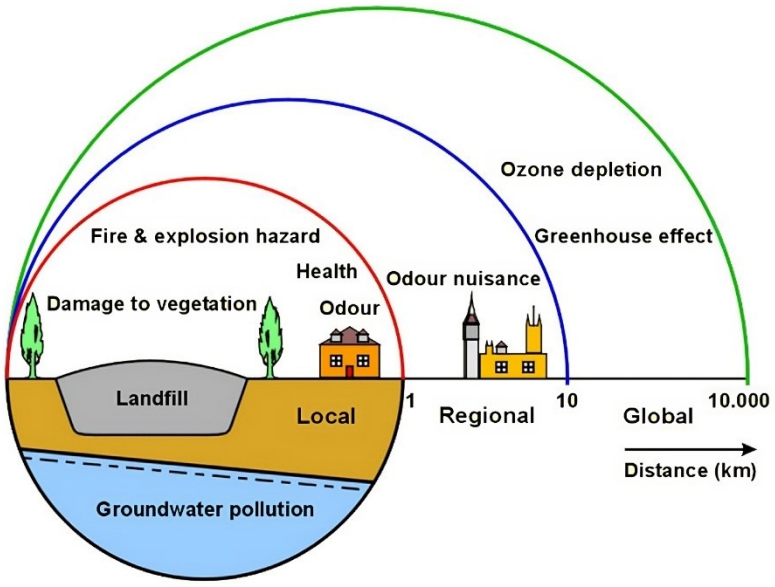

Figure 3.3 The different scales of LFG effects (Kjeldsen, 2018)

A study performed by Nastev et al. (2001) on landfill gas emissions highlighted how the main mass transport mechanisms of the gas in a landfill are advection in the liquid phase and advection and diffusion in the gas phase. On the other hand, heat transport occurs by means of conduction through solid material and fluid flow. The first issue, concerning the advection of gas into liquid phase, will not be assessed due to the fact that the liquid leachate is removed using the leachate collection system. Since the objective of this thesis is to address the design of the biogas collection layer, this issue won't be treated.

3.2.1 Advection in the gas phase

The advective flux of a gas constituent through a porous medium refers to the transport of the gas due to fluid flow through the interconnected void spaces within the medium. This process is governed by several factors, in which the most relevant are the pressure gradient and the permeability of the medium. When there is a pressure gradient present in the fluid, it causes it to move from regions of high pressure to regions of low pressure. This bulk fluid flow carries the gas constituent along with it, leading to the transport of the gas through the porous medium.

If the fluid considered is water, advection can be effectively described by Darcy's law in the following form:

$$Q = -\frac{k \cdot A}{\mu} \cdot \frac{dp}{dx} \qquad 3.1$$

where Q $[m^3/s]$ is the flow rate, k $[m/s]$ is the water permeability of the porous medium, A $[m^2]$ is the cross-sectional area, μ $[Pa \cdot s]$ is the dynamic viscosity of the fluid, and dp/dx is the pressure gradient that guides the flow. The LFG produced inside of the landfill or abrupt changes in the barometric pressure can both contribute to the pressure gradient's build-up.

However, *3.1* is valid for water flow and not gas flow, so a proper modification of this equation to adapt it to the biogas case should be carried out, and this issue will be discussed later in Chapter 4.

3.2.2 Diffusion in the gas phase

The transport of gas constituents through a porous medium driven by concentration gradients is referred to as diffusional fluxes. When gas concentrations vary within the medium, diffusion becomes an important mechanism for gas movement between different regions. Diffusion is the movement of gas molecules from a high concentration area to a low concentration area. This movement is caused by random molecular motion and is intended to balance the concentration distribution.

The Fick's first law for diffusion can be written as:

$$J = -D_0 \cdot \frac{dC}{dx} \qquad 3.2$$

where $J\ [g/m^2 \cdot s]$ is the diffusion flux, $D_0\ [m^2/s]$ is the diffusivity of the gas, and dC/dx is the concentration gradient. However, since the flux of gas in the soil fluctuates over time and does not occur under steady-state conditions, the processes that take place in the soil are more complicated than those that are taken into account by Fick's first law. It is important to define the diffusivity D_0, because this parameter is measured for the diffusion of a gas which is free to move, thus not taking into account the eventual presence of a porous media. For this reason, in presence of a porous media such as the BCL, gas diffusivity can be defined as (Neira et al., 2015):

$$D_P = D_0 \tau \varepsilon \tag{3.3}$$

with D_0 defined previously as the gas diffusivity in the air, corrected with two factors τ and ε. In particular, τ is the tortuosity of the soil (dimensionless), while ε is the soil air-filled porosity (ratio m^3 air / m^3 soil) and is mostly controlled by the total porosity and the water-filled porosity, which depend on the type of soil, the amount of organic matter, and management.

For many years, diffusional fluxes have been considered the most significant transport process for gas migration and emission. However, it has become clear in more recent years that advective processes can drive much higher gas fluxes from the waste, particularly if permeable soils have been used or there are areas that are poorly covered (Kjeldsen, 2018).

3.3 LANDFILL GAS COLLECTION SYSTEM

As stated previously in Chapter 3.2, the correct management of biogas produced in a landfill is vital to avoid different problems that may arise, both internally in the landfill (such as its stability and efficiency) and externally due to the release of greenhouse gases in the atmosphere. For this reason, every modern landfill should possess an effective biogas collection system capable to collect and, when possible, reuse the biogas.

Typically, a gas collection system is formed by the elements visible in **Figure 3.4**. The main constituents of this system are:

- Vertical extraction wells
- Horizontal collectors/trenches
- Superficial biogas collection layer

- Network of interconnected pipes
- Condensate management elements
- Flare systems
- Monitoring systems

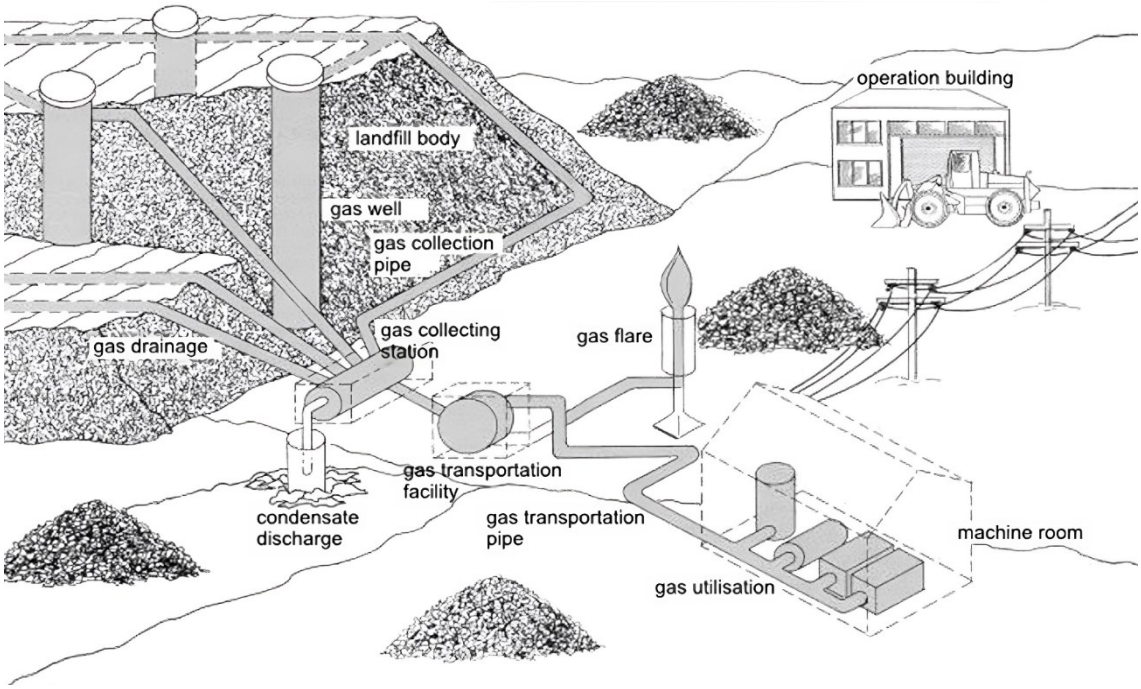

Figure 3.4 *Overview of a proper biogas collection system (Rettenberger, 2018)*

It is important to know that the biogas collection can be either active or passive. Using an active system, the gas is collected from the landfill using blowers, which typically provide vacuum pressures in the landfill body. On the other hand, under semi controlled conditions, passive gas collection systems use the positive pressure in the landfill body to transfer the gas out of the waste. A network of interconnected pipes is required to transport all the extracted gas to the different elements of the system.

3.3.1 Vertical extraction wells

The vertical extraction wells are the most typical method for recovering LFG. They are often installed in disposal areas that are already in operation. These wells can be coupled with vacuum pumps to extract the gas by creating a negative pressure (active system). It is important that gas wells are gastight against air intrusion, especially at the wellhead and the upper part of the well, so that air is not drawn in through the surface of the landfill. Wells drilled inside the waste typically reach a depth of 75% of the refuse.

The construction process often involves utilizing an auger to bore into the landfill. With a PVC or HDPE casing, the diameter varies, ranging commonly between 60 cm and 120 cm. The openings, which might be slots or holes, should be big enough to prevent clogging but less than the diameter of the gravel used to fill the well's surrounding area. A bentonite seal on top stops air infiltration.

Moreover, the wellhead includes a flow control valve, gas sampling port, pressure monitoring port, and optionally flow monitoring ports and thermometers. In **Figure 3.5**, a classic extraction well can be observed.

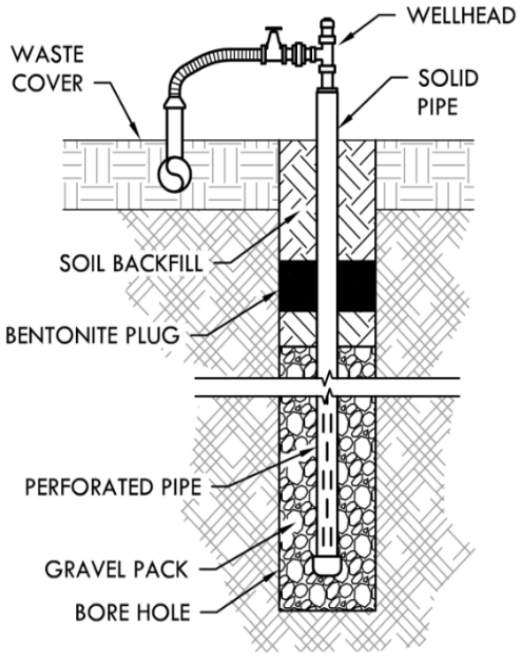

Figure 3.5 *Typical vertical gas extraction well (EPA, 2021)*

3.3.2 Horizontal collectors/trenches

Particularly in deeper landfills and in areas of active filling, horizontal piping laid in trenches in the waste may be an efficient way to extract biogas. They frequently work in conjunction with vertical wells. Due to the fact that these horizontal pipes are positioned at or below a layer of waste, they might not significantly affect landfill operations as much as vertical wells would.

Usually made of PVC or HDPE, horizontal collectors can be built using common earthmoving tools, but they are generally built like the vertical wells (**Figure 3.6**). They

can be positioned and covered with a permeable material, or they can be positioned in trenches, requiring excavation.

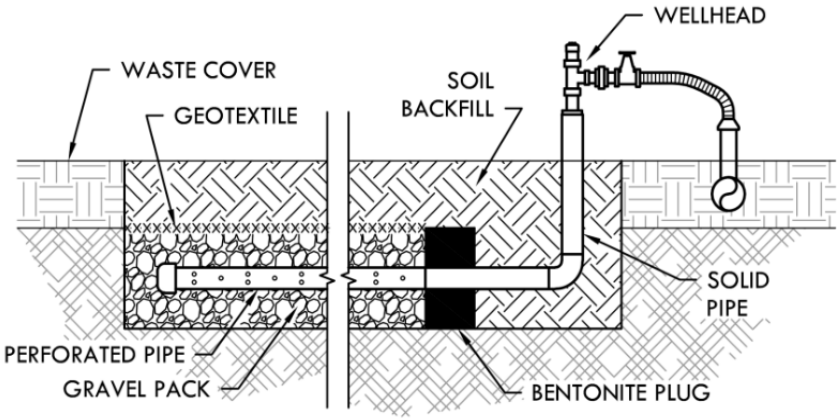

Figure 3.6 *Typical horizontal gas extraction pipe (EPA, 2021)*

3.3.3 Biogas collection layer

Main protagonist of this work, the gas collection layer is a layer whose specific function is to convey all the biogas to the extraction wells or pipes. This transmission of biogas to the pipes happens because of the homogenization of the media provided by this solution. It must have certain important characteristics, one of which is the right permeability. Further considerations on its requirements and design elements will be widely discussed in following chapters.

3.3.4 Network of interconnected pipes

The network is made up of artifacts and pipes that connect the landfill's intake points to the intake unit. The network configuration is determined by site characteristics, design choices, and economic factors. Furthermore, to reduce the effects of settling, it is necessary to minimize landfill crossings as much as possible and to locate the majority of the network on surrounding land. Appropriate substations are typically provided to collect biogas from wellheads and transport it in a single line to the suction plant.

3.3.5 Condensate management elements

Warm gas from the landfill cools as it passes through the GCS, forming condensate (water). Condensate can clog pipes and interfere with the LFG recovery process if it is not removed. Typically, traps enable condensate removal by gravity, meanwhile sumps collect it.

3.3.6 Flare systems

A flare is a device used to ignite and burn the biogas extracted from the waste. Flares are required to regulate LFG emissions while the energy recovery system is starting up and shutting down, as well as to manage situations in which more gas than the energy conversion equipment can handle is produced. Usually, flaring turns out to be the final stage for most plants geared only toward environmental remediation. A flare is also a cheap technique to progressively expand an operating landfill's electricity-producing system's capacity. The flare is used to manage extra gas and stop methane from leaking into the atmosphere when more waste is disposed of in the landfill (i.e., during the enlargement of the waste refuse).

In the flaring process, methane from biogas is burned in combustion to produce steam, carbon dioxide, sulphur oxides, and nitrogen oxides, with oxygen from the air acting as an oxidizer.

There are three main methods of flaring (**Figure 3.7**):

- **Static flares**: used in situations where forced biogas extraction and consequently centralized treatment are not feasible, static flares are placed directly on top of wells. However, to prevent open flames in the landfill area, it is preferable to install automatic extraction and combustion systems when it is feasible.
- **Open-flame flares**: the basic components of an open-flame flare are a burner mounted on top of a support structure with a small windbreak for protection, a pilot with an igniter, and a thermal flame detection system. Open-flame combustion results often in a difficult to control combustion temperature and a generally partial mixing of biogas with the air needed for combustion. Such flares hardly meet the necessary emission standards and, as a result, they are no longer widely used.
- **High-temperature flares**: these kinds of flares are, on the other hand, characterised by a large combustion chamber internally lined with refractory insulation and are equipped with a main and a secondary burner. They are designed to achieve high combustion efficiency and consequently very low emission values. The construction of this type of combustor allows biogas to be burned at high temperatures due to the presence of refractory material.

Figure 3.7 *Static flares (left) and high-temperature flare (CONVECO SRL, 2022)*

3.3.7 Monitoring systems

The LFG collection system needs to be permanently adjusted due to shifting conditions in the landfill body, changes in atmospheric pressure, rising landfill height and age, and shifting operational modes. Monitoring systems that operate automatically might be useful to control all the different factors that regulate the efficiency of the gas extraction. This includes monitoring gas collection rates, gas quality, system pressure, and other relevant parameters. Moreover, regular maintenance activities are needed, such as inspecting and repairing gas wells, pipes, and other components, as well as optimizing the gas extraction equipment for maximum efficiency.

3.4 UTILIZATION OF THE EXTRACTED BIOGAS

Before the input into the energy market of the extracted gas, it must be necessarily treated to meet specific requirements. Principally, LFG must be treated in energy recovery systems to get rid of extra moisture, particles, and contaminants. Treatment is based on the energy recovery system and site-specific factors. While gas turbines and microturbines could need siloxane and hydrogen sulfide removal, boilers and internal combustion engines only need minimum treatment. The price of gas purification depends mostly on the required degree of purity, with filtration systems being less expensive than systems that remove impurities like siloxane and sulfur.

Energy production is for sure the main application of the extracted gas, but it's not the only one (**Figure 3.8**). So, the main options are:

- **Energy Production**: to produce electricity and heat, biogas can be used as fuel in a gas engine or a gas turbine. The generated electricity can be transferred to the grid for wider distribution or used locally to power the waste treatment facility. The heat produced by combustion can be used for a variety of applications, such as industrial processes, water heating, and space heating.
- **Cogeneration or Combined Heat and Power (CHP)**: biogas can be used in cogeneration systems, where both electricity and heat are produced simultaneously. Cogeneration maximizes the energy efficiency of the biogas by utilizing the waste heat generated during the electricity generation process. This waste heat can be utilized for district heating, industrial processes, or other heating applications, further enhancing the overall energy efficiency of the system.
- **Biofuel Production**: biomethane can be created by upgrading and processing existing biogas to remove impurities, particularly carbon dioxide. A purified version of biogas with characteristics resembling those of natural gas is called biomethane. It can take the place of traditional fossil fuels as a renewable fuel for transportation. For greater distribution and use, biomethane can be injected into the natural gas grid or compressed and stored in the natural gas vehicle tanks.
- **Cooking and Heating**: biogas can be used for cooking and heating in homes and communities in places with limited access to clean cooking fuels. Similar to other gaseous fuels like LPG[4], biogas can be distributed in cylinders or through a network of pipelines. By replacing traditional fuels like wood, charcoal, or kerosene with biogas for cooking and heating, indoor air pollution and deforestation may be reduced.
- **Industrial Processes**: different industrial processes that call for heat or fuel can make use of biogas. It can be applied to any process that needs thermal energy, including the production of steam, but also in kilns, and boilers. It can be a good opportunity for industries to lessen their impact on the environment and emissions of greenhouse gases.

[4] Liquefied petroleum gas.

- **Agriculture and Farm Applications**: agricultural settings can use biogas for a variety of purposes. It can be used to heat greenhouses, power irrigation systems, and produce electricity for on-farm operations. It can also be used to heat livestock housing. Together with manure or agricultural waste, biogas can be used for anaerobic digestion to create a closed-loop waste management system and a renewable energy source.

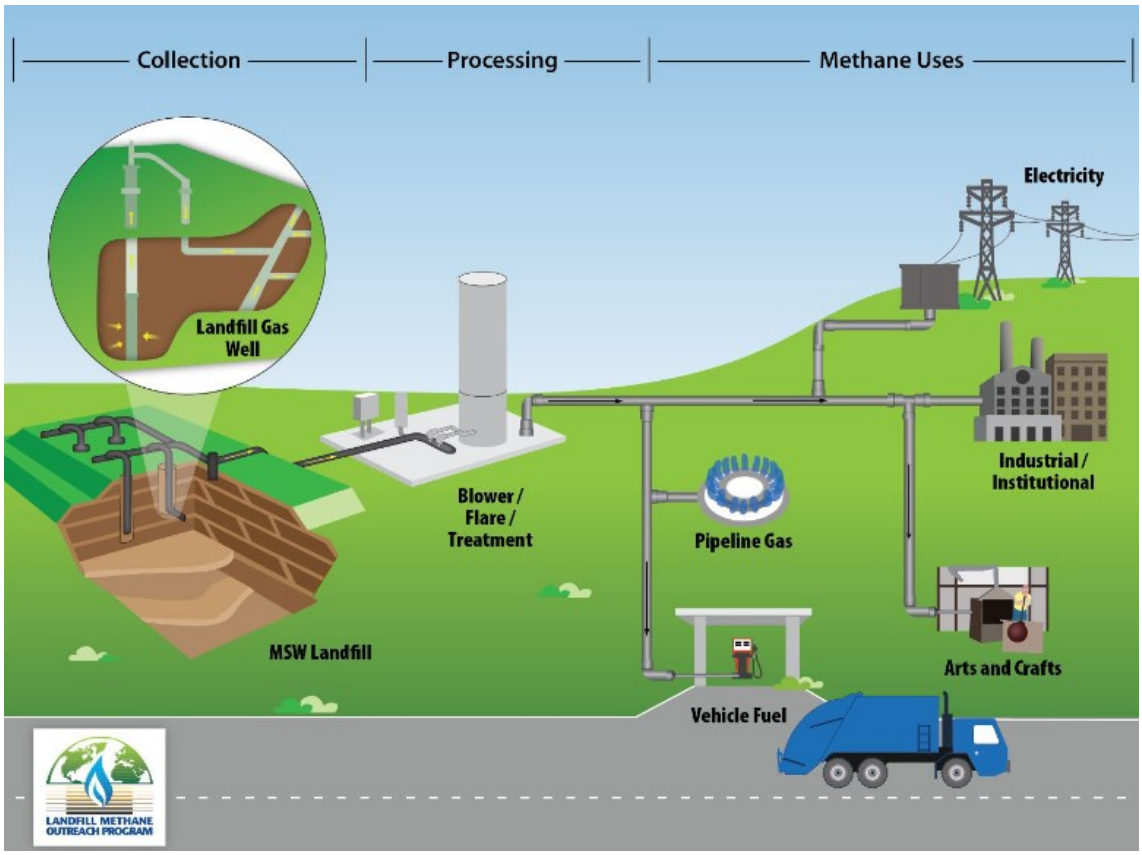

Figure 3.8 *Main applications of biogas (EPA, 2021)*

4 GAS COLLECTION LAYER DESIGN

In the top cover, laying directly above the base layer, the biogas collection layer is responsible for the gas transport through the porous media to the collection pipes. As it can be addressed from the Italian regulations reported in Chapter 2.2, the only limit imposed by the directive is that the gas collection layer of a landfill should have a thickness greater than 0.5 m, made of materials that guarantee a suitable transmissivity and gas permeability. The real problem lies right here: it is crucial to understand which value of transmissivity and permeability can be considered suitable. Only after the definition of a proper permeability it will be possible to understand if a certain material could be appropriate to be applied as granular filter.

The procedure to determine these parameters will be based mainly on the work carried out by Thiel (1998). The process that is presented consists in three principal steps:

1. Estimation of the maximum biogas flux in the landfill;
2. Slope stability analysis and FoS[5] definition;
3. Design of a passive vent system.

Then, when these steps are completed, the design hydraulic conductivity may be defined.

4.1 ESTIMATION OF MAXIMUM BIOGAS FLUX

The first important step in designing a biogas collection layer (BCL) is to assess the biogas production in the underlying waste mass. The maximum production of biogas will be later used to calculate the maximum biogas flux, essential in the design of the collection layer. Nowadays, various models to predict the yield of biogas have been presented. Depending on the exact landfill circumstances and data availability, each model has different strengths, limits, and applicability. The accuracy of biogas production assessments can be improved by combining numerous models or employing calibrated models based on site-specific data. However, to be considered reliable, a proper prediction model should include three submodels (Andreottola et al., 2018):

- **Stoichiometric**: this model delivers the highest theoretical yield of biogas from the organic waste fraction that will anaerobically decompose in a landfill. Some

[5]Factor of Safety.

models proposed in the literature are merely stoichiometric and provide only information on LFG yields as a result.

- **Kinetic**: this is a dynamic model that shows the time evolution of LFG generation rates. It can be an empiric model, which is based on a more or less simple equation of a defined order, a deterministic model, which is based on a set of equations describing the degradation of the various biodegradable MSW fractions, or an ecological model, which describes the dynamic of microbial populations and substrates within the landfill.
- **Diffusion**: this is a dynamic model that represents the variation of pressure, temperature, and gas composition within the landfill body across time and space. LFG emission rates may be determined, and the efficiency of the gas extraction system can be demonstrated.

All models consider as a primary factor the composition of the waste, related to the various fractions present (**Table 4.1**). So, the assessment of the type of waste and all its components is fundamental to guarantee a correct estimation of the biogas production.

__Table 4.1__ Typical composition of MSW organic fractions (Tchobanoglous et al., 1993)

	Wet Weight (%)	**Dry Weight (%)**	**Elemental Composition (%)**					
Component			**C**	**H**	**O**	**N**	**S**	**Ash**
Food wastes	11.4	4.6	4.7	4.7	4.4	13.0	10.0	4.0
Paper	42.8	55.0	50.8	53.0	61.3	18.5	60.0	55.2
Cardboard	7.5	9.8	9.2	9.4	11.1	3.7	10.0	8.0
Plastics	8.8	11.9	15.1	13.8	6.8	-	-	19.8
Textiles	2.5	3.1	3.6	3.3	2.4	14.8	-	1.4
Rubber	0.6	0.9	1.4	1.4	-	1.9	-	1.4
Leather	0.6	0.7	0.9	0.8	0.2	7.4	-	1.1
Yard wastes	23.3	11.2	11.4	10.8	10.8	40.7	20.0	8.3
Wood	2.5	2.8	2.9	2.8	3.0	-	-	0.6
Total	100	100	100	100	100	100	100	100

Nowadays, some of the most applied models include:

- **First-order Decay Model**: simple model used for the degradation of organic waste in landfills that assumes a first-order decay process. It calculates biogas generation based on the initial organic content of the waste, the waste's age or time since disposal, and a decay constant that represents the rate of organic waste decomposition. Although the model provides a quick estimate, it may oversimplify the complex processes that occur in landfills.
- **LandGEM**: the Landfill Gas Emissions Model (LandGEM) is a well-known software tool created by the United States Environmental Protection Agency (EPA). It estimates biogas generation and emission rates using site-specific data such as waste characteristics, climate, and landfill design. LandGEM takes into account both aerobic and anaerobic degradation processes, providing a more comprehensive assessment of biogas production.
- **FOD**: the FOD model, developed by the Intergovernmental Panel on Climate Change (IPCC), is one of the best methods for estimating methane generation in a landfill. Originally, the FOD model was created to quantify methane emissions from all landfills in a country in conjunction with national GHG inventories. It considers the evolution of LFG generation over time using first-order kinetics, estimating methane generation using waste compounds' biodegradable carbon content.

These are only a few of the large number of models developed, and the choice of one over another depends on various site-specific factors that need to be taken into consideration. The accuracy of biogas production assessments can be improved by combining multiple models or using calibrated models based on site-specific data. On-site monitoring and measurements of biogas production, however, are critical to guaranteeing a correct modeling approach. Field-scale data collection provides real-time and site-specific information for biogas production estimation, such as gas collection rates, gas composition analysis, and waste characterization. These data can be used to validate and improve model predictions.

4.1.1 Site specific flux estimation

For a clearer and more understandable procedure, the data from the case study of Torretta di Legnago landfill, presented in Chapter 2.3 will be taken into account.

The estimated maximum flow, referred to the theoretical biogas production, is shown in **Table 4.2** and **Figure 4.1**. The model used for the estimation of biogas production is, in this case, constructed specifically for this situation and does not refer to any classic literature model.

Table 4.2 *Estimated biogas production data for the Legnago site*

Year	*Theoretical Production (m^3/h)*	*Catchable (m^3/h)*	*Year*	*Theoretical Production (m^3/h)*	*Catchable (m^3/h)*	*Year*	*Theoretical Production (m^3/h)*	*Catchable (m^3/h)*
2010	4	2	2028	314	188	2046	169	101
2011	21	9	2029	335	201	2047	160	96
2012	50	23	2030	353	212	2048	152	91
2013	67	30	**2031**	**391**	**235**	2049	145	87
2014	88	40	2032	384	230	2050	139	83
2015	121	54	2033	378	227	2051	86	60
2016	149	67	2034	353	212	2052	82	57
2017	175	79	2035	328	197	2053	78	55
2018	199	119	2036	307	184	2054	75	53
2019	239	143	2037	286	172	2055	72	50
2020	239	143	2038	269	161	2056	68	48
2021	239	143	2039	252	151	2057	66	46
2022	227	136	2040	237	142	2058	63	44
2023	230	138	2041	224	134	2059	60	42
2024	249	149	2042	210	126	2060	58	41
2025	254	152	2043	198	119	2061	56	39
2026	266	160	2044	187	112	2062	55	39
2027	293	176	2045	179	107			

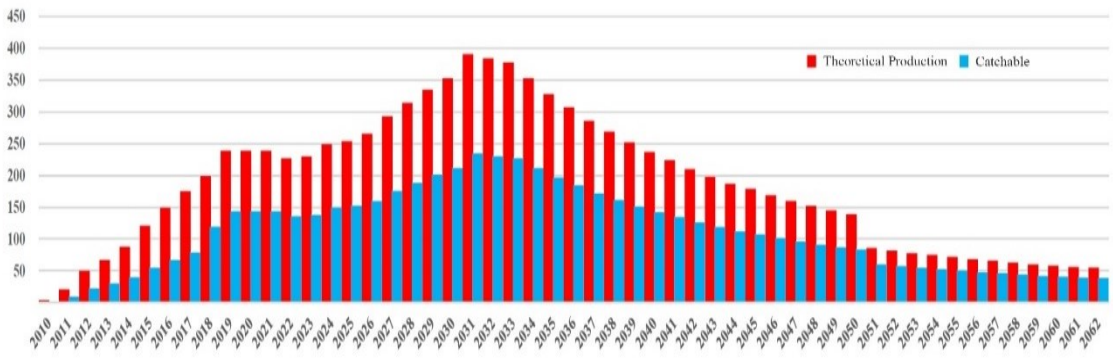

Figure 4.1 *Trend of biogas production for the Legnago site*

The maximum flow of biogas Q_b is expected in year 2031 and equal to 391 m^3/h, with a catchable flow of 235 m^3/h. Knowing the area of the surface in which the biogas propagation occurs, it's easy to calculate the maximum gas flux. Approximately, the area of the landfill totals 308200 m^2, thus the maximum flux is:

$$\Phi_b = \frac{Q_b}{A} = \frac{391\,m^3/h}{308200\,m^2} = 1.27 \cdot 10^{-6}\ \frac{m^3}{h \cdot m^2} \cdot \frac{1\,h}{3600\,s} = 3.52 \cdot 10^{-7}\,\frac{m^3}{s \cdot m^2} \quad 4.1$$

So, $3.52 \cdot 10^{-7}$ $m^3/m^2 \cdot s$ should be the value taken into account for the design of the BCL.
In addition, in his work, Thiel suggests an easy but effective way to calculate the maximum gas flux. Starting from literature values and adjusting them based on the observations in the United States' landfills, he calculated the gas generation rate:

$$r_g = 6.24 \cdot 10^{-3}\ \frac{m^3}{kg \cdot year} \quad 4.2$$

This rate indicates how much volume of biogas one kilogram of MSW is expected to produce in a year, at atmospheric pressure and ambient temperature. The assumption can be defined as highly precautionary, since it considers undifferentiated MSW with a high content of biodegradable organic fraction. The waste delivered to the Torretta di Legnago landfill, on the other hand, has a very low content of OFMSW[6], given the good quality of differentiated waste collection. For this reason, it is fair to say that the r_g in this specific case is definitely lower.
Using this parameter is possible to estimate the maximum flow rate per unit area q_b, that corresponds to the flux calculated above, using a simple equation:

$$q_b = r_g \cdot H_w \cdot \gamma_w \quad 4.3$$

where r_g is the above-mentioned gas generation rate, H_w the waste mass depth under the cover area, and γ_w the density of the waste.
Considering the case study under investigation, the waste mass has an average depth of 20 m, while the density can be considered equal to 800 kg/m^3. Thus, the flow rate is equal to:

[6] Organic Fraction of Municipal Solid Waste.

$$q_b = \Phi_b = 6.24 \cdot 10^{-3} \ \frac{m^3}{kg \cdot year} \cdot \frac{1\ year}{8760\ h} \cdot \frac{1\ h}{3600\ s} \cdot 20\ m \cdot 800 \frac{kg}{m^3}$$
$$= 3.16 \cdot 10^{-6} \frac{m^3}{s \cdot m^2} \qquad 4.4$$

The value obtained using this method is almost nine times greater than the value obtained in *4.1*. One of the main reasons is the already mentioned overestimation of the gas generation rate r_g. This could lead to an overestimation of the biogas produced and an oversizing of the extraction system. For this reason, for the design of the BCL, the value of $\Phi_b = 3.52 \cdot 10^{-7}\ m^3/s \cdot m^2$ will be used, in order to carry out more accurate calculations.

4.2 SLOPE STABILITY ANALYSIS

The study of slope stability assures the safety of landfill operations and the adjacent areas. In fact, landfills are frequently built on slopes to maximize space use, thus there is a possibility of slope failure without proper slope stability analysis. This is important to identify potential slope instability and adopt suitable mitigation measures to safeguard the safety of employees, infrastructure, and the surrounding environment.

However, this evaluation is central not only for landfills constructed on slopes, but for all landfill areas that present escarpments and inclinations of the top cover. In fact, the analysis carried out in this thesis is related to the Torretta di Legnago landfill, that lies above and below ground level, with slopes determined by the different gradients of the top covers and determined by the designers in the project phase.

The analysis allows to calculate the maximum permitted gas pressure that yields an acceptable overall static FoS. Gas pressure, in fact, constitutes a destabilizing effect on the stability of the top cover, acting as an uplifting force on the interface between the BCL and the non-woven geotextile or geomembrane that divide BCL and the superior hydraulic barrier (usually a compacted clay liner).

The purpose of this section is to understand how the biogas pressure will affect the overall stability of the capping, in order to obtain a FoS that can be considered safe.

4.2.1 Shear strength in presence of gas

To ensure a suitable permeability, BCL is, in most of the cases, formed by sand and granular coarse materials. This type of non-cohesive soils possesses a shear strength that is mainly due to frictional aspects, rather than mineralogy or over-consolidation ratio as it happens for clays. The main frictional factors include void ratio or relative density, particle shape and grain size distribution.

As Karl Terzaghi stated in 1936, the total principal stresses σ_1, σ_2, and σ_3 acting in a certain point can be used to calculate the stresses at each point in a section through a soil mass. The total principal stresses can be divided into two parts if the soil pores are filled with water at a pressure u, that acts in all directions with equal intensity in the water and solid phases and is known as neutral pressure. The differences $\sigma - u$, that can be called effective total stresses σ', represent an increase from the neutral pressure and are only found in the ground's solid phase. The effective principal stress will be defined as a fraction of the total principal stress. So:

$$\sigma' = \sigma - u \tag{4.5}$$

Moreover, Terzaghi added that any measurable effect of a stress state change, such as compression, distortion, or shear strength change, can only be attributed to changes in effective stresses.

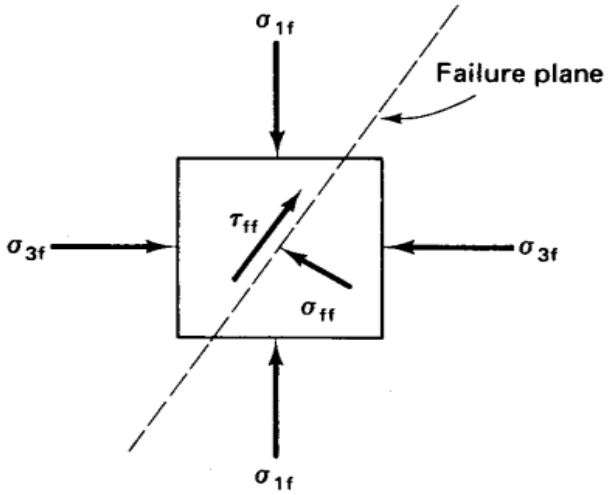

Figure 4.2 *Display of the forces acting on an element (Favaretti, 2022)*

As evident from *4.5*, an increase in water pressure leads to a decrease in effective stresses. This pressure, that is usually referred to water because of the most present fluid in soil,

could also be applied to gas. Gas is a fluid with different viscosities but the neutral pressure it induces in the soil can be assessed in the same way.

To address the shear strength of materials, the most widely used approach is the one proposed by Charles-Augustin de Coulomb and later refined by Christian Otto Mohr at the end of the 19th century, which affirms that materials fail when the shear stress on the failure plane reaches some unique function of the normal stress on that plane at the time of failure:

$$\tau_{ff} = f(\sigma_{ff}) \qquad 4.6$$

with τ_{ff} and σ_{ff} that represent shear stress and normal stress at failure. This theory takes as given the fact that a failure plane exists (**Figure 4.2**), but this assumption is most of the time true for elements like soil.

In particular, Mohr conducted various tests on the same specimen, using direct or triaxial shear tests, and plotting the results in the $\sigma - \tau$ plane he has been able to describe the shear behaviour of the soil at failure using the so-called "Mohr circles". Because the Mohr circles are calculated at failure, the failure envelope of the shear stress may be constructed.

This envelope, known as the Mohr failure envelope, expresses the actual connection between shear stress τ_{ff} and normal stress σ_{ff}. Any circle that is smaller than the Mohr failure envelope denotes a stable condition, with failure happening only when τ_{ff} and σ_{ff} are combined in such a way that the Mohr circle is tangent to the Mohr failure envelope (**Figure 4.3**).

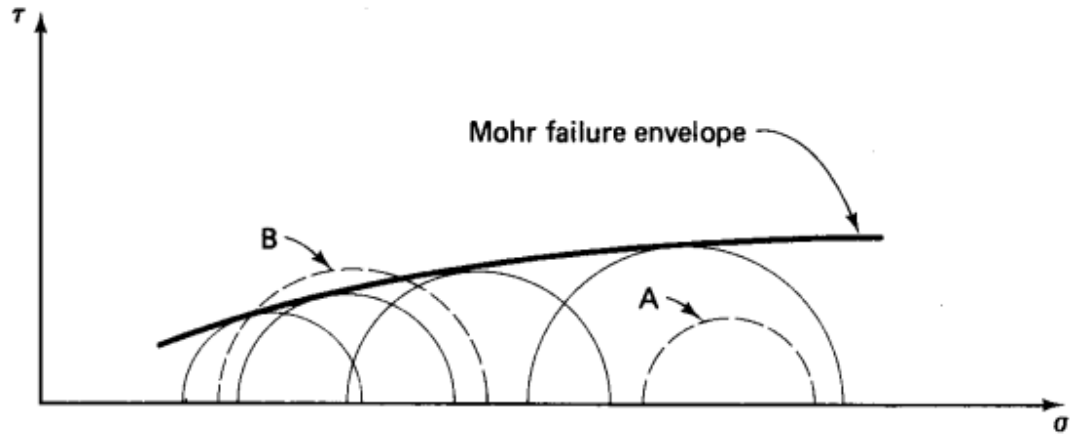

Figure 4.3 *Mohr failure envelope. Circle A is a stable condition, while circle B is an impossible condition, since the material would reach failure before reaching these stress states (Favaretti, 2022)*

Starting from all these considerations, Coulomb proposed a method to simply assess the shear strength of the soils, a straightforward formulation that only involves a first-order equation and known as Mohr-Coulomb failure criterion:

$$\tau_f = \sigma_f \tan\phi + c \qquad 4.7$$

where the shear strength at failure τ_f is directly related to normal stress at failure σ_f, and other two factors, ϕ and c. The first one, ϕ, is dependent on stress and is called angle of internal friction. The second, c, is independent on friction between particles and is the internal friction. This criterion approximates the Mohr failure envelope (a curve) with a straight line, easy to work with. From a merely geometric point of view, ϕ represents the slope of the failure envelope, while c represents the intercept between the failure envelope and the τ axis in the $\sigma - \tau$ plane (**Figure 4.4**).

When talking about slope stability, shear strength of the soil is the most important parameter that regulates the resistance of the whole mass of soil and, in this case, of the top landfill cover. After this little introduction, the following chapters will try to address the problems in stability related to the presence of biogas, whose presence determines a weakening in shear strength due to the decrease of the effective stresses.

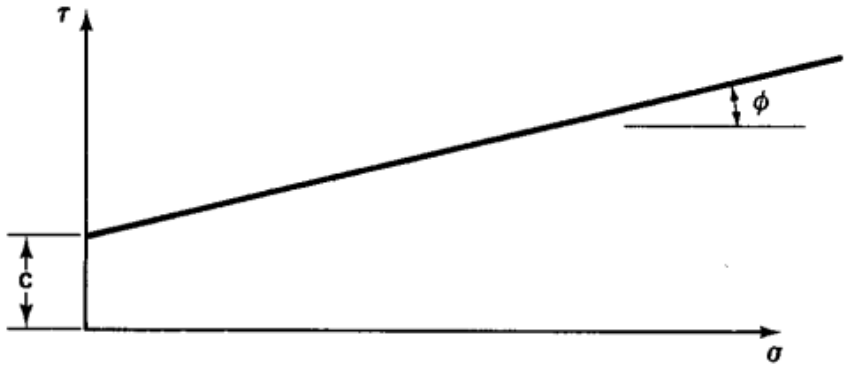

Figure 4.4 *The Mohr-Coulomb criterion (Favaretti, 2022)*

4.2.2 Choosing the model

It is up to the designer to use any cover slope stability model deemed appropriate for the project, but it must be able to incorporate gas pore pressures from below, as described in detail later. Several papers describing landfill cover veneer slope stability have been published, and exhaustive models have been developed, such as Koerner & Soong (1998) and Giroud et al. (2015). These models take into account a lot of factors and are very

reliable, considering they include different cases like the presence of seepage forces, seismic forces, toe buttressing forces, tapered slopes, and slope reinforcement.
However, most of these factors, like buttressing forces or reinforcements, are forces that act in favour of stability and usually result in a higher final FoS. For this reason, the infinite slope approach could also be useful and is the one that Thiel used to carry out its analyses. This approach, although less complex than the others, allows to evaluate the stability in a simple but effective way, not considering eventual supplementary stabilizing forces that act in favour of safety. For this reason, the infinite slope approach is considered a conservative option. Moreover, being the sliding surface expected to be between the discontinuities of the various layers composing the top cover, the critical interface can be considered parallel to the slope and thus the model can be applied.
For linear sliding surfaces, the FoS is defined as (**Figure 4.5**):

$$FoS = \frac{\sum F_R}{\sum F_M} = \frac{Sum\ of\ resisting\ forces}{Sum\ of\ mobilizing\ forces} \qquad 4.8$$

The choice of an appropriate factor of safety for the slope stability depends on various factors and is usually imposed by national or local regulations. Usually, a FoS of 1.3 is considered safe, but it depends on the specific situation. Liu et al. (1997), on the base of statistical analyses, assessed that the choice of the FoS depends mainly on the cost of failure and the uncertainty in the estimation of the interface shear strength of geosynthetics, principally due to:

- Material variability, both between batches and inside the same batch;
- Accuracy of testing methods;
- Moisture conditions;
- Post-peak strength reductions.

One of the aims of this work is to understand the effects of biogas pressure on the FoS.

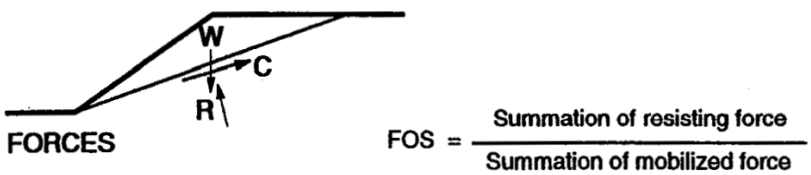

Figure 4.5 *FoS for linear critical interfaces (Favaretti, 2022)*

4.2.3 Infinite slope model construction

The infinite slope model is based on the following assumptions:

- Undefined slope length, or at least much larger than the depth of the potential slip surface;
- Rigid, perfectly plastic constitutive law;
- Constant slope angle;
- Homogeneous soil characteristics along the slope direction;
- Parallel to the slope failure or slip surface;
- Mohr-Coulomb's failure criterion.

Essential to perform the analysis is the individuation of the failure surface. Realistically, it can be deduced that potential failure surfaces are located along the discontinuities in the cover system. In **Figure 4.6**, a common combination of soil and materials right above the BCL is shown. From top to bottom, the elements are:

- Rainwater drainage layer (RDL);
- Geomembrane (GM);
- Compact clay liner (CCL)
- Non-woven geotextile (NWGT);
- Biogas collection layer (BCL).

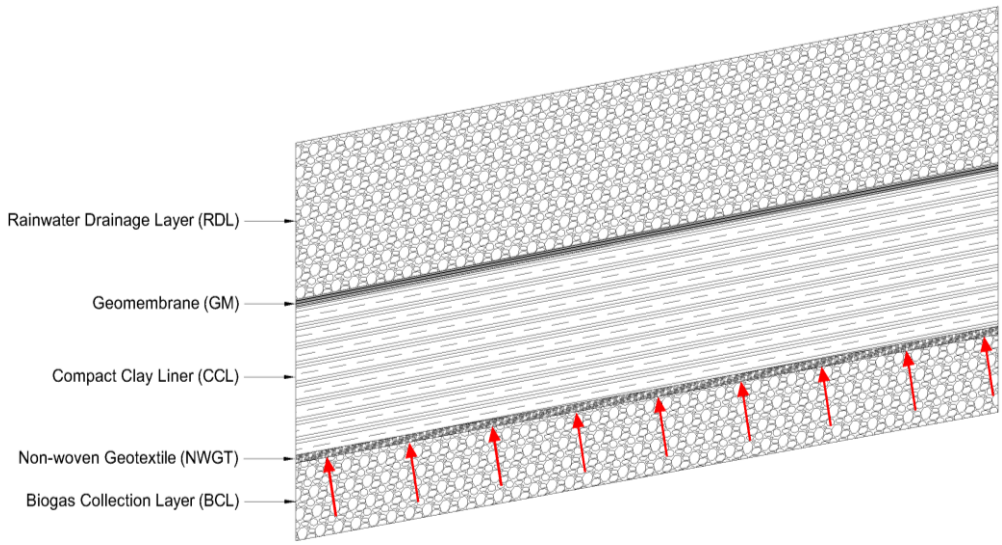

Figure 4.6 *Example of possible combination between BCL and RDL*

This combination will be taken as an example, but the considerations that will be made in the following paragraphs con suit all types of cases.

The gas, arriving from the underlying waste mass and making their way through the BCL (red arrows), produces an uplifting pressure on the upper elements. This pressure can induce additional stresses on the BCL-NWGT surface (in red), which becomes a potential slip surface.

It is important to note that other two considerations will be made for the sake of simplicity:

- As a precautionary measure, the cohesion of the soils c will be considered null;
- The weight of geomembranes and geotextiles will be approximated to zero.

In **Figure 4.7**, the free-body diagram and the force polygon can be observed.

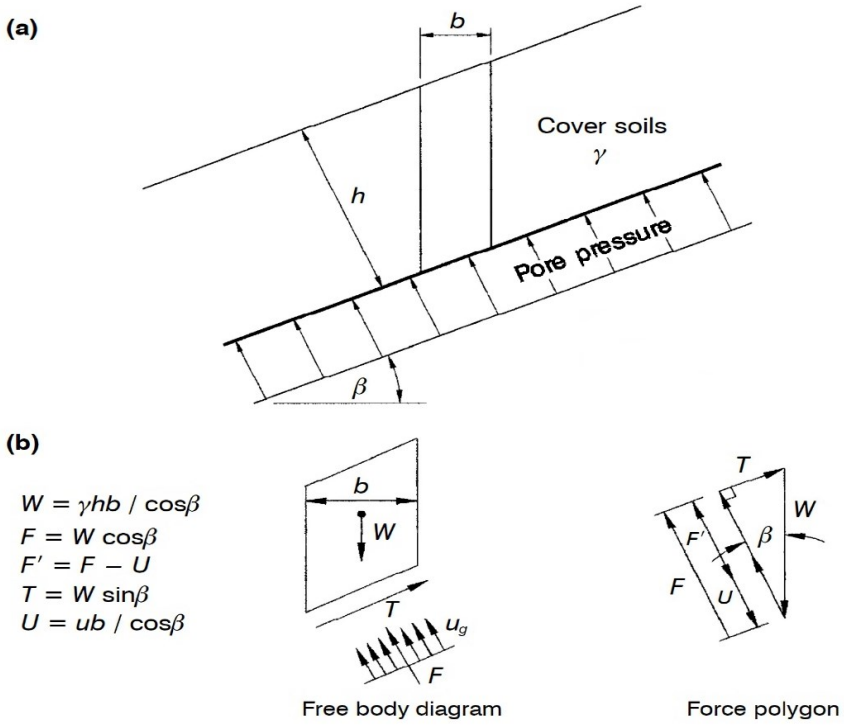

Figure 4.7 Components of forces on the failure surface (Thiel, 1998)

A representative slice of width b $[m]$ will be assessed, in a slope of inclination β [°]. The cover soil, that will be considered homogeneous[7], has a weight of:

$$W = \gamma \cdot h \cdot \frac{b}{\cos \beta} \qquad 4.9$$

[7] If not homogeneous, the weight can be easily calculated, for i layers, as $\sum \gamma_i \cdot h_i \cdot b / \cos \beta$

Where γ = unit weight of the material $[kN/m^3]$; h = thickness of the cover soil $[m]$. The unit weight can be dry or saturated, depending on the specific conditions of the case. The weight of the cover soil can be divided into two components, one parallel to the slope $W_{/\!/}$ and one perpendicular to the slope $W_{\perp}$.
The perpendicular component $W_{\perp}$ is:

$$W_{\perp} = W \cdot \cos\beta = \gamma \cdot h \cdot b \tag{4.10}$$

while the parallel component $W_{/\!/}$ is:

$$W_{/\!/} = W \cdot \sin\beta = \gamma \cdot h \cdot b \cdot \tan\beta \tag{4.11}$$

However, these are forces, and must be translated into stresses, simply considering them relative to the area in which they act. In this case, the area is the base of the slice $b/\cos\beta$. So, the total normal stress on the failure surface is:

$$\sigma = \frac{W_{\perp}}{b/\cos\beta} = \gamma h \cos\beta \tag{4.12}$$

and the tangent shear stress (mobilizing) is:

$$\tau_M = \frac{W_{/\!/}}{b/\cos\beta} = \gamma h \sin\beta \tag{4.13}$$

It has already been assessed that the gas pressure consists in an excess stress on the failure surface. Moreover, as Terzaghi stated, any change can be attributed to changes in effective stresses, thus making it mandatory to do the calculations in terms of effective stresses. The gas pressure u_g can be introduced in *4.12* using *4.5*, obtaining the effective normal stress acting on the failure surface:

$$\sigma' = \sigma - u_g = \gamma h \cos\beta - u_g \tag{4.14}$$

At the base of the slice, the resisting shear strength is determined by the shear strength along the interface between the material forming the BCL and the NWGT[8].

[8] Same considerations can be carried out if the interface is between soil and other types of geosynthetics.

It is important, to clearly understand the resisting force on the slip surface, what is the behaviour of geosynthetics in contact with other materials. Performing interface shear tests (**Figure 4.8**) it is possible to determine the two important parameters that characterize the geotextile: the effective adhesion parameter a' $[kN/m^2]$ and the effective interface friction angle δ' [°].

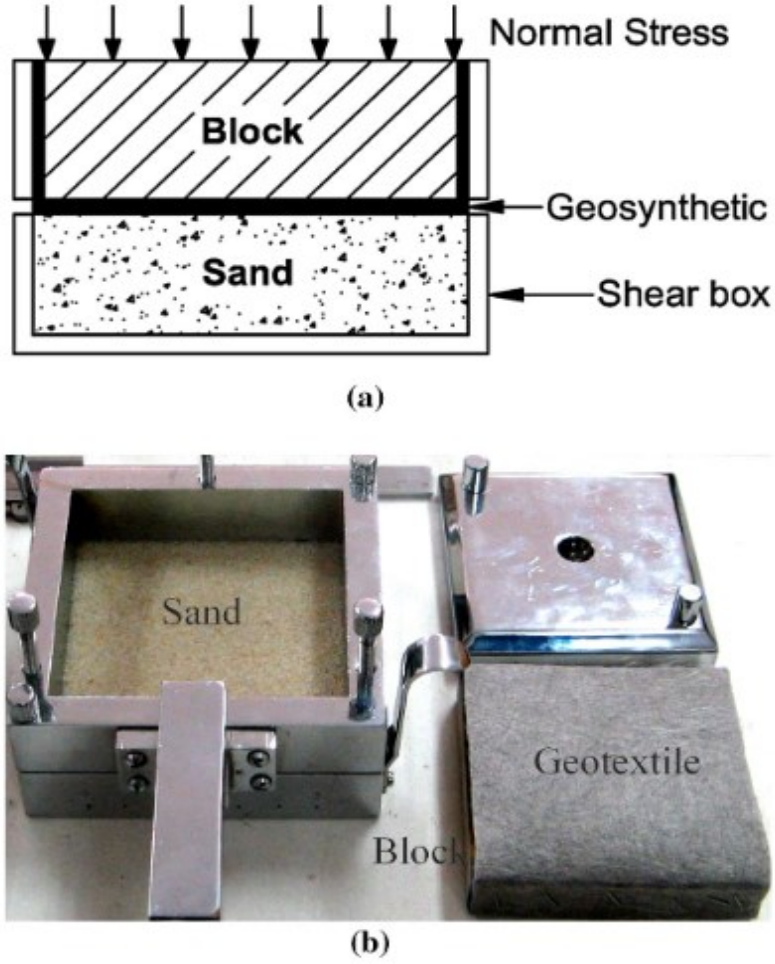

Figure 4.8 *Specimen configuration for sand–geotextile interface testing with the 100 mm shear box (Markou, 2018)*

The shear strength of a geosynthetic can then be expressed with an equation similar to the Mohr-Coulomb one:

$$\tau_{GS} = a' + \sigma' \tan \delta' \qquad 4.15$$

with a' and δ' representing, respectively, the intercept and the slope of the function in the $\sigma - \tau$ plane (**Figure 4.9**).

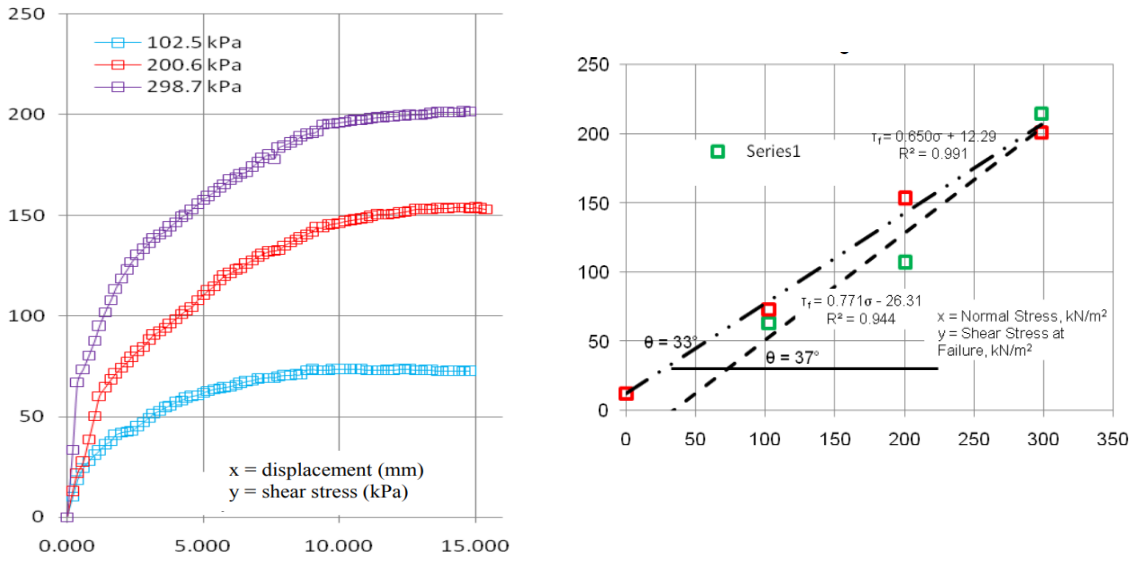

Figure 4.9 *Example of interface shear strength between NWGT and soil (Izzuddin Zaini et al., 2012)*

Some tests performed by Izzuddin Zaini et al. (2012) demonstrate that the contact friction angle of woven GCL is greater than that of non-woven GCL. Regarding adhesion, it is not significant for woven GCL but considerable for non-woven GCL. Considering also the tests performed by Söylemez & Arslan (2020) and Anubhav & Basudhar (2010), it is reasonable to consider the adhesion value for the interface between coarse soil and non-woven geotextiles oscillating in the interval 5-15 kPa. For cohesive soils, Nguyen & Ho (2021) determined higher values, around 25 kPa. However, due to the variety of geotextile properties and testing methods, laboratory evaluation of interface friction coefficients is important, if not required, in each specific case.

Inserting *4.14* in *4.15*, the resisting shear strength on the slip surface becomes:

$$\tau_R = \tau_{GS} = a' + \left(\gamma h \cos\beta - u_g\right) \tan\delta' \qquad 4.16$$

Finally, defining the FoS as in *4.8*, inserting all the considerations, the following relation can be obtained:

$$FoS = \frac{\tau_R}{\tau_M} = \frac{a' + \left(\gamma h \cos\beta - u_g\right) \tan\delta'}{\gamma h \sin\beta} \qquad 4.17$$

For fixed geometry parameters, this equation can be solved explicitly for u_g, determining the maximum allowable biogas pressure $u_{g,max}$ and obtaining the factor of safety.
Solving:

$$u_{g,max} = \gamma h \cos\beta - \frac{(FoS \cdot \gamma h \sin\beta - a')}{\tan\delta'} \qquad 4.18$$

In this way, it is now possible to predict the way FoS is influenced by biogas pressure.

4.3 DESIGN OF A PASSIVE VENT SYSTEM WITH STRIP DRAINS

4.3.1 Design equations

Now that $u_{g,max}$ has been evaluated, related to a proper FoS to obtain, the design of the collection system can be carried out. As previously assessed in Chapter 3.2.2, the majority of the gas fluxes in a landfill are driven by advective processes. These processes can be efficiently analysed when the flow is laminar, using Darcy's Law (*3.1*). Thus, it is important to understand the type of flow that the gas follows when passing through the BCL. To define the type of flow, the Reynold's number Re is a relation useful for this assessment. Technically, the Reynolds number is the ratio of inertial forces to viscous forces that distinguishes laminar flows from turbulent flows. It is defined by the equation:

$$Re = \frac{\rho v d}{\mu_f} \qquad 4.19$$

where ρ = fluid density, μ_f = fluid dynamic viscosity, v = fluid velocity, and d = characteristic flow dimension. This relation is studied for classic hydraulic situations, like the flow in pipes, but can be adapted to different conditions. For this reason, usually, the characteristic flow dimension d indicates the diameter of the pipe. In the case of flow in a porous media, the characteristic dimension will be different, because the movement occurs through the pores of the soil and the direct measurement of the pore size is a difficult task that will be discussed later in this paper.
Generally, the flow is considered laminar for values of $Re < 2000$ in classic hydraulics but, for the flow in porous media, experiments involving flow rates of various fluids show

that the critical Reynolds number below which the flow is laminar is somewhere between 1 and 10, with most references conservatively identifying a value of 1 as a safe limit for the applicability of Darcy's law (Thiel, 1998).

For the derivation of the design equations, the flow of gas inside the BCL will be considered laminar, thus making Darcy's law usable for the analysis. However, when performing calculations on specific cases, a precise evaluation of the Reynolds number will be made to ensure the applicability of this assumption.

This chapter considers the design of a collection system composed by a series of strip drains that run longitudinally along the benches or slopes, usually consisting in perforated pipes (**Figure 4.10**). Then, these strip drains will be connected to outlets that penetrate the cover system and help move the gas outside the landfill area.

Figure 4.10 *Perforated pipes for biogas extraction (CONVECO SRL, 2022)*

These elements will be disposed at a spacing D and will be considered as a passive system. This assumption has a conservative meaning, also if the final system is going to be an active system with pumps to collect the biogas. This is due to the possibility of malfunctioning of pumps or maintenance of the system, that is a concrete risk to take into account. For this reason, in this case the system would become equal to a passive one and, if this was not considered in the design phase, it could lead to potential gas overpressures and risk of instability.

An example of disposition of strip drains on a bench-slope system like that of the landfill can be observed in **Figure 4.11**. Moreover, the cross-section between two strip drains is visible in **Figure 4.12**. Note that, for the derivation of equations, the flux of biogas from the waste below is considered to move uniformly into the BCL. Since the flow can be considered symmetric, a length parameter $L = D/2$ can be defined. One-dimensional variable distance x will be considered zero on the axis of the strip drains and increase towards the centreline between the two drains. Furthermore, the width will be considered unitary. The volume of gas moving through the BCL is then considered to vary linearly from its maximum ($x = 0$) to zero ($x = L$).

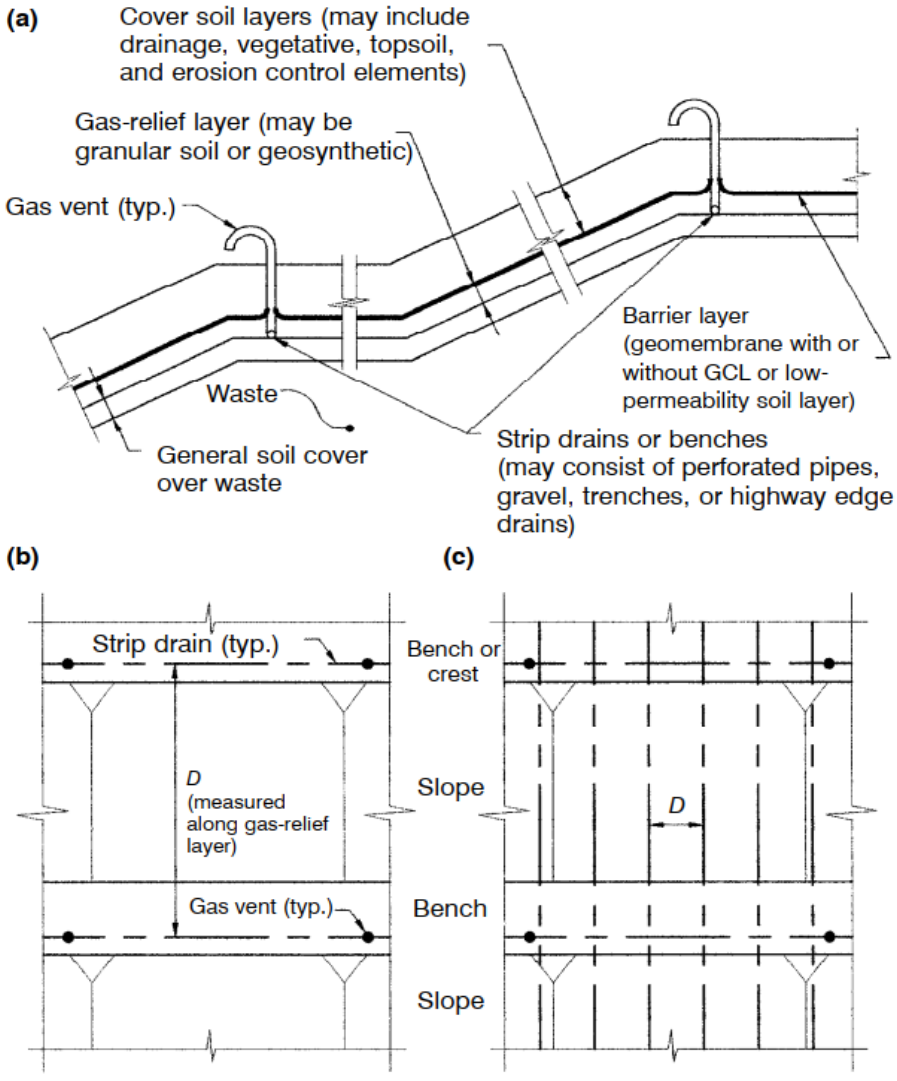

Figure 4.11 *Illustration depicting the design elements of the gas-relief layer: (a) final cover profile with gas-relief layer and strip drains; (b) plan view of strip-drain layout on benches only; (c) plan view of strip-drain layout on slopes and benches (Thiel, 1998)*

This last consideration could be written in terms of flow rate per unit width Q_x with this simple relation:

$$Q_x = \Phi_g(L - x) \tag{4.20}$$

where Φ_g is the gas flux flowing in the BCL already defined in Chapter 4.1.1.

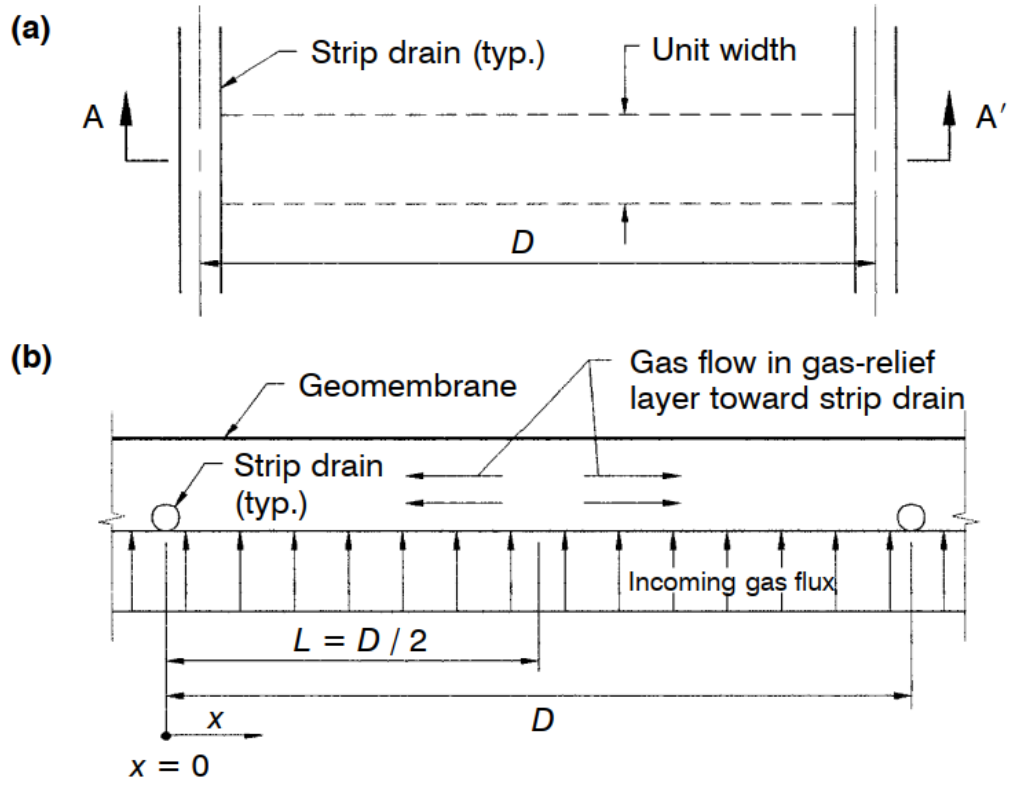

Figure 4.12 *Model of gas flow to strip drains: (a) plan view; (b) cross-section A-A' (Thiel, 1998)*

As recalled in the beginning of the paragraph, Darcy's law can be used for this situation. It can be written as:

$$Q_x = \left(\frac{k_g}{\gamma_g}\right) \cdot A \cdot \left(\frac{du_g}{dx}\right) \tag{4.21}$$

where k_g is the permeability of the porous media to the gas, γ_g is the unit weight of the gas, A the area in which the flow takes place, and u_g the gas pressure. Being the width equal to one and the thickness of the BCL equal to t, the area is $A = t$.

So, the relation becomes:

$$Q_x = \left(\frac{k_g \cdot t}{\gamma_g}\right) \cdot \left(\frac{du_g}{dx}\right) \tag{4.22}$$

It is now possible to define a new parameter, the transmissivity of the gas collection layer Ψ_g, that incorporates both permeability of the media and thickness of the layer, defined by the equation:

$$\Psi_g = k_g \cdot t \tag{4.23}$$

Through the definition of the transmissivity is possible to rewrite *4.22* as:

$$Q_x = \left(\frac{\Psi_g}{\gamma_g}\right) \cdot \left(\frac{du_g}{dx}\right) \tag{4.24}$$

and combining *4.20* and *4.24* the following relation is obtained:

$$\Phi_g(L - x) = \left(\frac{\Psi_g}{\gamma_g}\right) \cdot \left(\frac{du_g}{dx}\right) \tag{4.25}$$

Now, it is possible to obtain the value of the pressure of biogas u at any distance x from the strip drain, simply integrating *4.25* in terms of x:

$$\begin{aligned} \int_0^x \Phi_g(L - x)\, dx &= \int_0^x \left(\frac{\Psi_g}{\gamma_g}\right) \cdot \left(\frac{du_g}{dx}\right) dx \\ \Phi_g L x - \Phi_g \frac{x^2}{2} &= \frac{\Psi_g}{\gamma_g} u_{g,x} \end{aligned} \tag{4.26}$$

finally obtaining the pressure in function of the distance:

$$u_{g,x} = \frac{\gamma_g}{\Psi_g} \Phi_g \left(Lx - \frac{x^2}{2}\right) \tag{4.27}$$

For $x = L$, so in the middle between two strip drains, the pressure will be maximum:

$$u_{max} = \frac{\gamma_g}{\Psi_g} \Phi_g \left(\frac{L^2}{2}\right) \tag{4.28}$$

and null on the strip drain ($x = 0$):

$$u_{min} = \frac{\gamma_g}{\Psi_g} \Phi_g \left(Lx - \frac{x^2}{2} \right) = 0 \tag{4.29}$$

Equation *4.28* could be also written in terms of drain spacing D and, as we defined L as the half space between the drains ($L = D/2$), the following equation is obtained:

$$u_{max} = \frac{\gamma_g}{\Psi_g} \Phi_g \left(\frac{D^2}{8} \right) \tag{4.30}$$

If the maximum pressure is known, and there is the need to design a proper spacing of the drains, D can be made explicit as:

$$D = \sqrt{\frac{8 u_{max} \Psi_g}{\gamma_g \Phi_g}} \tag{4.31}$$

4.3.2 Calculation of the needed material permeability to gas

When deriving the equations for the BCL design, the gas transmissivity $\Psi_g = k_g \cdot t$ has been defined. However, there is a problem since little data is present regarding transmissivity for the different materials. In fact, usually, the permeability of a porous material is referred to water permeability k_w and not gas permeability k_g. The solution to this problem lies in the concept of intrinsic permeability.

When writing Darcy's law in these terms:

$$q = \frac{Q}{A} = \frac{k}{\mu} \cdot \frac{dp}{dx} \tag{4.32}$$

the coefficient k $[m/s]$ denotes the hydraulic conductivity of the porous medium and is related to the type of fluid and characteristics of the medium. It is, in brief, a factor that encompasses the characteristics of both the medium and the fluid and consequently is dependent on both. But these two parts can be divided.

Hydraulic conductivity present in *4.32* can be expressed as:

$$k = \frac{K \rho g}{\mu} = \frac{K \gamma}{\mu} \tag{4.33}$$

where γ = unit weight of the fluid; μ = dynamic viscosity of the fluid; K = intrinsic permeability of the fluid. The part that is dependent on the fluid characteristics can be defined as fluidity $f = \mu/\gamma$, whereas the intrinsic permeability K is a function of the pore structure and geometry of the porous media (Tindall et al., 1999). Since pores are not smooth, straight and parallel to each other, the path followed by a fluid in the structure is not regular.

The intrinsic permeability has a unit of measure of m^2:

$$K = \frac{\mu k}{\rho g} = \frac{\left[\frac{kg}{m/s}\right] \cdot \left[\frac{m}{s}\right]}{\left[\frac{kg}{m^3}\right] \cdot \left[\frac{m}{s^2}\right]} = [m^2] \tag{4.34}$$

Considering one porous media and two different fluids (i.e., water and gas), it is then possible to obtain the hydraulic conductivity of one of the fluids in relation to the other, since the intrinsic permeability is the same (porous media is the same). Therefore, if the two fluids considered are gas and water, with respective intrinsic permeabilities K_g and K_w, the relation would be:

$$K_w = K_g \tag{4.35}$$

and, consequently, the explicit expression:

$$\frac{k_w \cdot \mu_w}{\gamma_w} = \frac{k_g \cdot \mu_g}{\gamma_g} \tag{4.36}$$

can be written as:

$$\frac{k_w}{k_g} = \frac{\gamma_w}{\gamma_g} \cdot \frac{\mu_g}{\mu_w} \tag{4.37}$$

This equation permits to convert the gas permeability into water permeability (and then transmissivity), much easier to calculate and conventionally used when designing. The fact that intrinsic permeability K doesn't depend on the porous medium has been proven by Muskat & Wyckoff (1937) with a series of experiments that aimed to measure intrinsic permeability on sands, all with water permeability values k_w ranging from 10^{-3} to 10^{-6}

m/s. The experiments were operated on the same samples with both air and liquids, resulting in almost identical values (**Table 4.3**).

For design purposes, the assessment of the relationship between permeability to water and permeability to LFG will be performed. On the base of LFG composition presented in **Table 3.1**, counting only the major components, LFG could be considered as formed on average by 55% of methane (CH_4) and 45% of carbon dioxide (CO_2).

Table 4.3 *Intrinsic permeabilities of different soil samples measured using air and liquids (Muskat & Wyckoff, 1937)*

Sample	K (air)	K (liquid)
0- to 45-mesh sand	139.13	139.40
80- to 100-mesh sand	24.90	22.00
No. 1 sandstone (Woodbine)	1.18	1.20
No. 2 sandstone (Woodbine)	1.56	1.57
No. 3 sandstone (Woodbine)	1.63	1.63
No. 4 sandstone (Berea)	1.54	1.50

At 20°C and 1 bar of pressure, the viscosities of the two components are $\mu_{CH4} = 10.9 \cdot 10^{-6}\ N \cdot s/m^2$ and $\mu_{CO2} = 14.7 \cdot 10^{-6}\ N \cdot s/m^2$. The unit weights are $\gamma_{CH4} = 6.47\ N/m^3$ and $\gamma_{CO2} = 17.8\ N/m^3$. Knowing these values, a weighted average may be calculated and used as a reference for LFG. So:

$$\gamma_{LFG} = 0.55 \cdot \gamma_{CH4} + 0.45 \cdot \gamma_{CO2} = 11.6\ N/m^3 \qquad 4.38$$

and

$$\mu_{LFG} = 0.55 \cdot \mu_{CH4} + 0.45 \cdot \mu_{CO2} = 12.6 \cdot 10^{-6}\ N \cdot s/m^2 \qquad 4.39$$

All these values can be visualized in **Table 4.4**.

Table 4.4 *Unit weights and viscosities of different fluids, at 20°C and 1 bar, considering LFG = 55% CH_4 + 45% CO_2 (The Engineering Toolbox, 2003)*

Fluid	Unit Weight γ [N/m³]	Dynamic Viscosity μ [N·s/m²]
Water	9780.6	$1.0 \cdot 10^{-3}$
Methane CH_4	6.5	$10.9 \cdot 10^{-6}$
Carbon Dioxide CO_2	17.8	$14.7 \cdot 10^{-6}$

LFG	11.6	$12.6 \cdot 10^{-6}$

With these values now available, the relationship between permeability to water and permeability to LFG may be evaluated with Equation *4.37*, in this case made explicit for water permeability k_w:

$$k_w = \frac{\gamma_w}{\gamma_{LFG}} \cdot \frac{\mu_{LFG}}{\mu_w} \cdot k_{LFG} = \frac{9780.6}{11.6} \cdot \frac{12.6 \cdot 10^{-6}}{1.0 \cdot 10^{-3}} \cdot k_{LFG} = 10.6\, k_{LFG} \qquad 4.40$$

thus, demonstrating that the permeability of a porous media to water that is more than ten times higher than the permeability to LFG. So, the following relation can be obtained:

$$k_w = 10\, k_{LFG} \qquad 4.41$$

Although this relation may sound counterintuitive, it may be due to different reasons. One of these reasons could be the difference in the kinetic diameters of the gas and water particles. The kinetic diameter is a metric for atoms and molecules that reflects the possibility of a molecule colliding with another molecule in a gas, essentially indicating the size of the molecule as a target. Kinetic diameter is mainly related to the mean free path[9], the molecule size and the molecular structure. Some data about common molecules are reported in **Table 4.5**.

Table 4.5 *Kinetic diameters for different elements (1 Å = 10^{-10} m) (Gnanasekaran & Reddy, 2013)*

Molecule	**Kinetic Diameter [Å]**
H_2	2.89
O_2	3.46
CH_4	3.80
CO_2	3.30
H_2O	2.65

[9] Average distance travelled by a moving particle before significantly changing its direction or energy (or, in some cases, other attributes), often as a result of one or more repeated collisions with other particles.

A study performed by Chen et al. (2018) on the behaviour of different molecules in polymers showed a correlation between kinetic diameter and permeability.

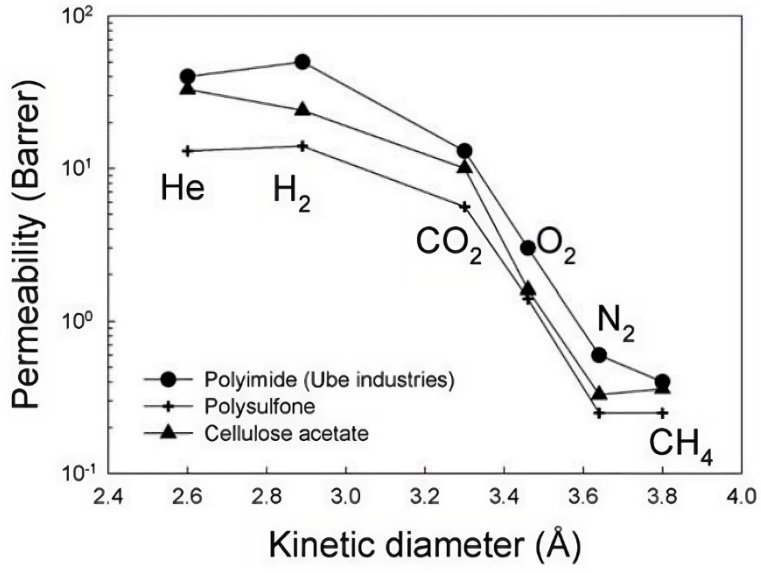

Figure 4.13 *Permeability as function of kinetic diameter for six gases in three glassy polymers (Chen et al., 2018)*

In particular, tests highlighted that the permeability of a membrane was inversely proportional to the kinetic diameter of the molecule (**Figure 4.13**). Since, as indicated in **Table 4.5**, the kinetic diameter of CH_4 and CO_2 are larger than H_2O, this could be one of the possible reasons for the result obtained in *4.40*.

Another possible explanation to the higher permeability to water than to gas could be identified in the capillary action, so the flow of water within the pores of a porous medium caused by adhesion, cohesion, and surface tension forces. This phenomenon allows water to move against gravity and flow through smaller pore spaces. On the other hand, capillary action is not as significant for gas molecules due to their weaker adhesive forces with solid surfaces, limiting their ability to move against the force of gravity. However, this phenomenon is of higher concern when regarding fine, cohesive soil.

Although series of experiments by Tanikawa et al. (2006) show that gas permeability is larger than water permeability by several times to one order of magnitude (mainly on cohesive soils), the previously presented concepts could explain the different behaviour and point out that the result obtained in *4.40* is plausible.

4.3.3 Effect of moisture on permeability

The BCL is, in all cases, located below a hydraulic barrier, usually consisting in a compacted clay layer. This layer provides protection against infiltration of rainwater and

other liquids that penetrate the top cover. For this reason, the BCL is usually considered unsaturated, and water is not taken into account. However, it is important to note that moisture may be present in the BCL. Moisture could be the result of infiltrations during the construction phase of the top cover but also of the fact that LFG is generally saturated, and this could lead to condensate forming in the layer.

The first studies on the dependency of permeability on the degree of saturation of a soil have been performed by Brooks & Corey (1964), that described the coefficient of permeability as a singular function of the degree of saturation S. To understand the final result of their studies, it is important to define some central concepts first. In fact, the degree of saturation has traditionally been regarded as a function of matric suction.

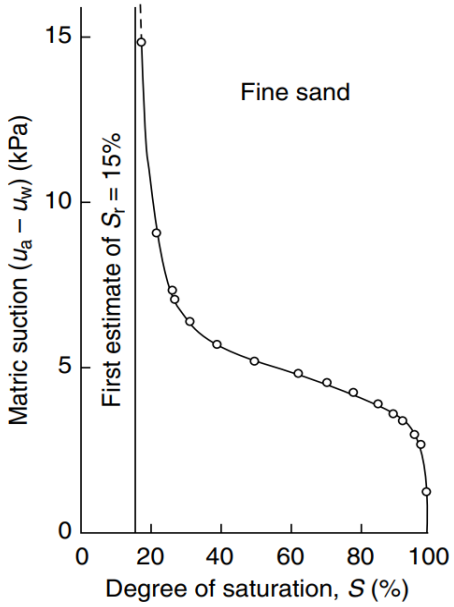

Figure 4.14 Matric suction versus degree of saturation curve (Wang-Wai & Menzies, 2007)

Matric suction $(u_a - u_w)$ can be roughly defined as the pressure that dry soil exerts on adjacent soils in order to equalize the moisture content of the entire block of soil. The curve that describes the relationship of this quantity with the degree of saturation is shown in **Figure 4.14**.

From this curve, three parameters can be obtained: the air entry value of the soil $(u_a - u_w)_b$, the residual degree of saturation S_r, and the pore size distribution index λ. Defining the effective degree of saturation S_e as:

$$S_e = \frac{S - S_r}{1 - S_r} \qquad 4.42$$

These parameters can be visualized in a matric suction versus effective degree of saturation graph (**Figure 4.15**).

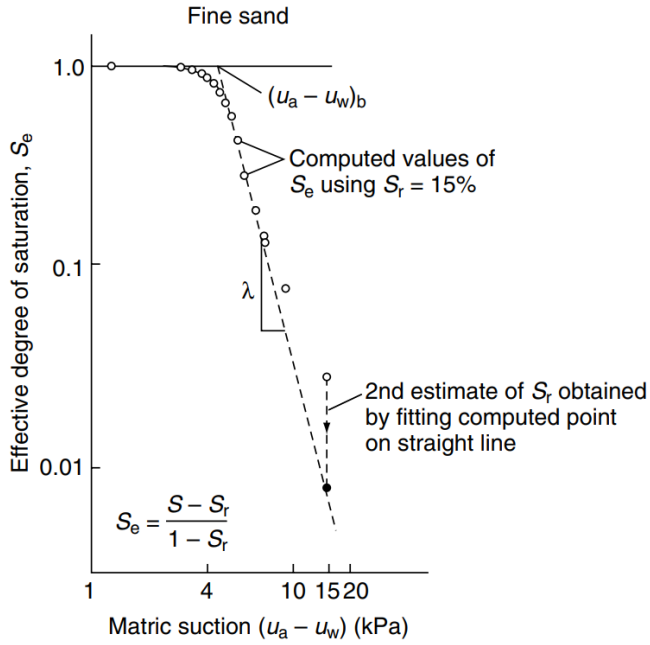

Figure 4.15 *Effective degree of saturation vs matric suction curve (Wang-Wai & Menzies, 2007)*

In particular:

- The air-entry value $(u_a - u_w)_b$ is the matric suction needed to cause desaturation of the largest pores, i.e., the suction value beyond which air begins to enter the saturated soil pores. The intersection point between the straight sloping line and the saturation ordinate (i.e., $S_e = 1.0$) is the air entry value of the soil.
- The pore size distribution index λ is defined as the negative slope of the $(u_a - u_w) - S_e$ curve. In general, small values of λ are found in soils with a wide range of pore sizes while λ increases with the degree of uniformity in the distribution of pore sizes in a soil. Usually, this number varies from circa 2 (for porous rocks) to infinity (uniform sands).
- The residual degree of saturation S_r is the saturation level at which an increase in matric suction does not significantly alter the saturation level.

Brooks & Corey (1964) tried to express the relationship between the permeability of a medium to a gas and the degree of saturation of the porous medium, for the conditions in which $(u_a - u_w) > (u_a - u_w)_b$.

This relationship can be written as:

$$k_g = k_d \cdot (1 - S_e)^2 \cdot \left(1 - S_e^{\frac{2+\lambda}{\lambda}}\right) \quad 4.43$$

with k_g = coefficient of permeability to gas; k_d = coefficient of permeability with respect to the air phase for a dry soil ($S = 0$); S_e = effective degree of saturation; λ = pore size distribution index.

Using typical moisture field capacities, it can be calculated that the gas permeability of a typical sand would be decreased by 25–50%. Thiel (1998) suggests that, based on field experience and available data, these recommendations should be followed when evaluating the gas permeability of the BCL:

- For fine sands containing less than 10-15% fines, the field-gas permeability can be calculated by dividing the dry-gas permeability by a factor of 5 to 10 to account for the presence of field moisture;
- For clean medium and coarse sands, the field-gas permeability can be calculated as the dry-gas permeability divided by two (one-half the dry value) to account for field moisture.

So, finally, when analysing the material to utilise for the construction of the BCL, these reductions should be taken into consideration. For the purposes of this paper, considering a value of field-gas permeability equal to the dry gas permeability divided by a reduction factor $RF_m = 2$ could be a possible solution, implying:

$$k_w = 10 \cdot k_{LFG} \cdot \frac{1}{RF_m} = 5\ k_{LFG} \quad 4.44$$

4.3.4 Calculation of the final design permeability

Once a suitable FoS has been chosen and the maximum uplift pressure calculated, the minimum required gas transmissivity $\Psi_{g,min}$ can be expressed reformulating Equation *4.30* as:

$$\Psi_{g,min} = \frac{\gamma_g}{u_{max}} \Phi_g \left(\frac{D^2}{8}\right) \quad 4.45$$

However, Thiel's analysis considers the BCL as an isotropic media, with no intrusions and difficulties for the gas to flow in the layer. This is not the real situation, because certain factors will tend to penalize the porous medium's transmissivity efficiency under real-world operational conditions. Thus, some corrective factors introduced in the *GC8 Standard* by the GRI ("Geosynthetic Research Institute") accounting for possible different conditions that may be present in the real situations need to be applied to increase the gas transmissivity in favour of safety.

It will be then possible to derive the design minimum gas transmissivity, to use for the final evaluation of the required permeability of the material. The design gas transmissivity is then:

$$\Psi_{g,d} = \Psi_{g,min} \cdot \prod_{i=1}^{4} CF_i \qquad 4.46$$

with:

$$\prod_{i=1}^{4} CF_i = CF_{IN} \cdot CF_{BC} \cdot CF_{CC} \cdot CF_{UC} \qquad 4.47$$

The different correction factors are explained in **Table 4.6**.

Table 4.6 *Correction factors for the gas transmissivity* (Geosynthetic Institute, 2013)

Correction Factor		Range	Adopted Value
$\boldsymbol{CF_{IN}}$	Potential intrusion of the overlying GT within the BCL	1 ÷ 1.2	1.1
$\boldsymbol{CF_{BC}}$	Biological clogging	1 ÷ 1.2	1
$\boldsymbol{CF_{CC}}$	Chemical clogging	1.2 ÷ 1.5	1.2
$\boldsymbol{CF_{UC}}$	Uncertainty of the model	2 ÷ 3	2

Using the adopted values to address the magnitude of *4.47*, the final expression for the design gas transmissivity is:

$$\Psi_{g,d} = \Psi_{g,min} \cdot \prod_{i=1}^{4} CF_i = 2.64\, \Psi_{g,min} \qquad 4.48$$

Through this relation and through the definition of gas transmissivity expressed in Equation *4.23*, it is possible to calculate the final design permeability coefficient to water $k_{w,d}$ to use for the selection of the material of the BCL. Knowing the thickness of the BCL t, the procedure for the evaluation of $k_{w,d}$ based on the considerations made in this chapter is:

$$k_{w,d} = 5\, k_{g,d} = 5 \cdot \frac{\Psi_{g,d}}{t} = 5 \cdot \frac{2.64\, \Psi_{g,min}}{t} = 13.2 \cdot \frac{\Psi_{g,min}}{t} \qquad 4.49$$

5 THE LEGNAGO LANDFILL CASE

In this section, all the procedures covered in the previous chapters will be applied to the case of a real landfill. The Torretta di Legnago landfill, already presented in Chapter 2.3, will be the subject of the study. The choice of this specific site has been made because, also since the project of 2009 that involved the expansion of the area with the concurrent realization of lots D, E and F, some parts of the site are prone to potential instability issues when in presence of biogas pressures. Built based on the *D. Lgs. 36/2003*, the escarpments show a slope ratio of 1:2.5 that equals approximately 21.8° (**Figure 5.1**).

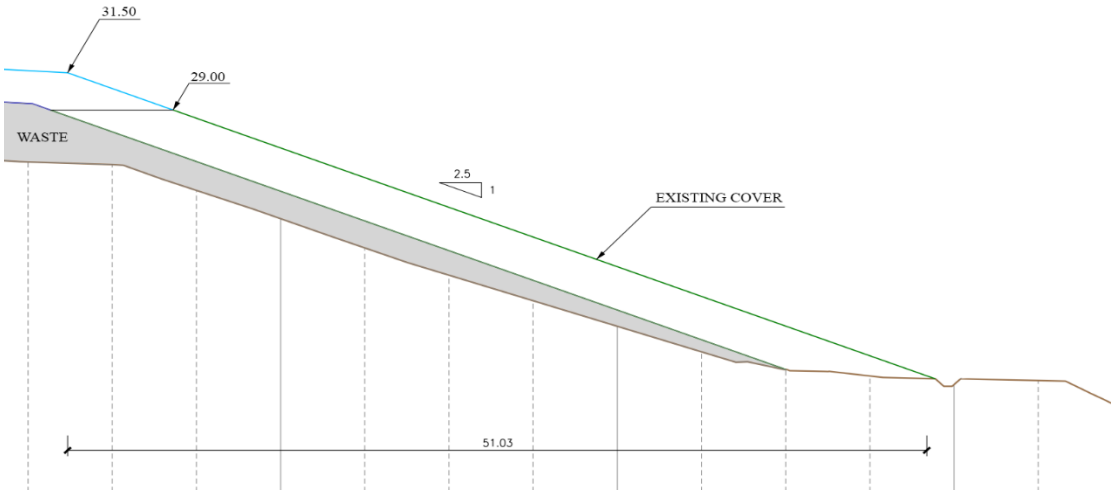

Figure 5.1 *Cross section of the escarpment in the lot E, measures in meters*

The slope analysed in this chapters, designed based on *D. Lgs. 36/2003*, possesses the stratification displayed in **Figure 5.2**.

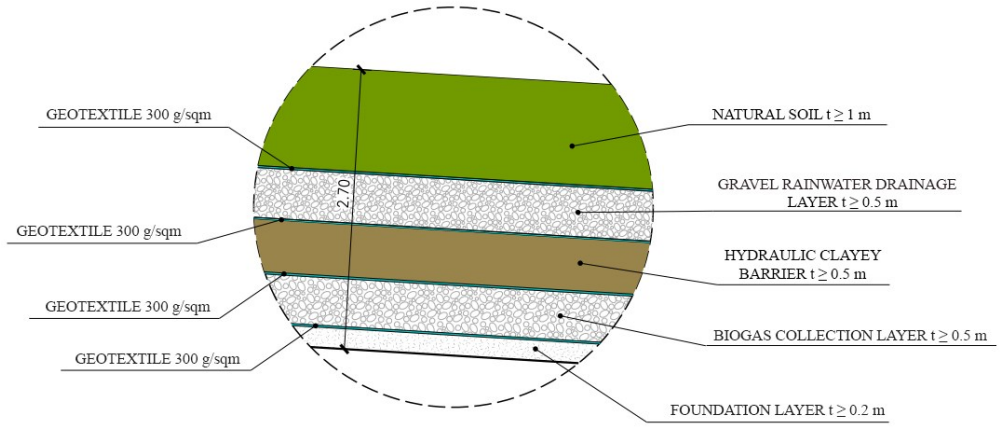

Figure 5.2 *Particular of the existing top cover*

In this case, the slope of the escarpment is 21.8° and the failure surface can be any of the discontinuities between the layers. However, given the objective of this thesis, the failure surface that will be studied will be, as already discussed in Chapter 4, the interface between BCL and the hydraulic clay barrier, that includes the use of a non-woven geotextile as separation. Here, as shown before, the biogas pressure builds from the underlying waste mass, inducing an additional uplifting force that could translate into the risk of sliding of all layers above the BCL.

Therefore, the analysis of Thiel will be performed on this situation. However, an additional method to assess the slope stability in presence of biogas will be utilized, in particular a modified version of the method of Koerner & Soong (1998). This solution has been chosen because, in the first place, the infinite slope model is a largely conservative model, which is likely to produce values that are safe but that can lead to considerable overestimations. Secondly, the Koerner & Soong method permits, in spite of being a bit more complex, to address in a more accurate way the forces and the resistance of the materials on the slope. In the end, all results will be compared to see how the two methods work in this case.

It is still important to note that the top cover planned in the new projects (**Figure 5.3**), that follows the prescriptions of *D. Lgs. 121/2020*, will not be taken into account for the calculations[10].

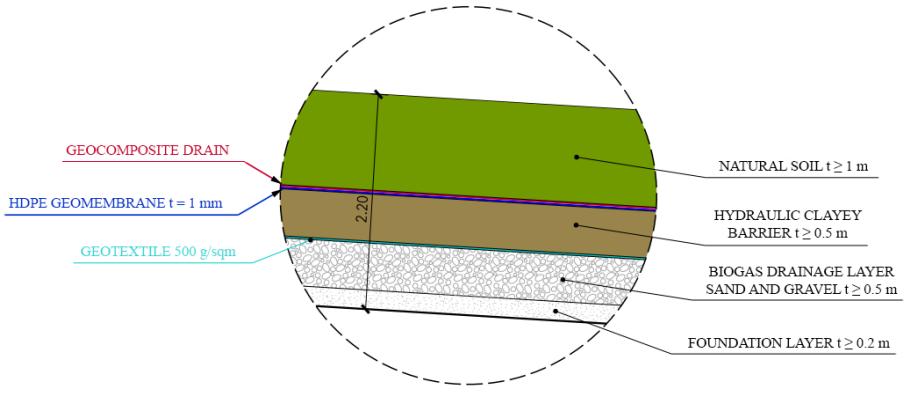

Figure 5.3 *Particular of the new top cover with the geocomposite drain*

[10] The final top cover for new projects based on *D. Lgs. 121/2020* will use a draining geocomposite instead of a classic gravel rainwater drainage layer. However, since a geomembrane is mandatory between the layers, a weak plastic-plastic surface prone to sliding failure is created. To address this problem, a 3D geogrid is introduced. The geogrid traction replaces the low attritional resistance of the interface between the two polymeric materials and indirectly also solves the stability issue between the BCL and hydraulic clayey barrier, by acting as an anchorage and preventing the clayey layer from the potential sliding due to excessive biogas pressures. Thus, this case is not considered in latter calculations.

5.1 THE KOERNER & SOONG METHOD

Figure 5.4 depicts a typical situation including a limited length, uniformly thick cover soil applied over a liner material at a slope angle of β. It has a passive wedge at the toe as well as a tension fracture on the crest. This method considers two wedges: the first is trapezoidal and defined as "active wedge", whereas the second is triangular and is defined as "passive wedge".

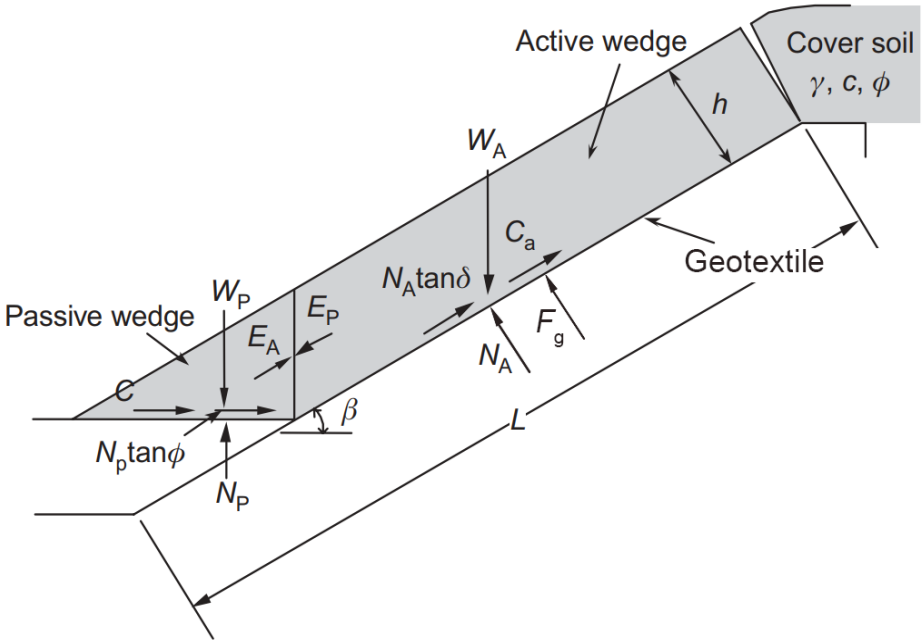

Figure 5.4 Limit equilibrium forces involved in a finite length slope analysis for a uniformly thick cover soil (Koerner & Soong, 1998)

The factors that are taken into consideration are:

- γ = unit weight of the cover soil;
- h = thickness of the cover soil;
- L = length of the slope measured along the geotextile;
- β = slope angle;
- u_g = biogas pressure;
- ϕ = friction angle of the cover soil;
- δ = interface friction angle between soil and geotextile;
- c_a = adhesion between soil and geotextile;
- c = cohesion of the cover soil.

The forces acting on the interface are:

- W_A = total weight of the active wedge;
- W_P = total weight of the passive wedge;
- N_A = effective force normal to the failure plane of the active wedge;
- N_P = effective force normal to the failure plane of the passive wedge;
- C_a = adhesive force between cover soil of the active wedge and the geotextile;
- C = cohesive force along the failure plane of the passive wedge;
- F_g = force applied on the interface by the uplifting biogas pressure;
- E_A = interwedge force acting on the active wedge from the passive wedge;
- E_P = interwedge force acting on the passive wedge from the active wedge;

FS will then identify the factor of safety for sliding.

It is important to note that, when calculating the friction at the interface between soil and geotextile, the lowest values (i.e., for δ and c_a) should be taken, which are the ones that determine the sliding surface.

The forces concerning the active wedge are:

$$W_A = \gamma h^2 \left(\frac{L}{h} - \frac{1}{\tan\beta} - \frac{\tan\beta}{2}\right) \quad 5.1$$

$$F_g = u_g h \left(L - \frac{h}{\tan\beta} - h\frac{\tan\beta}{2}\right) \quad 5.2$$

$$C_a = c_a \left(L - \frac{h}{\tan\beta}\right) \quad 5.3$$

$$N_A = W_A cos\beta - F_g \quad 5.4$$

Balancing the forces in the vertical direction, the following equation results:

$$E_A \sin\beta = W_A - N_A \cos\beta - F_g \cos\beta - \frac{N_A \tan\delta + C_a}{FS} \sin\beta \quad 5.5$$

That permits to define E_A:

$$E_A = \frac{(FS)[W_A(1 - \cos^2\beta)] - (N_A \tan\delta + C_A)\sin\beta}{(FS)\sin\beta} \quad 5.6$$

Considering the passive wedge, the forces are:

$$W_P = \frac{\gamma h^2}{\sin 2\beta} \quad 5.7$$

$$C_P = \frac{ch}{\sin \beta} \quad 5.8$$

$$N_P = W_P + E_P \sin \beta \quad 5.9$$

Balancing the forces in the horizontal direction:

$$E_P \cos \beta = \frac{C_P + N_P \tan \phi}{FS} \quad 5.10$$

Therefore obtaining:

$$E_P = \frac{C_P + W_P \tan \phi}{\cos \beta \, (FS) - \sin \beta \tan \phi} \quad 5.11$$

For the equilibrium, it must be $E_A = E_P$. Equalling the two expressions, a quadratic equation in the variable FS can be obtained:

$$a(FS)^2 + b(FS) + c = 0 \quad 5.12$$

Where the three coefficients are:

$$a = \cos \beta \, (W_A \sin^2 \beta) \quad 5.13$$

$$b = \sin \beta \tan \phi \, (-W_A \sin^2 \beta) - \sin \beta \cos \beta \, (N_A \tan \delta + C_a) - \sin \beta \, (C_P + W_P \tan \phi) \quad 5.14$$

$$c = \sin^2 \beta \tan \phi \, (C_a + N_A \tan \delta) \quad 5.15$$

Solving this equation and considering the positive solution, the value of FS can be obtained.

5.2 ANALYSIS AND COMPARISON OF THE RESULTS

As previously stated, the calculations on the Legnago landfill have been performed using the two methods of slope stability analysis (infinite slope and Koerner & Soong). These two methods permitted to establish the maximum allowable biogas pressure, once a proper FS has been chosen. When a u_{max} has been found, the calculation of the required permeability of the material will be carried out using the equations presented in Chapter 4.3. The unit weights of the layers above the BCL are shown in **Table 5.1**.

In the calculation of the total weight of the cover soil, for the sake of simplicity, a single layer of soil will be considered, of thickness $h = \sum h_{layer} = 2\ m$ and unit weight equal to the weighted average of the layers' unit weights, thus $\gamma_{cover} = 18.64\ kN/m^3$.

Table 5.1 *Weight of top cover soil layers*

LAYERS	h (m)	γ (kN/m³)
Clay	0,5	20
Gravel	0,5	18
Natural soil	1	18
TOTAL	**2**	**18,64**

Regarding interface coefficients, the interface friction angle (**Table 5.2**) will be taken as equal to $\delta = 28°$ and the adhesion coefficient $c_a = 5\ kPa$, based on the considerations made in Chapter 4.2.3.

Table 5.2 *Example of interface friction angles (TeMa Corporation, 2021)*

	Non-woven geotextile	HDPE smooth GM	Sand	Gravel	Topsoil
Non-woven geotextile		8°-14°	28°-30°	30°-33°	24°-26°
HDPE smooth GM	10°-12°		14°-18°		
Sand	28°-30°	8°-14°			

Gravel	32°-34°				
Topsoil	24°-28°				

For the cover soil, the internal friction angle will be considered $\phi = 30°$ and the cohesion c equal to zero. Moreover, when it comes to the FS to use in the calculations, a value of FS = 1.3 will be considered sufficient to ensure the safety to the sliding along the failure surface.

5.2.1 Escarpment: Infinite slope (IS) stability analysis

The Legnago landfill, in the worst case, possesses long escarpments ($L = 54.66\ m$) and a slope angle of $\beta = 21.8°$. With the parameters defined in the previous paragraphs of this section, the value of the maximum allowable pressure $u_{g,max}$ can be obtained using Equation *4.18*:

$$u_{g,max} = \gamma h \cos\beta - \frac{(FoS \cdot \gamma h \sin\beta - c_a)}{\tan\delta} \qquad 5.16$$

The correlation between u_g and FS is displayed in **Table 5.3** and **Figure 5.5**.

Table 5.3 *Values of FS related to different biogas pressures (escarpment, IS)*

$u_{g,max}$	FS		$u_{g,max}$	FS
0	1,690454		**9,5**	1,325668
0,5	1,671255		**10**	1,306469
1	1,652056		**10,5**	1,287269
1,5	1,632857		**11**	1,26807
2	1,613657		**11,5**	1,248871
2,5	1,594458		**12**	1,229672
3	1,575259		**12,5**	1,210472
3,5	1,556059		**13**	1,191273
4	1,53686		**13,5**	1,172074
4,5	1,517661		**14**	1,152874
5	1,498462		**14,5**	1,133675
5,5	1,479262		**15**	1,114476
6	1,460063		**15,5**	1,095277

6,5	1,440864		**16**	1,076077
7	1,421664		**16,5**	1,056878
7,5	1,402465		**17**	1,037679
8	1,383266		**17,5**	1,018479
8,5	1,364067		**18**	0,99928
9	1,344867		**18,5**	0,980081

From this analysis, for a FS of 1.3 corresponds a biogas pressure $u_{g,max} = 10.17\ kPa$, while to a FS of 1 (limit state) corresponds a pressure $u_{g,max} = 17.75\ kPa$. Thus, considering a value of $u_g = 10.17\ kPa$, it is possible to carry out the calculations described in Chapter 4.3 as proposed by Thiel. Being the biogas flux in the landfill equal to $\Phi_g = 3.52 \cdot 10^{-7}\ m^3/s \cdot m^2$ (Equation *4.1*) , the BCL thickness $t = 0.5\ m$, and the biogas unit weight $\gamma_g = 11.6\ N/m^3$ (Equation *4.38*), it is then possible to extrapolate the required water permeability k_w of the material forming the BCL, related to the distance between the two biogas strip drains D, using the following expressions already explained in Chapter 4.3.4:

$$\Psi_{g,min} = \frac{\gamma_g}{u_{g,max}} \Phi_g \left(\frac{D^2}{8}\right) \quad 5.17$$

$$\Psi_{g,d} = \Psi_{g,min} \cdot \prod_{i=1}^{4} CF_i \quad 5.18$$

$$k_g = \frac{\Psi_{g,design}}{t} \quad 5.19$$

$$k_w = 5 \cdot k_g \quad 5.20$$

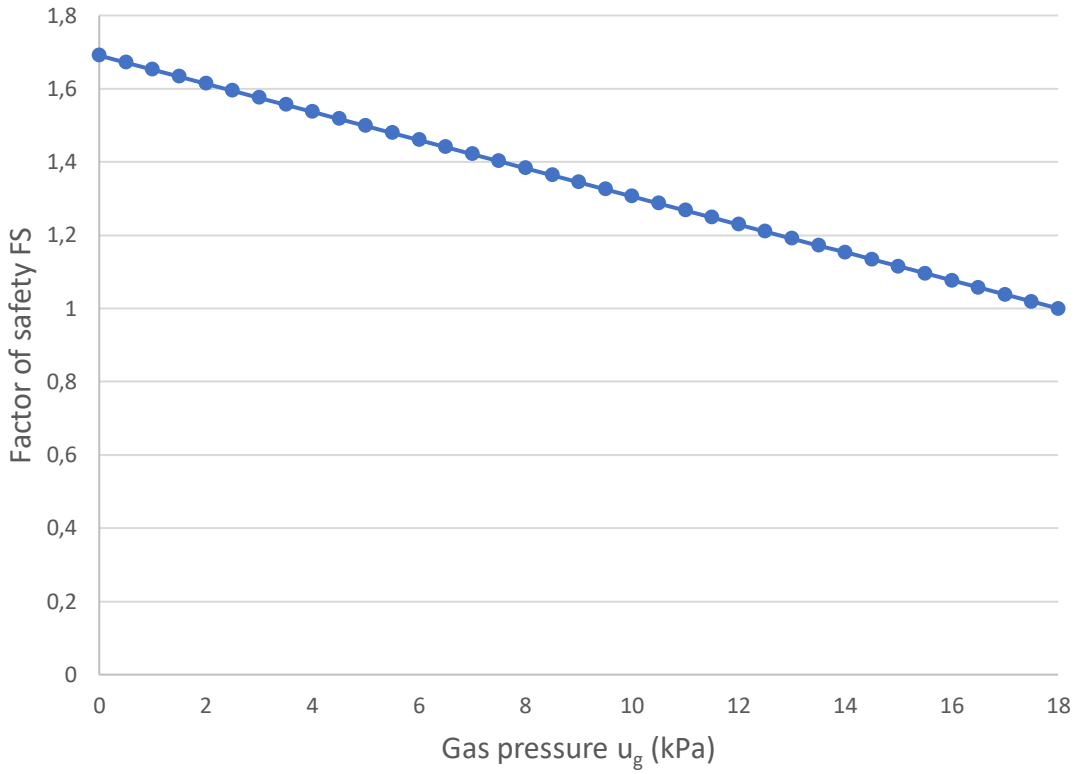

Figure 5.5 Correlation between u_g and FS (escarpment, IS)

Table 5.4 and **Figure 5.6** show the correlation between spacing of the gas vents and the hydraulic required permeability.

Table 5.4 Permeability to water required for different vent distances (escarpment, IS)

$D\ (m)$	ψ_{min}	ψ_d	k_g	k_w
0	0	0	0	0
1	5,02E-08	1,32E-07	2,65E-07	1,32E-06
2	2,01E-07	5,30E-07	1,06E-06	5,30E-06
3	4,52E-07	1,19E-06	2,38E-06	1,19E-05
4	8,03E-07	2,12E-06	4,24E-06	2,12E-05
5	1,25E-06	3,31E-06	6,62E-06	3,31E-05
6	1,81E-06	4,77E-06	9,54E-06	4,77E-05
7	2,46E-06	6,49E-06	1,30E-05	6,49E-05
8	3,21E-06	8,48E-06	1,70E-05	8,48E-05
9	4,07E-06	1,07E-05	2,15E-05	1,07E-04
10	5,02E-06	1,32E-05	2,65E-05	1,32E-04
11	6,07E-06	1,60E-05	3,21E-05	1,60E-04

12	7,23E-06	1,91E-05	3,82E-05	1,91E-04
13	8,48E-06	2,24E-05	4,48E-05	2,24E-04
14	9,84E-06	2,60E-05	5,19E-05	2,60E-04
15	1,13E-05	2,98E-05	5,96E-05	2,98E-04
16	1,28E-05	3,39E-05	6,78E-05	3,39E-04
17	1,45E-05	3,83E-05	7,66E-05	3,83E-04
18	1,63E-05	4,29E-05	8,59E-05	4,29E-04
19	1,81E-05	4,78E-05	9,57E-05	4,78E-04
20	2,01E-05	5,30E-05	1,06E-04	5,30E-04
21	2,21E-05	5,84E-05	1,17E-04	5,84E-04
22	2,43E-05	6,41E-05	1,28E-04	6,41E-04
23	2,65E-05	7,01E-05	1,40E-04	7,01E-04
24	2,89E-05	7,63E-05	1,53E-04	7,63E-04
25	3,14E-05	8,28E-05	1,66E-04	8,28E-04

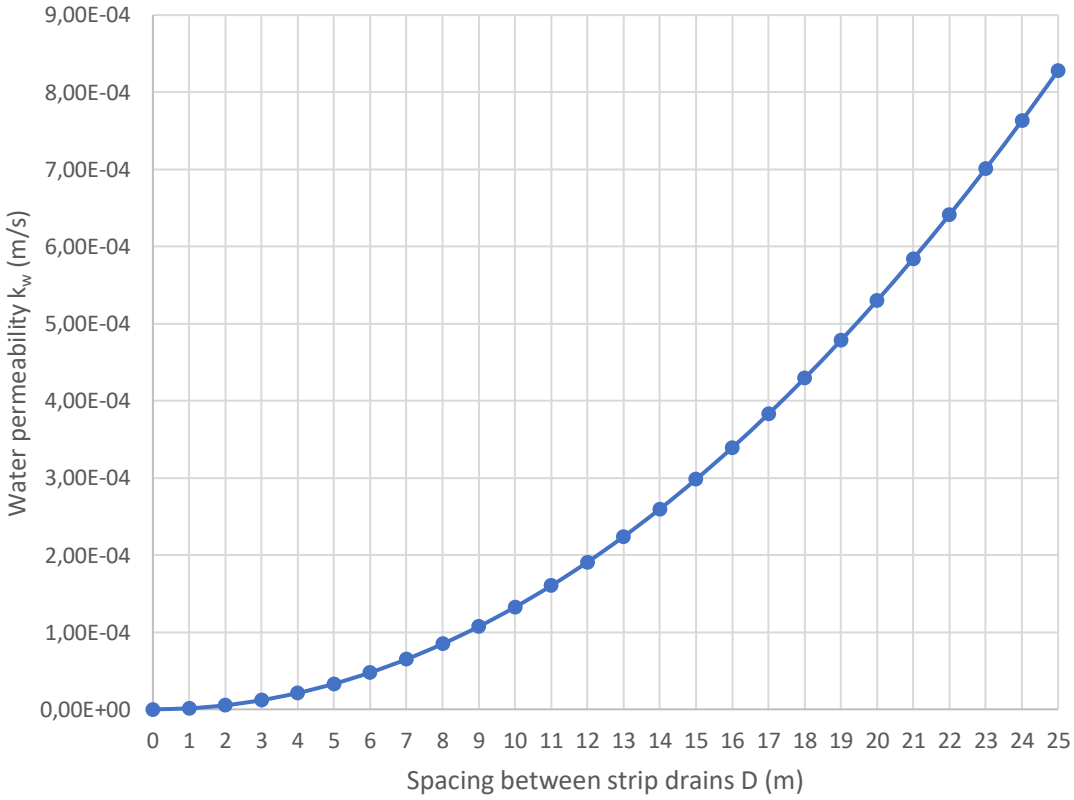

Figure 5.6 *Graph showing the correlation between distance D and permeability required (escarpment, IS)*

Once the distance between the gas collection strips running along the BCL has been determined, these calculations allow the designer to select a suitable material with the appropriate coefficient of permeability to water. However, it is important to underline

that k_w is not the only parameter to take into consideration when choosing the material for the construction of the BCL, but this matter will be discussed later in Chapter 6.

5.2.2 Escarpment: Koerner & Soong (KS) stability analysis

Using the same geometric and material parameters just selected, the analysis will be carried out using the Koerner & Soong method to determine the FS. It is reasonable to expect higher FS values respect to the ones given by the infinite slope method, related to the same values of u_g, since this method is less conservative.

Using the equations presented in Chapter 5.1, the results are presented in **Table 5.5** and **Figure 5.7**. In fact, this case, to a FS of 1.3 equals a biogas pressure $u_{g,max} = 13.4\ kPa$. Using the same equations as Chapter 5.2.1, it is then possible to determine the correlation between k_w and D, that will be used to efficiently design the BCL. The final results are shown in **Table 5.6** and **Figure 5.8**.

__Table 5.5__ Values of FS related to different biogas pressures (escarpment, KS)

$u_{g,max}$	F_g	N_A	a	b	c	FS
0	0,000	1705,382	235,196	-475,776	91,972	1,806
0,5	24,630	1680,753	235,196	-471,261	90,929	1,787
1	49,260	1656,123	235,196	-466,745	89,886	1,768
1,5	73,890	1631,493	235,196	-462,229	88,844	1,749
2	98,519	1606,863	235,196	-457,714	87,801	1,730
2,5	123,149	1582,233	235,196	-453,198	86,758	1,711
3	147,779	1557,603	235,196	-448,683	85,715	1,692
3,5	172,409	1532,974	235,196	-444,167	84,673	1,673
4	197,039	1508,344	235,196	-439,651	83,630	1,654
4,5	221,669	1483,714	235,196	-435,136	82,587	1,635
5	246,298	1459,084	235,196	-430,620	81,544	1,616
5,5	270,928	1434,454	235,196	-426,105	80,501	1,597
6	295,558	1409,824	235,196	-421,589	79,459	1,578
6,5	320,188	1385,195	235,196	-417,073	78,416	1,560
7	344,818	1360,565	235,196	-412,558	77,373	1,541
7,5	369,448	1335,935	235,196	-408,042	76,330	1,522
8	394,077	1311,305	235,196	-403,527	75,288	1,503
8,5	418,707	1286,675	235,196	-399,011	74,245	1,484

9	443,337	1262,045	235,196	-394,495	73,202	1,465
9,5	467,967	1237,416	235,196	-389,980	72,159	1,446
10	492,597	1212,786	235,196	-385,464	71,117	1,427
10,5	517,227	1188,156	235,196	-380,949	70,074	1,408
11	541,856	1163,526	235,196	-376,433	69,031	1,389
11,5	566,486	1138,896	235,196	-371,917	67,988	1,370
12	591,116	1114,266	235,196	-367,402	66,946	1,351
12,5	615,746	1089,637	235,196	-362,886	65,903	1,333
13	640,376	1065,007	235,196	-358,371	64,860	1,314
13,5	665,006	1040,377	235,196	-353,855	63,817	1,295
14	689,635	1015,747	235,196	-349,339	62,775	1,276
14,5	714,265	991,117	235,196	-344,824	61,732	1,257
15	738,895	966,487	235,196	-340,308	60,689	1,239

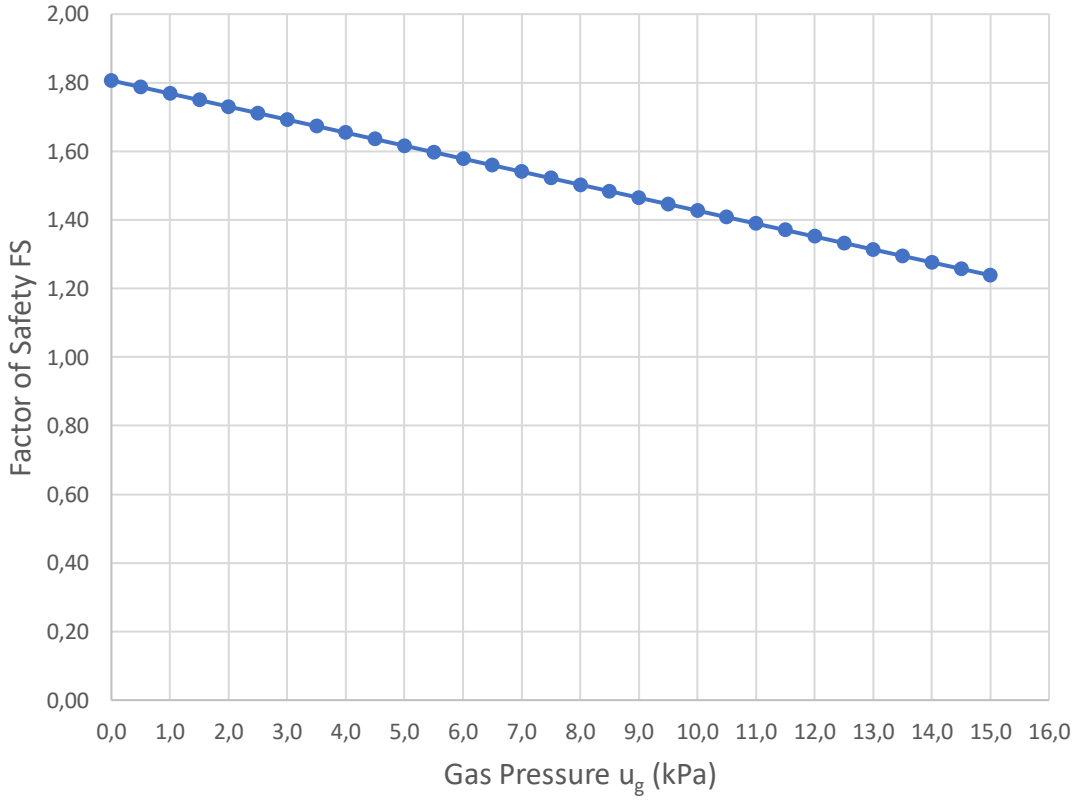

Figure 5.7 *Correlation between u_g and FS (escarpment, KS)*

Table 5.6 Permeability to water required for different vent distances (escarpment, KS)

$D\ (m)$	ψ_{min}	ψ_d	k_g	k_w
0	0	0	0	0
1	3,81E-08	1,01E-07	2,01E-07	1,01E-06
2	1,52E-07	4,02E-07	8,04E-07	4,02E-06
3	3,43E-07	9,05E-07	1,81E-06	9,05E-06
4	6,09E-07	1,61E-06	3,22E-06	1,61E-05
5	9,52E-07	2,51E-06	5,03E-06	2,51E-05
6	1,37E-06	3,62E-06	7,24E-06	3,62E-05
7	1,87E-06	4,93E-06	9,85E-06	4,93E-05
8	2,44E-06	6,44E-06	1,29E-05	6,44E-05
9	3,09E-06	8,15E-06	1,63E-05	8,15E-05
10	3,81E-06	1,01E-05	2,01E-05	1,01E-04
11	4,61E-06	1,22E-05	2,43E-05	1,22E-04
12	5,48E-06	1,45E-05	2,90E-05	1,45E-04
13	6,44E-06	1,70E-05	3,40E-05	1,70E-04
14	7,47E-06	1,97E-05	3,94E-05	1,97E-04
15	8,57E-06	2,26E-05	4,53E-05	2,26E-04
16	9,75E-06	2,57E-05	5,15E-05	2,57E-04
17	1,10E-05	2,91E-05	5,81E-05	2,91E-04
18	1,23E-05	3,26E-05	6,52E-05	3,26E-04
19	1,38E-05	3,63E-05	7,26E-05	3,63E-04
20	1,52E-05	4,02E-05	8,04E-05	4,02E-04
21	1,68E-05	4,43E-05	8,87E-05	4,43E-04
22	1,84E-05	4,87E-05	9,73E-05	4,87E-04
23	2,01E-05	5,32E-05	1,06E-04	5,32E-04
24	2,19E-05	5,79E-05	1,16E-04	5,79E-04
25	2,38E-05	6,28E-05	1,26E-04	6,28E-04

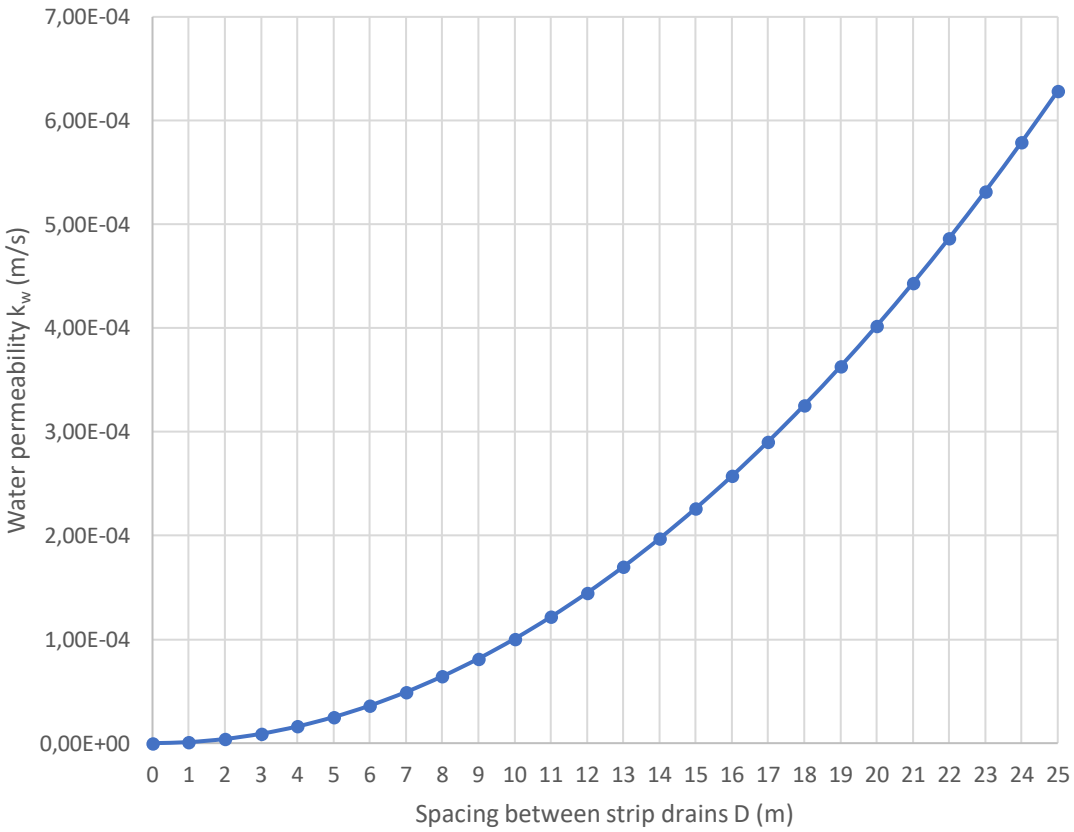

Figure 5.8 *Graph showing the correlation between distance D and permeability required (escarpment, KS)*

5.2.3 Summit cover: Infinite slope (IS) stability analysis

For the sake of completeness, the results regarding the summit cover will be presented. The cover located in the upper part of the landfill has the same exact characteristics as the one on the escarpment, but possesses a much less inclined slope, with a gradient of $\beta = 5.4°$. For this reason, the stability of this part of the cover is not of particular interest but will be treated also to understand the weight of β in the two different cases.

Tables**Table 5.7** and**Table 5.8** together with Figures**Figure 5.9** and**Figure 5.10** display the results obtained.

Table 5.7 Values of FS related to different biogas pressures (summit cover, IS)

$u_{g,max}$	FS		$u_{g,max}$	FS
0	7,050		**21**	3,868
1	6,898		**22**	3,716
2	6,747		**23**	3,565
3	6,595		**24**	3,413
4	6,444		**25**	3,262
5	6,292		**26**	3,110
6	6,141		**27**	2,959
7	5,989		**28**	2,807
8	5,838		**29**	2,656
9	5,686		**30**	2,504
10	5,535		**31**	2,352
11	5,383		**32**	2,201
12	5,231		**33**	2,049
13	5,080		**34**	1,898
14	4,928		**35**	1,746
15	4,777		**36**	1,595
16	4,625		**37**	1,443
17	4,474		**38**	1,292
18	4,322		**39**	1,140
19	4,171		**40**	0,989
20	4,019		**41**	0,837

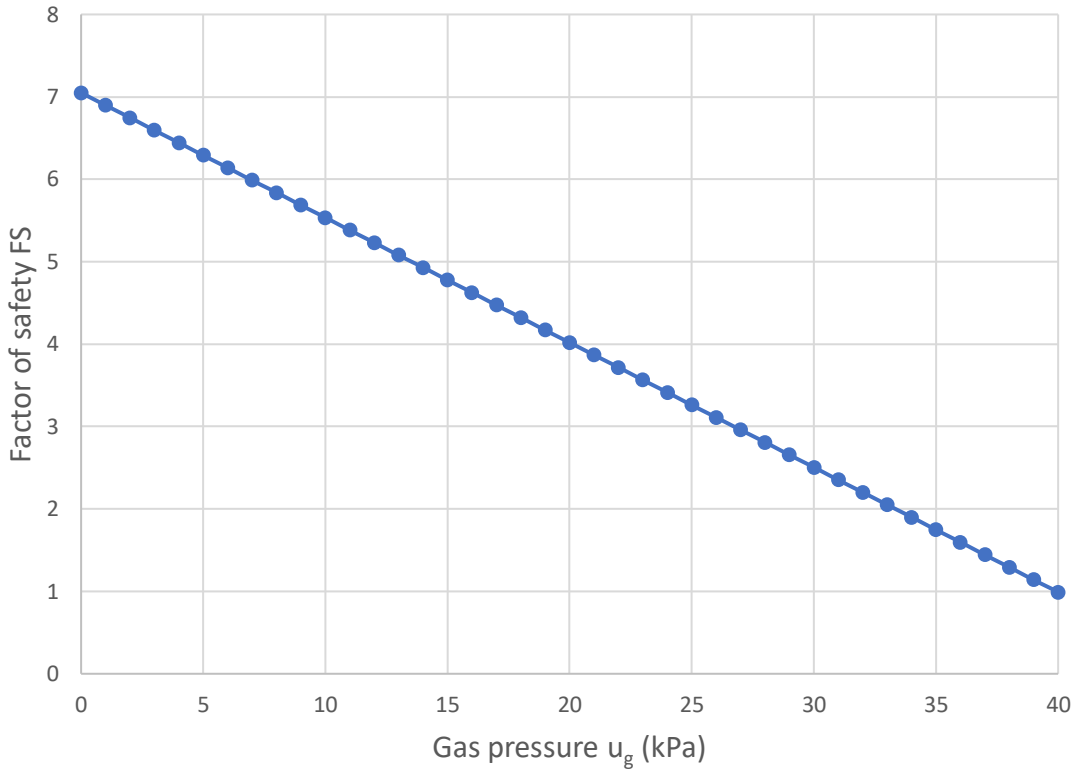

Figure 5.9 *Correlation between ug and FS (summit cover, IS)*

Factor of Safety FS is 1.3 with $u_g = 37.5\ kPa$.

Table 5.8 *Permeability to water required for different vent distances (summit cover, IS)*

$D\ (m)$	ψ_{min}	ψ_d	k_g	k_w
0	0	0	0	0
1	1,36E-08	3,59E-08	7,19E-08	3,59E-07
2	5,44E-08	1,44E-07	2,87E-07	1,44E-06
3	1,22E-07	3,23E-07	6,47E-07	3,23E-06
4	2,18E-07	5,75E-07	1,15E-06	5,75E-06
5	3,40E-07	8,98E-07	1,80E-06	8,98E-06
6	4,90E-07	1,29E-06	2,59E-06	1,29E-05
7	6,67E-07	1,76E-06	3,52E-06	1,76E-05
8	8,71E-07	2,30E-06	4,60E-06	2,30E-05
9	1,10E-06	2,91E-06	5,82E-06	2,91E-05
10	1,36E-06	3,59E-06	7,19E-06	3,59E-05
11	1,65E-06	4,35E-06	8,70E-06	4,35E-05

12	1,96E-06	5,17E-06	1,03E-05	5,17E-05
13	2,30E-06	6,07E-06	1,21E-05	6,07E-05
14	2,67E-06	7,04E-06	1,41E-05	7,04E-05
15	3,06E-06	8,08E-06	1,62E-05	8,08E-05
16	3,48E-06	9,20E-06	1,84E-05	9,20E-05
17	3,93E-06	1,04E-05	2,08E-05	1,04E-04
18	4,41E-06	1,16E-05	2,33E-05	1,16E-04
19	4,91E-06	1,30E-05	2,59E-05	1,30E-04
20	5,44E-06	1,44E-05	2,87E-05	1,44E-04
21	6,00E-06	1,58E-05	3,17E-05	1,58E-04
22	6,59E-06	1,74E-05	3,48E-05	1,74E-04
23	7,20E-06	1,90E-05	3,80E-05	1,90E-04
24	7,84E-06	2,07E-05	4,14E-05	2,07E-04
25	8,51E-06	2,25E-05	4,49E-05	2,25E-04

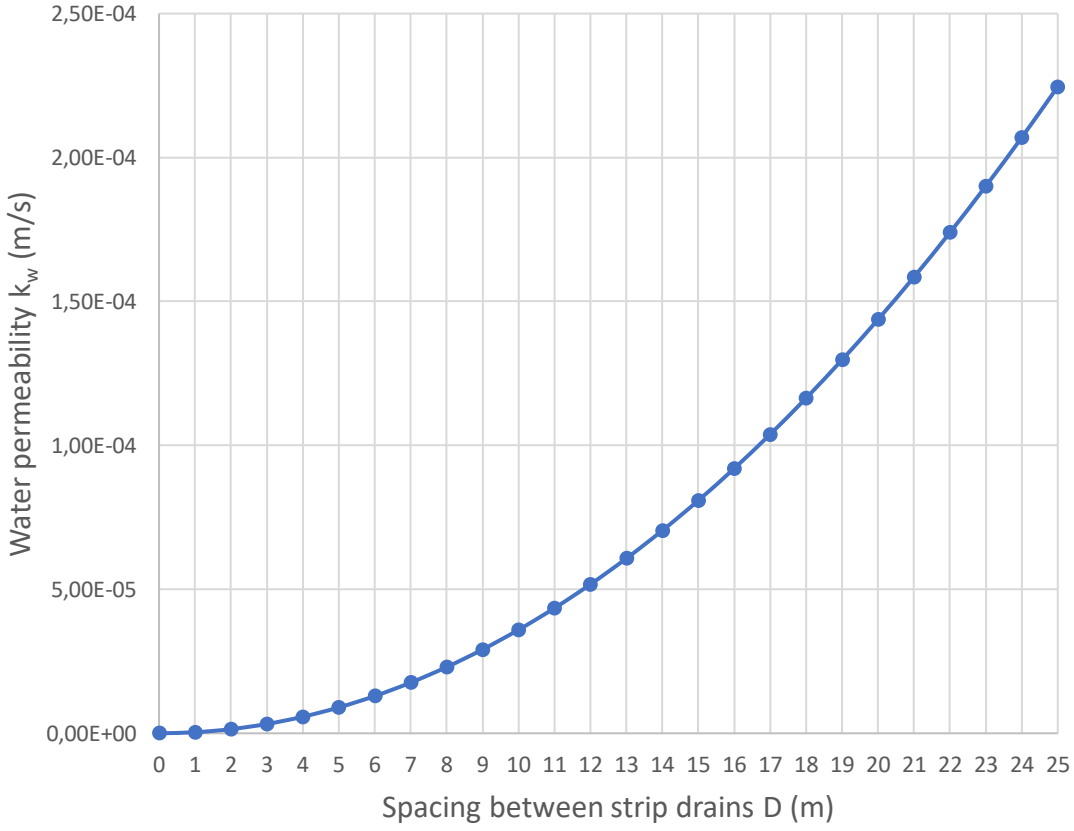

Figure 5.10 *Graph showing the correlation between distance D and permeability required (summit cover, IS)*

5.2.4 Summit cover: Koerner & Soong (KS) stability analysis

Tables**Table 5.9** and**Table 5.10**, together with Figures **Figure 5.11** and **Figure 5.12**, display the results obtained using the Koerner & Soong stability analysis on the summit cover.

Table 5.9 *Values of FS related to different biogas pressures (summit cover, KS)*

u_g	F_g	N_A	a	b	c	FS
0,0	0,00	3739,89	33,12	-256,98	12,75	7,71
1,5	151,12	3588,76	33,12	-249,45	12,34	7,48
3,0	302,24	3437,64	33,12	-241,92	11,92	7,25
4,5	453,36	3286,52	33,12	-234,39	11,51	7,03
6,0	604,49	3135,40	33,12	-226,86	11,10	6,80
7,5	755,61	2984,28	33,12	-219,34	10,69	6,57
9,0	906,73	2833,16	33,12	-211,81	10,28	6,35
10,5	1057,85	2682,04	33,12	-204,28	9,87	6,12
12,0	1208,97	2530,91	33,12	-196,75	9,46	5,89
13,5	1360,09	2379,79	33,12	-189,22	9,05	5,66
15,0	1511,22	2228,67	33,12	-181,69	8,64	5,44
16,5	1662,34	2077,55	33,12	-174,17	8,23	5,21
18,0	1813,46	1926,43	33,12	-166,64	7,82	4,98
19,5	1964,58	1775,31	33,12	-159,11	7,40	4,76
21,0	2115,70	1624,18	33,12	-151,58	6,99	4,53
22,5	2266,82	1473,06	33,12	-144,05	6,58	4,30
24,0	2417,94	1321,94	33,12	-136,53	6,17	4,08
25,5	2569,07	1170,82	33,12	-129,00	5,76	3,85
27,0	2720,19	1019,70	33,12	-121,47	5,35	3,62
28,5	2871,31	868,58	33,12	-113,94	4,94	3,40
30,0	3022,43	717,46	33,12	-106,41	4,53	3,17
31,5	3173,55	566,33	33,12	-98,88	4,12	2,94
33,0	3324,67	415,21	33,12	-91,36	3,71	2,72
34,5	3475,80	264,09	33,12	-83,83	3,30	2,49
36,0	3626,92	112,97	33,12	-76,30	2,89	2,27
37,5	3778,04	-38,15	33,12	-68,77	2,47	2,04
39,0	3929,16	-189,27	33,12	-61,24	2,06	1,81
40,5	4080,28	-340,40	33,12	-53,71	1,65	1,59

42,0	4231,40	-491,52	33,12	-46,19	1,24	1,37
43,5	4382,52	-642,64	33,12	-38,66	0,83	1,15
45,0	4533,65	-793,76	33,12	-31,13	0,42	0,93

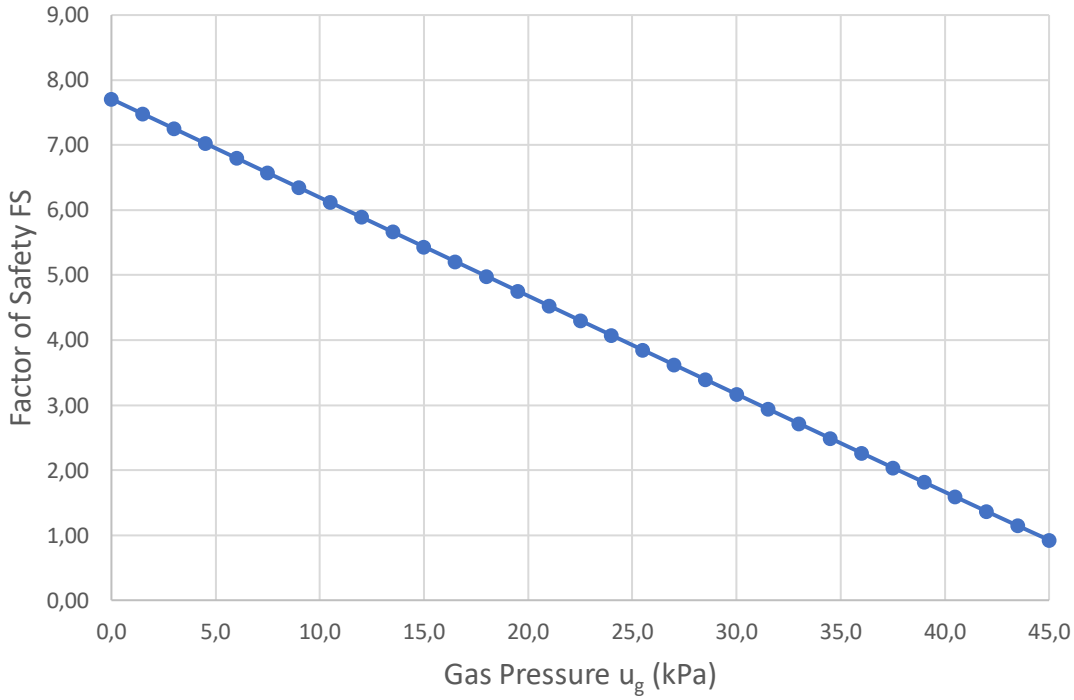

Figure 5.11 *Correlation between ug and FS (summit cover, KS)*

In this case, to a FS of 1.3 corresponds a gas pressure $u_g = 42.4\ kPa$.

Table 5.10 *Permeability to water required for different vent distances (summit cover, KS)*

$D\ (m)$	ψ_{min}	ψ_d	k_g	k_w
0	0	0	0	0
1	1,20E-08	3,18E-08	6,36E-08	3,18E-07
2	4,82E-08	1,27E-07	2,54E-07	1,27E-06
3	1,08E-07	2,86E-07	5,72E-07	2,86E-06
4	1,93E-07	5,08E-07	1,02E-06	5,08E-06
5	3,01E-07	7,94E-07	1,59E-06	7,94E-06
6	4,33E-07	1,14E-06	2,29E-06	1,14E-05
7	5,90E-07	1,56E-06	3,11E-06	1,56E-05
8	7,70E-07	2,03E-06	4,07E-06	2,03E-05
9	9,75E-07	2,57E-06	5,15E-06	2,57E-05

10	1,20E-06	3,18E-06	6,36E-06	3,18E-05
11	1,46E-06	3,85E-06	7,69E-06	3,85E-05
12	1,73E-06	4,58E-06	9,15E-06	4,58E-05
13	2,03E-06	5,37E-06	1,07E-05	5,37E-05
14	2,36E-06	6,23E-06	1,25E-05	6,23E-05
15	2,71E-06	7,15E-06	1,43E-05	7,15E-05
16	3,08E-06	8,14E-06	1,63E-05	8,14E-05
17	3,48E-06	9,18E-06	1,84E-05	9,18E-05
18	3,90E-06	1,03E-05	2,06E-05	1,03E-04
19	4,35E-06	1,15E-05	2,29E-05	1,15E-04
20	4,82E-06	1,27E-05	2,54E-05	1,27E-04
21	5,31E-06	1,40E-05	2,80E-05	1,40E-04
22	5,83E-06	1,54E-05	3,08E-05	1,54E-04
23	6,37E-06	1,68E-05	3,36E-05	1,68E-04
24	6,93E-06	1,83E-05	3,66E-05	1,83E-04
25	7,52E-06	1,99E-05	3,97E-05	1,99E-04

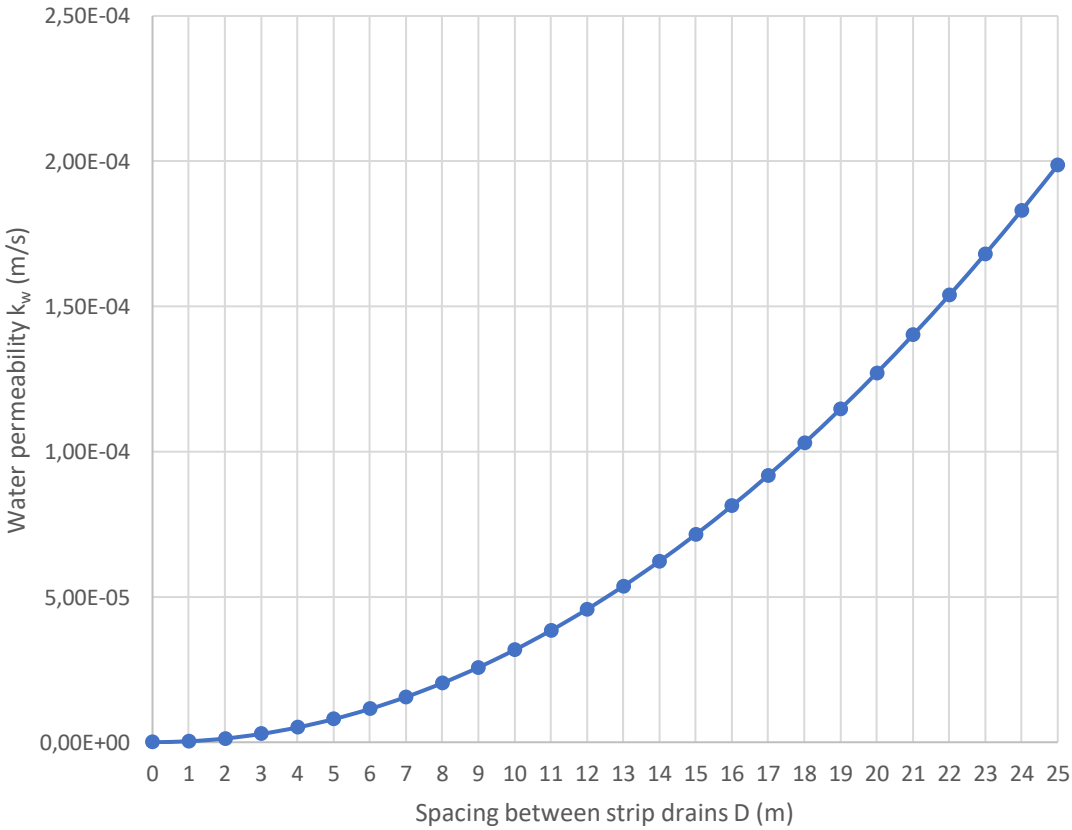

Figure 5.12 *Graph showing the correlation between distance D and permeability required (summit cover, KS)*

5.3 VALIDITY OF THE HYPOTESIS

When first deriving the design equations in Chapter 4.3.1, the assumption of laminar flow inside the porous media of the BCL has been assumed as true, to allow the use of the Darcy's law. To address a feasible method to confirm the hypothesis, an example of a possible case that could be also suited for the Legnago landfill will be examined.

The condition for the flow to be laminar is considered to be $Re < 1$ for the flow of fluid in porous media (Chapter 4.3.1). Supposing the thickness of the BCL $t = 0.5\,m$ and a distance between strip drains equal to $D = 25\,m$, the hypothetical material will be a medium sand, with an average particle size $d = 1\,mm$. The gas flow through the BCL will be the one used for the calculations, thus $\Phi_g = 3.52 \cdot 10^{-7}\,m^3/s \cdot m^2$.

With these parameters it is possible to calculate the maximum gas flow rate, Q, from the half-distance between strip drains per unit width:

$$Q = \Phi_g \cdot \frac{D}{2} \cdot 1 = 3.52 \cdot 10^{-7} \left[\frac{m^3}{s \cdot m^2}\right] \cdot \frac{25\ [m]}{2} \cdot 1\ [m] = 4.4 \cdot 10^{-6}\ \frac{m^3}{s} \qquad 5.21$$

Being the Reynolds number defined as:

$$Re = \frac{\rho v d}{\mu} \qquad 5.22$$

with, for this case, ρ = biogas density, μ = biogas dynamic viscosity, v = biogas velocity, and d = average particle size.

Velocity can be easily calculated as:

$$v = \frac{Q}{A} = \frac{4.4 \cdot 10^{-6}\ [m^3/s]}{0.5\ [m] \cdot 1\ [m]} = 8.8 \cdot 10^{-6}\ \frac{m}{s} \qquad 5.23$$

and, considering the biogas density $\rho = 1.18\ kg/m^3$ and the biogas dynamic viscosity $\mu = 12.6 \cdot 10^{-6}\,kg/s \cdot m$, it is possible to calculate the corresponding Reynolds number:

$$Re = \frac{1.18\ [kg/m^3] \cdot 8.8 \cdot 10^{-6}\ [m/s] \cdot 0.001\ [m]}{12.6 \cdot 10^{-6}[kg/s \cdot m]} = 8.2 \cdot 10^{-4} \ll 1 \qquad 5.24$$

Thus, for this case, since the Reynolds number is significantly lower than 1, the flow can be safely considered laminar and Darcy's law can be applied.

5.4 THE DESIGN CHOICE

Until this point of the thesis, the work of Thiel has been taken as model to perform the calculations, therefore considering the gas vents as linear drains that run along the slope. However, this one is not the only possible solution for the design of the collection system, as the case of Legnago landfill shows. In fact, in Legnago, the collection system consists in coil-shaped pipes disposed all over the landfill area (**Figure 5.13**).

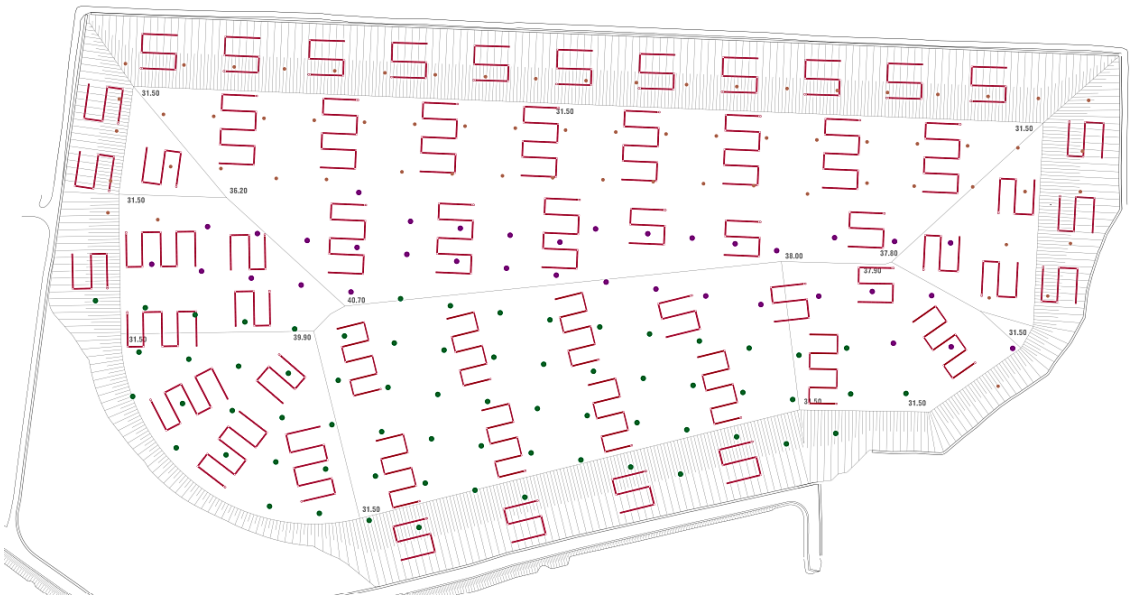

Figure 5.13 *Gas collection system for the Torretta di Legnago landfill, consisting in coil-shaped pipes (in red) and gas extraction wells (points)*

This solution, not widely utilised, could indeed help to improve the collection efficiency of the extraction system, with a possibility of savings in terms of material usage and costs. In fact, this disposition involves a larger zone of influence compared with the linear drains. However, the assessment of the magnitude of the effect of coil-shaped drains is based on a lot of different factors, mainly fluid dynamic related, that can be successfully evaluated using methods such as Computational Fluid Dynamics (CFD) or Finite Element Method (FEM).

Based on the assumptions made in the previous sections of this work, using the model of Thiel, an example of possible disposition of the pipes is shown in **Figure 5.14**.

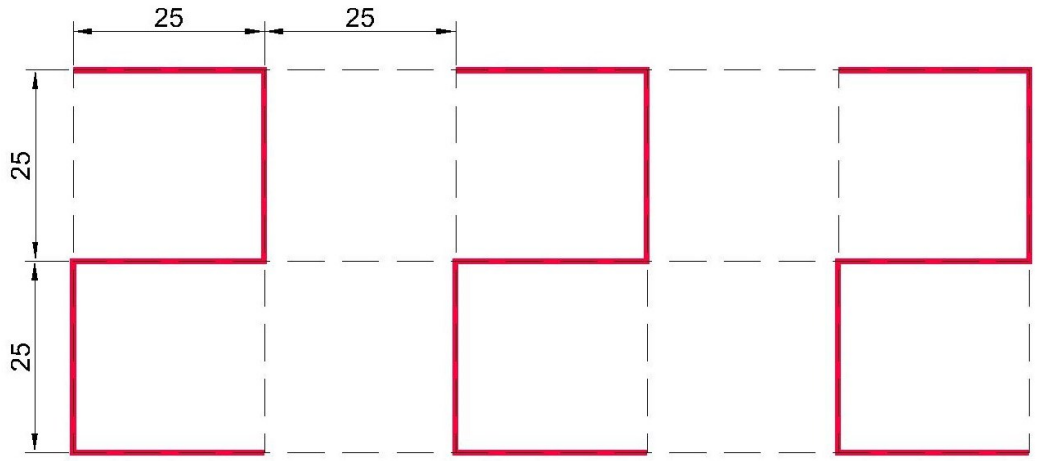

Figure 5.14 Possible disposition of coil-shaped pipes

For example, in this case, considering these pipes as linear at a distance of 25 meters from each other, if located on the escarpment of the landfill, the coefficient of permeability to water of the porous media to ensure the cover stability can be retrieved from **Table 5.6**. It can be seen that to a distance $D = 25\,m$ corresponds a permeability $k_w = 6.28 \cdot 10^{-4}\ m/s$, that can be approximated at $k_w = 1 \cdot 10^{-3}\ m/s$ for the sake of simplicity and safety. As stated before, this is an approximation that does not take into account the positive effect that this particular shape could have on the efficiency, thus it is legitimate to expect lower values of k_w. However, the assessment of the magnitude of the shape effect is not considered in this work.

It is important to note that, usually, the use of horizontal collectors is not common practice, and the gas extraction systems only relies on vertical wells. These wells, usually positioned at a distance of 25 – 30 m from each other, in many cases do not succeed to ensure an optimal extraction efficiency, risking to compromise the stability of the top cover. This is due to the fact that, more than based on case-specific calculations, the decision of the distance between the wells is based on common practice.

However, from the results of the analyses performed in the previous chapter, it is clear that the biogas has a serious effect on the stability of the cover, even with low pressures. Thus, when constructing the BCL, it should be important to follow a specific procedure like the one presented in this work, to avoid neglecting this crucial problem. For this reason, the use of horizontal collectors instead of vertical wells (or together) should be considered as a good, if not needed, design solution. In fact, this solution helps providing

a more homogeneous collection of the biogas, avoiding the eventual formation of preferred pathways or “dead spots” which could result in excessive pressures on the top cover. In addition, the use of horizontal collectors is less invasive in terms of construction and operation, since it does not require deep excavation like the vertical wells.

6 MATERIALS FOR BCL DESIGN

In the analysis carried out in the previous sections of this thesis, the principal parameter determined regarding the material to be used for the construction of the BCL is the hydraulic conductivity k_w. Undoubtedly, the conductivity is an important factor to take into account when it comes to the selection of a suitable material, but it is certainly not the only aspect that must be considered. In fact, Raut (2006) identifies three main requisites that a generic granular filter must possess:

1. As indicated in **Figure 6.1**, the filter must be fine enough to capture some of the larger particles of the protected core material (also known as the base soil). These trapped particles clog the filter voids, retaining the finer fraction of the base soil;
2. The filter must be coarse enough to allow seepage flow to pass through it, preventing the accumulation of high internal pore pressures and emptying all seepage water from the dam, avoiding saturation of the downstream fill;
3. The filter must be non-cohesive. Within the cohesive core soils, cavities or cracks may occur. Thus, to be effective, the protective filter must have low cohesion.

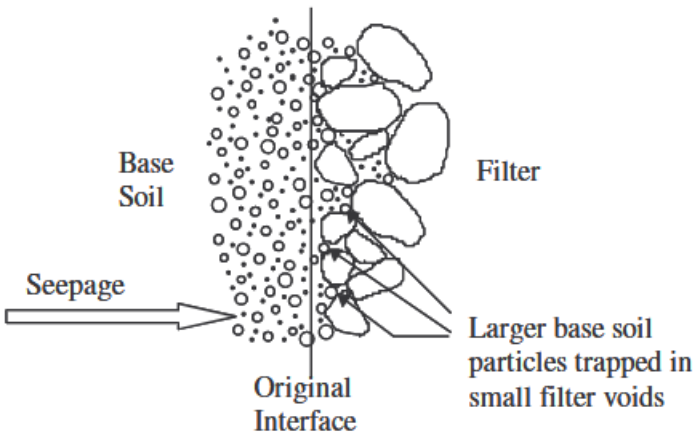

Figure 6.1 *A stable base-filter interface during seepage (Raut, 2006)*

When studying the feasibility of a new material for its application as a granular filter for the design of a biogas collection layer, it may be required to achieve suitable standards in terms of:

- **Landfill conferability**: the material must be considered "landfill-eligible" in order to be used in the landfill; thus, the analytical limits related to the eligibility

criteria for non-hazardous waste, as regulated by *D. Lgs. 121/2020*, must be checked during acceptance verification;

- **Mechanical strength and resilience**: it is important to determine whether the grain size distribution (GSD) remains unchanged in the face of the stresses that might develop as a result of the construction-induced loads of the overlying layers;
- **Granulometric compatibility**: in order to prevent the coarser particle size classes from passing the base layer underneath them, penetrating it, and thereby depleting the biogas drainage layer of such fractions, it is crucial to define the minimum diameters of these particle size classes;
- **Internal stability**: this procedure seeks to determine if the layer within it has the capacity to hold all of the particle size fractions in order to avoid their migration to the outside, which would deplete the particle composition;
- **Hydraulic conductivity**: the material must possess an appropriate permeability to permit the flow of biogas without the development of excessive pore pressures inside the filter.

In this section, the framework for the acceptance of a material to be used for the BCL construction will be presented (scheme in **Figure 6.2**).

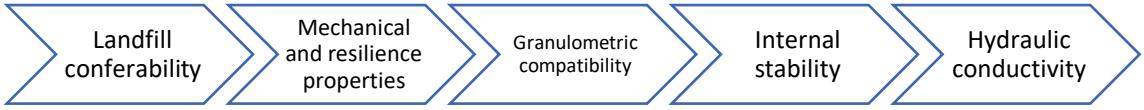

Figure 6.2 *Procedure for the acceptance of a BCL-forming material*

6.1 LANDFILL CONFERABILITY

Since the aim of this thesis is to find proper waste materials to use as granular filter for the BCL, the first step for the assessment is the evaluation of its admissibility in the landfill. *D. Lgs. 121/2020* sets the rules for the type of waste that can be introduced. In fact, a certain type of waste shall be accepted exclusively if it meets the eligibility criteria of the corresponding landfill category. As a first step, every incoming waste must undergo a treatment as indicated in D. Lgs. 152/2006 before disposal in the landfill.

The most quantitatively significant treatment operations are:

- Biological treatments;

- Physicochemical treatments;
- Preliminary grouping and reconditioning treatments;
- Incineration.

However, treatment is not mandatory in the case of inert materials that cannot technically undergo the process. Moreover, when disposing wastes containing or contaminated with persistent organic pollutants, the provisions of *Regulation (EU) No. 2019/1021* must be followed.

After the treatment, in order to determine the eligibility of waste in each landfill category, the waste producer is required to carry out basic characterization, mandatory for each type of waste delivered to the landfill. Characterization must be carried out prior to landfilling or after the last treatment performed, by persons and institutions independent and qualified. Laboratories must have demonstrated experience sampling and analysing waste, as well as an effective quality control system. Waste producers or operators may conduct sampling and analytical determinations if they have established an appropriate quality assurance system, including independent periodic monitoring.

Sampling of the waste mass to be subjected to subsequent analysis should be carried out taking into account the merceological composition, according to the *CII-Uni 9246 Standard*. On the other hand, for the purpose of chemical and physical characterization, the analysis shall be carried out in such a way as to obtain a representative sample according to the criteria, procedures, and methods of *Uni 10802*, *Uni En 14899*, and *Uni En 15002*.

For example, *D. Lgs. 121/2020* sets concentration limits in the eluates for acceptability of stable and non-reactive hazardous waste in landfills for non-hazardous waste (**Table 6.1**).

Table 6.1 *Eluate concentration limits for acceptability of stable non-reactive hazardous waste in landfills for non-hazardous waste (D. Lgs. 121/2020)*

Parameter	Concentration (mg/l)
As	0.2
Ba	10
Cd	0.1
Total Cr	1
Cu	5

Hg	0.02
Mo	1
Ni	1
Pb	1
Sb	0.07
Se	0.05
Zn	5
Chlorides	1500
Fluorides	15
Sulphides	2000
DOC [11]	80
TDS [12]	6000

Moreover, another important parameter to evaluate is the TOC ("Total Organic Carbon") present in the sample, the limit of which is fixed at 5% of the total.

It is only after a correct determination of the chemical and physical characteristics of the waste, confirming its eligibility to be disposed in the landfill, that all the other considerations can be carried out.

6.2 MECHANICAL STRENGHT AND RESILIENCE

One important concept that must be kept in mind is that, when performing evaluations on the material properties, the sample should undergo a process to determine its strength and resistance. In fact, the material can show excellent properties if the tests are performed as it is on its arrival on the site. The problem is that, when it is applied on the BCL, the particles could undergo crushing and erosion processes, as a result of the loadings that it must endure during its installation and lifecycle. Particle crushing must be minimized to prevent unfavourable production of fines, which inevitably affect material permeability. This may compromise the achievement of the granulometric compatibility and, thus, the stability of the structure. This eventuality could result in serious depletion of the layer properties, posing the risk of unexpected problems.

[11] Dissolved Organic Carbon.
[12] Total Dissolved Solids.

However, it may be worthwhile, before proceeding with more accurate tests, to have a general understanding of the order of magnitude of the hydraulic permeability of the material under examination. This could be very useful because it can give the designer immediate feedback to help understand if it is worth it to go ahead with the procedure or if the material is not likely to meet the desired requirements.

To perform this evaluation, some formulas that correlate GSD and hydraulic permeability have been developed. Maybe the most used one, generally for loose sands, is the Hazen formula:

$$k_w = c \cdot (D_{10})^2 \tag{6.1}$$

that calculates the hydraulic permeability k_w $[cm/s]$ in relation to D_{10} $[cm]$, which is the sieve width that allows 10% by weight of the granular material sample to pass through. The constant c can be assumed equal to 100.

Another empiric formula that can be utilized is the following:

$$k_w = 1.02 \cdot (D_5 \cdot D_{10})^{0.93} \tag{6.2}$$

where k_w $[cm/s]$ is correlated both to D_{10} and D_5 (sieve width that allows 5% by weight of the granular material sample to pass through).

As already stated, these formulas are useful to provide the designer with a first glance at the possible order of magnitude of k_w, but later it is mandatory to determine the exact value of the permeability using more accurate tests, such as constant head or variable head permeameters.

After this first evaluation, it is important to find a way to test how the material will work under the conditions that will be present on the site. To provide a solution to this challenge, Cortellazzo et al. (2021) came up with an innovative test, referred to as Cyclic Static Punching (CSP) test. In particular, its use has been studied for the evaluation of the properties of glass cullet before and after crushing phenomena.

It is, for example, important for the material to not show possible relevant interlocking tendency. Interlocking in granular materials can be defined qualitatively as a situation in which particles or grains lock together and give additional resistance to deformation. Any granular assembly's interlocking is solely a geometrical property (Bindal et al., 2020). Various studies derive interlocking indirectly from microscopic properties of granular

materials such as friction, cohesion, form, rotation, and translation. Interlocking in granular materials has traditionally been regarded as shearing resistance, and hence intergranular friction is increased to account for this effect.

The goal of the test is to replicate the stress states that the material experiences as a result of specific quasi-static loading situations brought on in situ by the compaction machine's slow passage over the mineral liners. These quasi-static loading conditions are replicated through a sequence of successive static punchings, performed using an oleo-pneumatic piston press. When the design pressure is reached (correspondent to the specific site conditions), it is maintained for around one second. After dry sieving the specimen as it is, to determine the initial GSD, CSP test is performed placing the material in a mold, subject to a loading by a circular plate of different diameters for comparative purposes. The first one has a diameter D = 130 mm and the second a diameter D = 150 mm.

The number of static punchings is set at 10, based on the estimated number of dumpers passes in situ, and the rate of loading and unloading phases is indicative of in situ observed conditions. After that, another dry sieving is performed to determine the final GSD. Finally, two constant head permeability tests are performed: the first on the material as it is; the second on the material after being subjected to compaction using the 130 mm circular plate. In this way, it is possible to determine how the change in void ratio and in GSD can possibly alter the conductivity values of the material.

For example, for glass cullet, the void ratio evolution during the CSP test can be observed in **Figure 6.3**. During the experiments, the void ratio increased by 18% to 25% after the first punching and 23% to 32% after ten punchings.

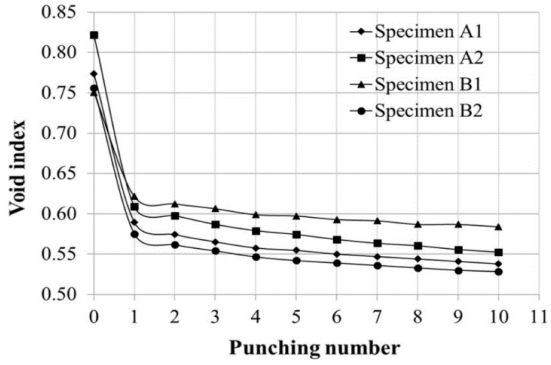

Figure 6.3 *Void index variation during CSP tests on glass cullet as a consequence of particle breakage and particle adjustment due to rolling and sliding (Cortellazzo et al., 2021)*

Following CSP tests, the GSD curves of tested representative portions (**Figure 6.4**) evolve similarly as a result of particle breaking processes that occur under loading.

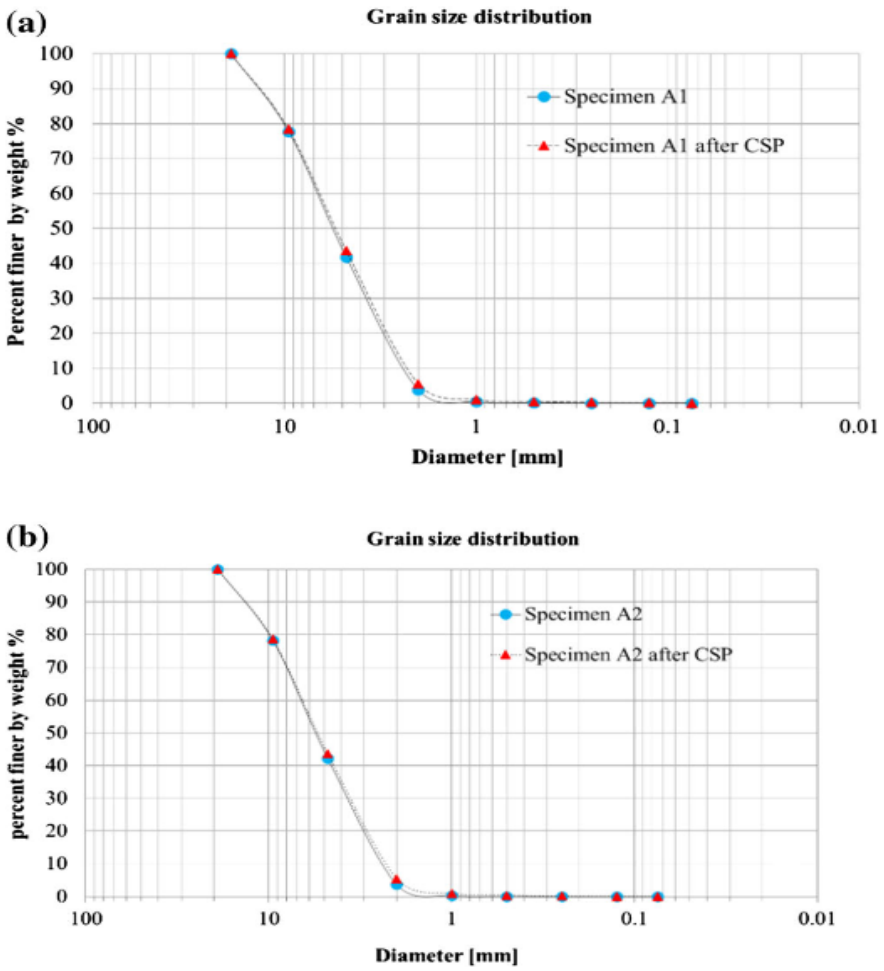

Figure 6.4 GSD curves before and after CSP tests for two glass cullet specimens (Cortellazzo et al., 2021)

In that case, the change in GSD due to the loading conditions and the consequent particle breakage has shown no significant changes in the permeability of the specimen. For a general case, it is important to evaluate all properties only after performing this type of test, to be sure that the results are related to the in-situ performance of the chosen material.

6.3 GRANULOMETRIC COMPATIBILITY

After the aforementioned CSP test, the evaluation of the granulometric compatibility between the materials forming the BCL and the underlying base layer is needed to verify that they are compatible with each other. In short, granulometric compatibility analysis is intended to establish the minimum diameters of the larger particle size classes so that they do not cross the underlying base layer (as a result of dragging by fluids and/or mechanical

actions and vibrations) by interpenetrating it and, thus, depleting the biogas drainage layer from such fractions. In particular, two criteria must be satisfied:

1. **Retention criterion**: voids should be sufficiently small to prevent fine particle migration from the finer grain material to the filter, resulting in fine grain material erosion and filter clogging;
2. **Permeability criterion**: to prevent the buildup of interstitial fluid pressures, the filter should be more permeable than the fine grain material with which it is in contact.

In 1922, Karl Terzaghi calculated two equations to assess the satisfaction of these two criteria, respectively *6.3* for the retention and *6.4* for the permeability:

$$\frac{D_{15f}}{D_{85b}} < 4 \qquad 6.3$$

and

$$\frac{D_{15f}}{D_{15b}} > 4 \qquad 6.4$$

where D_{85} and D_{15} are, respectively, the sieve widths that allow 85% and 10% by weight of the granular material sample to pass through; additionally, letter f refers to the material forming the filter (like the BCL), while letter b to the material forming the base (or material to be protected). If these equations are satisfied, it is possible to proceed with the assessment of the internal stability of the material.

6.4 INTERNAL STABILITY

Internal stability of a granular material, also known as “self-healing”, is a property that indicates the ability of the granular material to retain all particle size fractions within itself, including the finest, in order to prevent their migration outward, depleting the particle composition. In summary, the finer particle size classes of the BCL must be held by the layer's coarser size classes. Thus, the shape of the grain size curve of the material constituting the layer plays an important role in defining the internal stability. Each particle size class in a self-healing porous media must develop "voids" way of maintaining finer particles mobilized by vibrations and/or filtration processes.

Various authors developed effective methods to assess the internal stability of a granular material, such as the empirical one by Kezdi (1969) and the statistical-probabilistic by Musso & Federico (1982). However, the most commonly used is the one elaborated by Kenney & Lau (1985).

6.4.1 Kenney & Lau verification method

Kenney & Lau noticed that, within granular materials, there is a "primary structure" that is mainly responsible for stress transfer and a "secondary structure" that consists of finer particles displaced within the voids formed between the primary structure's grains. Unlike particles in the primary structure, which can be considered to be in a fixed position, particles in the secondary structure tend to move within the intergranular voids due to the effect of external stresses caused, for example, by filtration motions or vibrations. Thus, these moving, finer particles are considered responsible for a material's potential internal instability.

In these terms, the primary structure is comparable to a filter, while the secondary structure is equivalent to the material that must be protected. When a mobile particle reaches a sufficiently small constriction to be retained during its migration, the particle begins to become part of the load-carrying skeleton (primary structure). So, thinking in these terms, an internally unstable material is characterized by an insufficient number of grains of a certain size to form constrictions large enough to block smaller particles. These excessively large constrictions then promote erosion of the layer due to migration of fine particles.

Kenney & Lau criterion utilizes the shape of the GSD by determining, for each value of the passing weight F to which the diameter D is associated, the weight percentage H comprised between the diameters D and $4D$ (**Figure 6.5**). By plotting the $H - F$ curve on a graph, it is possible to evaluate the position of that curve with respect to the limit line that indicates the minimum value of H required for the material to be internally stable. Such a limit line has the following equation:

$$H = F \tag{6.5}$$

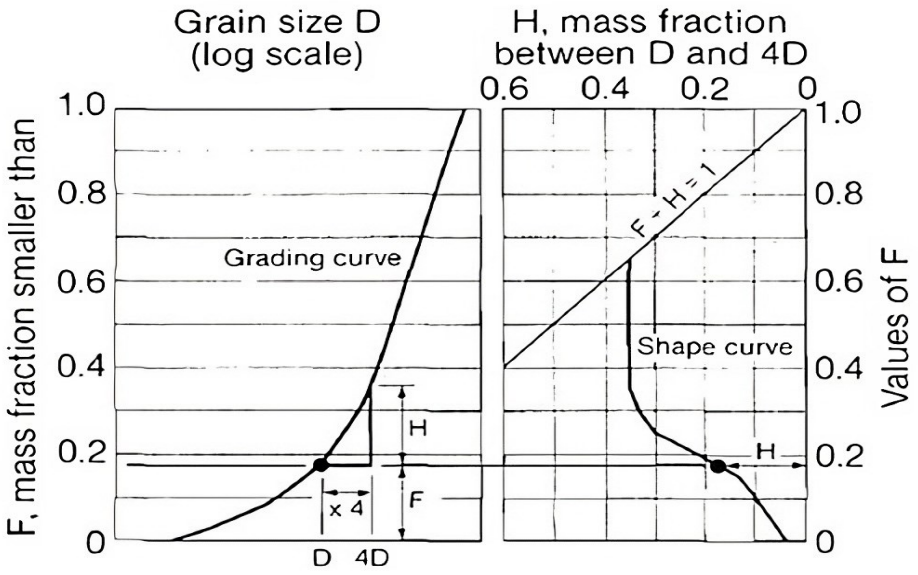

Figure 6.5 *Graphs showing the relationships of the Kenney & Lau verification method (Kenney & Lau, 1985)*

However, it is not necessary for the entire curve describing the shape of the GSD to lie above the limit line $H = F$ for the material to be internally stable. In fact, only the fraction representing the mobile particles, which is responsible for much of the internal instability of granular soils, must meet this criterion. As a result, in materials with not so wide grain size curve, the Kenney & Lau criterion must be verified for $0 < F < 0.3$, whereas in materials with wider grain size curves, this range is reduced to $0 < F < 0.2$. In any case, if the diameter $4D$ exceeds the maximum diameter of the grain size curve, verification will be terminated at the diameter D.

As an example, the case of a recycled material will be taken into account. This material consists of the upper part of the sieving of heavy slag coming from the incineration of MSW (**Figure 6.6**). Since it is obtained from a sieving process, the granulometry has already been inspected. The grain size distribution curve of the material can be seen in **Figure 6.7** and, from this graph, it is possible to determine the two parameters required to perform the Kenney & Lau verification:

- F = passing fraction correspondent to the sieve diameter D;
- H = passing fraction correspondent to the sieve diameter $4D$, from which is subtracted the value F for the same diameter D.

Values of F and H are displayed in

Table **6.2**.

Figure 6.6 *Heavy slag from MSW incineration (Ad Rem, 2020)*

d (mm)	%
70,00	100%
46,00	90%
32,00	80%
25,00	70%
21,00	60%
18,00	50%
15,50	40%
13,00	30%
10,50	20%
5,40	10%
4,50	8%
3,70	6%
2,60	4%
1,70	2%
1,00	0%

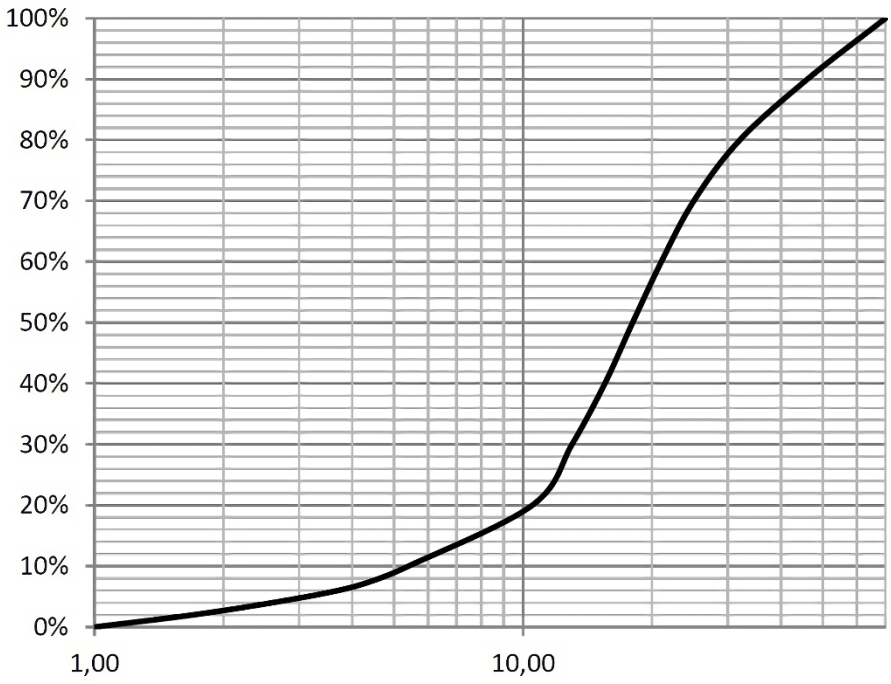

Figure 6.7 *Grain size distribution curve of the selected material*

Table 6.2 Parameters derived from the GSD curve

D (mm)	Passing %	4D	F	H
70,00	1,00	280,00		
46,00	0,90	184,00		
32,00	0,80	128,00		
25,00	0,70	100,00		
21,00	0,60	84,00		
18,00	0,50	72,00		
15,50	0,40	62,00	0,40	0,56
13,00	0,30	52,00	0,30	0,62
10,50	0,20	42,00	0,20	0,66
5,40	0,10	21,60	0,10	0,44
4,50	0,08	18,00	0,08	0,38
3,70	0,06	14,80	0,06	0,31
2,60	0,04	10,40	0,04	0,19
1,70	0,02	6,80	0,02	0,10
1,00		4,00	0,00	0,06

With the values derived from the GSD curve is now possible to plot the $H(F)$ curve that, in this case, lies completely above the $H = F$ line (**Figure 6.8**). For this reason, it is safe to say that the investigated material is "internally stable" and, thus, suitable for design purposes.

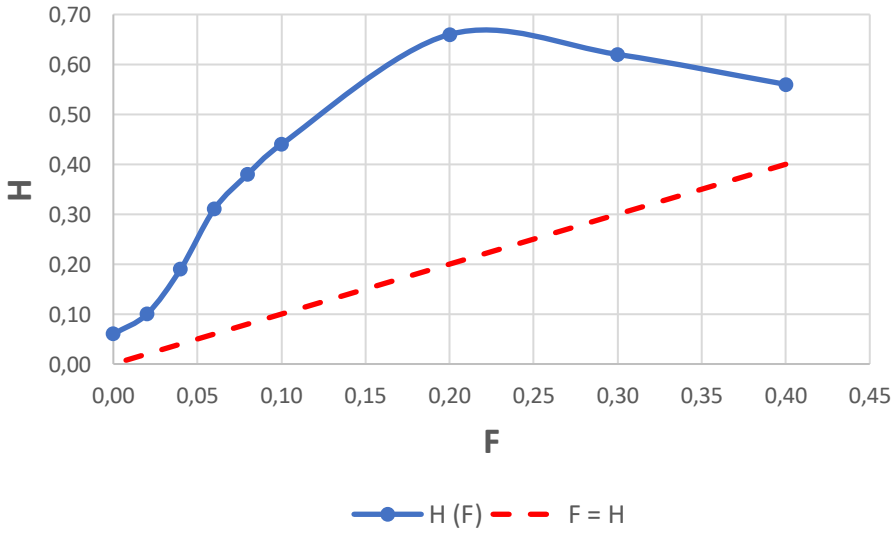

Figure 6.8 Resulting graph for the Kenney & Lau verification method

6.5 PERMEABILITY

Finally, the assessment of the permeability can be carried out. This operation aims to achieve a precise estimation of the coefficient of permeability k_w. There are several laboratory methods commonly used to assess the permeability coefficient of soil. The choice of method depends on factors such as the type of soil, the required accuracy, and the specific testing objectives. However, the most used tests are the constant head permeameter test and the falling head permeameter test.

Briefly, these tests possess the following characteristics:

- **Constant Head Permeameter Test:** the constant head permeameter test is used to measure the hydraulic conductivity of coarse-grained soils (sands and gravels) with relatively high permeability. In this test, a soil sample is placed in a cylindrical column (permeameter) with a known cross-sectional area. The bottom of the column is connected to a constant water head via a standpipe filled with water, that is allowed to flow through the soil sample under the influence of gravity. The rate of flow is measured as the water level in the standpipe remains constant. The hydraulic gradient is determined by measuring the elevation difference between the water surface in the reservoir and the water level in the standpipe, and Darcy's law is used to calculate the hydraulic conductivity of the soil sample.
- **Falling Head Permeameter Test**: the falling head permeameter test is used to determine the hydraulic conductivity of soils with lower permeability, including fine-grained soils (clays and silts). In this test, a soil sample is placed in a cylindrical column similar to the constant head permeameter. However, instead of maintaining a constant water head, a known volume of water is introduced into the top of the column, and the water level is allowed to fall under gravity. As water flows through the soil sample and the level drops, measurements of time and falling water level are recorded. The hydraulic conductivity is then determined using a formula that accounts for the change in water level with time and the properties of the soil sample. The falling head permeameter test is suitable for soils with lower permeability because it measures the time it takes for water to

flow through the sample, which can be more practical for slow-draining soils compared to the constant head test.

Once the k_w of the material has been evaluated, the value must be equal or greater to the one needed for the design of a safe and efficient drainage layer such as the one determined using the method shown in Chapters 4 and 5.

If this relation is satisfied, along with all the other verifications presented in this chapter, the material could be safely considered suitable for the formation of the biogas drainage layer.

CONCLUSIONS

This work's main objective is to give designers a practical example, which comprises the necessary steps for the development of the calculations needed when planning the construction of a BCL in an effective manner. The method proposed in 1998 by Richard Thiel is the base upon which all considerations are carried out, incorporating slope stability analyses and fluid dynamics for the evaluation of a suitable permeability of the porous media forming the BCL.

This model has been applied to the Torretta di Legnago landfill, starting from the evaluation of the maximum flux of biogas that has been calculated from site specific data. Based on the biogas production models, year 2031 is expected to present the maximum flow $Q_b = 391\ m^3/h$, from which is calculated the maximum flux $\Phi_b = 3.52 \cdot 10^{-7}\ m^3/s \cdot m^2$.

As a second step, the stability of the landfill top cover has been analysed using two methods, the infinite slope (IS) approach and a slightly modified version of the one developed by Koerner & Soong (KS) in 1998. Both the escarpments (21.8°) and the summit cover (5.4°) have been taken into account. This step aimed to calculate the maximum biogas pressure u_g that is considered admissible for the top cover to ensure a FS of 1.3. For the escarpments, to a FS of 1.3 correspond a biogas pressure $u_{g,max} = 10.2\ kPa$ using IS and $u_{g,max} = 13.4\ kPa$ using KS. As expected, summit cover can withstand higher pressures due to its low gradient, in particular $u_{g,max} = 37.5\ kPa$ using IS and $u_{g,max} = 42.4\ kPa$ using KS. These values encompass the great implication derived from these analyses: when in presence of slopes, even low biogas pressures result in a serious drop of the factor of safety, making it mandatory to correctly quantify the destabilizing action that the biogas yields on the top cover.

So, once these values of flux and pressure have been defined, fluid dynamic equations as presented by Thiel's works have been applied to evaluate the design water permeability of the material in relation to the distance between the linear gas collection drains present in the BCL, considered as passive (no vacuum for gas extraction) for precautionary reasons. Design permeability has been calculated applying a series of correction factors to account for the effects of intrusion of the geotextile, clogging, and moisture.

Considering a distance between the strip drains $D = 25\ m$, the resulting permeability coefficients are, for the escarpments, $k_w = 8.28 \cdot 10^{-4}\ m/s$ (IS) and $k_w = 6.28 \cdot 10^{-4}\ m/s$ (KS); for the summit cover are $k_w = 2.25 \cdot 10^{-4}\ m/s$ (IS) and $k_w = 1.99 \cdot 10^{-4}\ m/s$ (KS). Throughout this paper, strip drains have been considered as the design choice based on the considerations carried out by Thiel. However, vertical wells are the usual biogas collection method, and their distance and placement often rely on common practice rather than site-specific calculations. Since it has been proved that, even at modest pressures, biogas has a major impact on the cover's stability, the use of horizontal collectors rather than vertical wells should be the preferred design choice. This method, besides being less invasive in terms of construction, permits a more uniform biogas collection, avoiding the eventual formation favoured paths or "dead spots" for the gas, which could lead to instability problems. As a result, it is safe to say that strip drains parallel to the slope are indispensable for an effective biogas extraction.

In the final part of the work, after the calculation of the different permeability coefficients, Chapter 6 presents a procedure for the acceptance of a suitable material to use as a filter in the BCL. Five steps have been identified as crucial for the choice of the material: landfill conferability, mechanical strength and resilience, granulometric compatibility, internal stability and permeability. Moreover, the cyclic static punching (CSP) test is here described as a proper procedure to assess the mechanical resilience of the material against phenomena such as particle fragmentation.

Finally, as an example, the granulometric curve derived from sieving of a specimen of heavy slag for MSW incineration has been used to show its suitability in terms of internal stability. In particular, the verification method proposed by Kenney & Lau has given positive results, thus allowing to define the material as internally stable.

BIBLIOGRAPHY

Ad Rem. (2020). *Incineration slag*. https://www.adrecyclingmachines.com/en/machines/incineration-slag-1

Andreottola, G., Cossu, R., & Ritzkowski, M. (2018). Landfill Gas Generation Modeling. *Solid Waste Landfilling: Concepts, Processes, Technologies*, 419–437. https://doi.org/10.1016/B978-0-12-407721-8.00020-6

Anubhav, & Basudhar, P. K. (2010). Modeling of soil-woven geotextile interface behavior from direct shear test results. *Geotextiles and Geomembranes*, *28*(4), 403–408. https://doi.org/10.1016/j.geotexmem.2009.12.005

ATSDR. (2001). *Landfill Gas Primer - Chapter 2: Landfill Gas Basics*. https://www.atsdr.cdc.gov/hac/landfill/html/ch2.html

Bindal, A. K., Das, A., & Das, A. (2020). Study on Effect of Particle Shape on Interlocking. *Lecture Notes in Civil Engineering*, *56*, 455–466. https://doi.org/10.1007/978-981-15-0890-5_38/FIGURES/8

Brooks, R. H., & Corey, A. T. (1964). *Hydraulic properties of porous media* (Vol. 3). Colorado State University.

Chen, X. Y., Kaliaguine, S., & Rodrigue, D. (2018). Correlation between Performances of Hollow Fibers and Flat Membranes for Gas Separation. In *Separation and Purification Reviews* (Vol. 47, Issue 1, pp. 66–87). Taylor and Francis Inc. https://doi.org/10.1080/15422119.2017.1324490

CONVECO SRL. (2022). *Biogas extraction & combustion*. https://www.conveco.com/en/biogas-extraction-combustion.html

Cortellazzo, G., Bellò, E., Busana, S., & Favaretti, M. (2021). Experimental Acceptance Procedure for Using Cullet in the Gas Collection Layer of MSW Landfill. *Indian Geotechnical Journal*, *51*(5), 877–886. https://doi.org/10.1007/s40098-020-00472-w

Cossu, R., & Stegmann, R. (2018). Landfill Planning and Design. *Solid Waste Landfilling: Concepts, Processes, Technologies*, 755–772. https://doi.org/10.1016/B978-0-12-407721-8.00035-8

Decreto Legislativo 3 aprile 2006, n. 152 “Norme in materia ambientale, Allegato B alla parte IV.”

EPA. (2021). LFG Energy Project Development Handbook. In *LFG Energy Project Development Handbook* (Vol. 7).

The European Green Deal, (2020). https://eur-lex.europa.eu/resource.html?uri=cellar:b828d165-1c22-11ea-8c1f-01aa75ed71a1.0002.02/DOC_1&format=PDF

Eurostat. (2023). *Waste statistics - Statistics Explained*. https://ec.europa.eu/eurostat/statistics-explained/index.php?title=Waste_statistics

Favaretti, M. (2022). *Environmental Geotechnics: course slides*.

Geosynthetic Institute. (2013). *GRI Standard GC8: Determination of the allowable flow rate of a drainage geocomposite*.

Giroud, J. P., Williams, N. D., Pelte, T., & Beech, J. F. (2015). Stability of Geosynthetic-Soil Layered Systems on Slopes. https://doi.org/10.1680/GEIN.2.0048

Gnanasekaran, D., & Reddy, B. S. R. (2013). Cost effective poly(urethane-imide)-POSS membranes for environmental and energy-related processes. *Clean Technologies and Environmental Policy*, *15*(2), 383–389. https://doi.org/10.1007/s10098-012-0500-7

Google Earth. (2023). https://earth.google.com/web

Izzuddin Zaini, M., Kasa, A., & Anuar Mohd Nayan, K. (2012). Interface Shear Strength of Geosynthetic Clay Liner (GCL) and Residual Soil. *International Journal on Advanced Science Engineering Information Technology*, *2*, 43–45.

Kenney, T. C., & Lau, D. (1985). Internal stability of granular filters. *Canadian Geotechnical Journal*, *22*(2), 215–225. https://doi.org/10.1139/t85-029

Kezdi, A. (1969). *Increase of protective capacity of flood control dikes*. Department of Geotechnique, Technical University Budapest.

Kjeldsen, P. (2018). LFG Migration. *Solid Waste Landfilling: Concepts, Processes, Technologies*, 975–984. https://doi.org/10.1016/B978-0-12-407721-8.00047-4

Koerner, R. M., & Soong, T. Y. (1998). Analysis and design of veneer cover soils. *Sixth International Conference on Geosynthetics*, *12*(1).

Liu, C., Gilbert, R., Thiel, R., & Wright, S. (1997). What is an appropriate factor of safety for landfill cover slopes? *Geosynthetics '97*, 481–496.

Markou, I. (2018). A Study on Geotextile—Sand Interface Behavior Based on Direct Shear and Triaxial Compression Tests. *International Journal of Geosynthetics and Ground Engineering*, *4*. https://doi.org/10.1007/s40891-017-0121-7

Meegoda, J. N., Hettiarachchi, H., & Hettiaratchi, P. (2016). Landfill design and operation. *Sustainable Solid Waste Management*, 577–604. https://doi.org/10.1061/9780784414101.CH18

Muskat, M., & Wyckoff, R. D. (1937). *The flow of homogeneous fluids through porous media* (1st ed.). McGraw-Hill Book Company, Inc.

Musso, A., & Federico, F. (1982). Un metodo geometrico-probabilistico per la verifica dei filtri. *Rivista Italiana Di Geotecnica*, *4*.

Nastev, M., Therrien, R., Lefebvre, R., & Geélinas, P. (2001). Gas production and migration in landfills and geological materials. *Journal of Contaminant Hydrology*, *52*(1–4), 187–211. https://doi.org/10.1016/S0169-7722(01)00158-9

Neira, J., Ortiz, M., Morales, L., & Acevedo, E. (2015). Oxygen diffusion in soils: Understanding the factors and processes needed for modeling. *Chilean Journal of Agricultural Research*, *75*, 35–44. https://doi.org/10.4067/S0718-58392015000300005

Nguyen, M.-D., & Ho, M.-P. (2021). The influence of saturation on the interface shear strength of clay and nonwoven geotextile. *Journal of Science and Technology in Civil Engineering (STCE) - NUCE*, *15*(1), 41–54. https://doi.org/10.31814/stce.nuce2021-15(1)-04

OECD. (2019). *Global Plastics Outlook*. https://www.oecd-ilibrary.org/environment/data/global-plastic-outlook_c0821f81-en

Othman, M. (2016). *Interface Behaviour and Stability of Geocomposite Drain/Soil Systems*. https://doi.org/10.13140/RG.2.2.22646.91204

Raut, A. K. (2006). *Mathematical modelling of granular filters and constriction-based filter design criteria* [PhD Thesis, University of Wollogong]. http://ro.uow.edu.au/theses/44

Rettenberger, G. (2018). Collection and Disposal of Landfill Gas. *Solid Waste Landfilling*, 449–462. https://doi.org/10.1016/B978-0-12-407721-8.00022-X

Söylemez, M., & Arslan, S. (2020). Experimental investigation of influence of clay in soil on interface friction between geotextile and clayey soil. *Arabian Journal of Geosciences*, *13*(10). https://doi.org/10.1007/s12517-020-05339-1

Tanikawa, W., Shimamoto, T., Tanikawa, W., & Shimamoto, T. (2006). Klinkenberg effect for gas permeability and its comparison to water permeability for porous sedimentary rocks. *HESSD*, *3*(4), 1315–1338. https://doi.org/10.5194/HESSD-3-1315-2006

Tchobanoglous, G., Theisen, H., & Vigil, S. (1993). *Integrated solid waste management: engineering principles and management issues*. McGraw-Hill.

TeMa Corporation. (2021). *Discariche e siti contaminati*. https://www.temacorporation.com/geo-applicazioni/discariche-e-siti-contaminati/

The Engineering Toolbox. (2003). *Viscosity - Absolute (Dynamic) vs. Kinematic*. https://www.engineeringtoolbox.com/dynamic-absolute-kinematic-viscosity-d_412.html

Thiel, R. (1998). Design methodology for a gas pressure relief layer below a geomembrane landfill cover to improve slope stability. *Geosynthetics International*, *5*(6), 589–6116.

Thurgood, M. (1999). *Decision-maker's guide to solid waste landfills*.

Tindall, J. A., Kunkel, J. R., & Anderson, D. E. (1999). Unsaturated zone hydrology for scientists and engineers. In *Saturated water flow in soil* (pp. 165–182). Prentice Hall.

UNI. (2002). *CNR-UNI 10006 "Classificazione dei terreni HRB-AASHTO."*

Ünvar, S., Ibrahim, A., Üniversitesi, Ç., Kocer, A., Yilmaz, A., Koçer, A., & Aygün, B. (2018). Factors Affecting the Production of Biogas. *International Journal of Scientific and Engineering Research*, *9*(5).

Wang-Wai, C., & Menzies, B. (2007). *Advanced unsaturated soil mechanics and engineering*. Taylor & Francis Group.

RINGRAZIAMENTI